Utilisation of Line Surge Arrestors to Improve Overhead HVAC and EHVDC Line Performance under Lightning Conditions

by

Eddie Singh

881118288

A thesis submitted in fulfilment of the academic requirements for the degree

Doctor of Philosophy in Engineering in the School of Engineering

University of KwaZulu-Natal, Durban, South Africa

Supervisor: Professor I.E. Davidson

July 2020

CERTIFICATION

I, Hariram Singh, hereby certify that the research work presented in this thesis entitled ''Utilisation of Line Surge Arrestors to Improve Overhead HVAC and EHVDC Line Performance under Lightning Conditions'' is an authentic record of my own work carried out under the guidance Professor Innocent E. Davidson. The work contained in this thesis has not been previously submitted in part or whole for an award of any degree at this or any other University/higher education institution. To the best of my knowledge, this thesis contains no material previously published or written by another person except where due references have been made.

Signed: ………………………………………………

Hariram Singh

Date: July 2020

As the candidate's Supervisor I agree / do not agree to the submission of this thesis.

………………………………………………   …………………………………..

Prof. IE Davidson   Date

DECLARATION 1 - PLAGIARISM

I, Hariram Singh declare that

1. The research reported in this thesis, except where otherwise indicated, is my original research.

2. This thesis has not been submitted for any degree or examination at any other university.

3. This thesis does not contain other persons' data, pictures, graphs or other information, unless specifically acknowledged as being sourced from other persons.

4. This thesis does not contain other persons' writing, unless specifically acknowledged as being sourced from other researchers. Where other written sources have been quoted, then:
    a. Their words have been re-written but the general information attributed to them has been referenced
    b. Where their exact words have been used, then their writing has been placed in italics and inside quotation marks, and referenced.

5. This thesis does not contain text, graphics or tables copied and pasted from the Internet, unless specifically acknowledged, and the source being detailed in the thesis and in the References sections.

Signed

…………………………………………………………………………

DECLARATION 2 - PUBLICATIONS

Publications emanating from the PhD research study are as follows:

[1]   Eddie Singh and Innocent E. Davidson, "Utilization of Line Surge Arrestors to Improve Overhead EHV DC Line Performance under Lightning Conditions", *International Journal of Applied Engineering Research, Vol 14, Number 21,* 2019, pp 4030 – 4041, ISSN0973 – 4562

[2]   Eddie Singh and Innocent E. Davidson, "Improving Overhead HV AC Line Performance using Line Surge Arrestors under Lightning Conditions with Economic Analysis", *International Journal of Applied Engineering Research, Vol 14, Number 22,* 2019, pp 4126 – 4135, ISSN0973 – 4562

[3]   E. Singh, I.E. Davidson and G.K. Venayagamoorthy, "Methodology for Measuring and Enhancing Tower Footing Resistance for Lightning Protection in an 88KV Line". *In Proceedings of the 25th South African Universities Power Engineering Conference,* 30 January – 1st February 2017, Stellenbosch, South Africa, pp. 655-659, ISBN 978-0-620-74503-1.

[4]   Sindi Malanda, Innocent Davidson, Elutunji Buraimoh and Eddie Singh, "Analysis of Soil Resistivity and its Impact on Grounding Systems Design". *Proceedings of the IEEE Power Africa Conference,* 26 – 29 June, 2018, Cape Town, South Africa, pp. 522-527

[5]   Eddie Singh and Innocent Davidson, "Utilization of Line Surge Arrestors to Improve Overhead HV AC Line Performance under Lightning Conditions". *In Proceedings of the 2019 South African Universities Power Engineering Conference/Robotics and Mechatronics/Pattern Recognition Association of South Africa (SAUPEC/RobMech/ PRASA),* 28 – 30 January 2019, Central University of Technology, Free State, Bloemfontein, South Africa, pp. 412 - 419. ISBN: 978-1-7281-0368-6.

[6]   E. Singh, "Fault Mitigation and Performance Improvement of an 88kV line using Line Surge Arrestors and Counters". University of Kwa Zulu Natal 2016 Postgraduate Research Day, Durban, South Africa, November 2016.

Signed:

July 2020

DEDICATION

This research work is wholly dedicated in the memory of my late Dad, Mr Chunun Singh.

ACKNOWLEDGEMENTS

First, I would like to give thanks to Lord Narayan (My Lord) the almighty, the all great without whom I could not have completed this educational endeavour. .Without his guidance, ability, wisdom, intellect, and strength this research work would never have come to reality. By chanting his name I can achieve all things.

I would like to convey my honest and deepest gratitude to my supervisor Prof Innocent E. Davidson of Durban University of Technology (DUT) for providing me with brilliant guidance, mentorship and for sharing his knowledge and expertise. In addition the confidence he inspired during the period of my PhD research during key stages is a revelation. It has been an impressive special honour for me to work under his supervision.

Many thanks to all faculty members, School of Engineering, various paper reviewers for their constructive comments, which aided and supported my thought process in the completion of this Ph.D. thesis.

Special thanks to my adored family for their unconditional affection, prayers, word of encouragement and support in my entire life. I would like to apologize to my wife and children for my absence during the time I was away conducting this research. Their support and patience during these four years will always be valued.

ABSTRACT

In high lightning areas, lightning strokes play an important role in the performance of overhead EHV AC and DC lines. A single lightning stroke, that terminate on the earthwire and/or tower can lead to back flashovers. This flashover depends on factors such as conductor type, tower, soil resistivity and magnitude of the stroke. The flashover across the insulator and the resultant fault current surge will propagate along the line, until it is extinguished or the breaker operates. This movement of the surge currents tend to damage and reduce the life span of associated equipment such and circuits breakers, insulators, transformers and impact network performance adversely. Furthermore this operation of the protective devices leads to power interruption to consumers on that network, and loss of production, thus negatively impacting the economy.

This thesis investigates the incidences of network failure due to lightining strokes occuring on Eskom HVAC network as well as HVDC networks, considering soil resistivity, tower footing resistance and factors that influence the earthing resistances. Tower footing resistance needs to be kept uniform and as low as possible to extinguish the surge across the tower and hence reducing the back flashovers across the insulator under lightning conditions. Theoretical simulations were conducted on the different methods that are available to improve the tower footing resistance values. A case study was undertaken to ascertain the tower footing resistance of an 88kV Eskom line. The crows earthing configuration was then utilized to reduce the footing resistance to a value less than 30 ohms, using line surge arrestors (LSA) which are devices that can drain power surges to ground, if placed adequately and in sufficient numbers.

Furthermore the thesis determines the relationship between the magnitude of the lightning stroke, the tower top voltage, tower footing resistance and hence the back flashover voltage that would appear on the line, which would lead to power interruptions. Surge arrestors were modelled using MATLAB software. The required number of surge arrestors per phase is thus determined that is required to drain the surge current down to earth., thus preventing power interruptions. EHV AC and DC cases studies are simulated and results are presented snd discussed.

Table of Contents

List of Figures

List of Tables

List of Abbreviations

A.C	Alternating Current
BFO	Back Flash Over
CIGRE	Conseil International des Grands Reseaux Electriques
CIRED	Congrès International des Réseaux Electriques de Distribution
D.C.	Direct Current
DPL	DIgSILENT Programming Language
DTL	Definite Time Lag
DVR	Dynamic Voltage Restorer
EHVDC	Extra High Voltage Direct Current
EMTP	Electromagnetic Transient Program
FALLS	Fault Analysis and the Lightning Location System
HV	High Voltage
HVAC	High Voltage Alternating Current
EHVDC	High Voltage Direct Current
Hz	Hertz
IDMT	Inverse Definite Mean Time
IEC	International Electrotechnical Committee
IEEE	Institute of Electrical and Electronic Engineers
kA	Kilo Amps
kV	Kilo Voltage.
LCC	Line of Common Coupling
LSA	Line Surge Arrestors
LV	Low Voltage
MATLAB	Matrix Laboratory
MOSA	Metal Oxide Surge Arrestor
MTDC	Multi Terminal Direct Current
MV	Medium Voltage
NEPS	Network and Equipment Performance System
NERSA	National Energy Regulator of South Africa
PCC	Point of Common Coupling
PQ	Power Quality
pu	Per Unit
QOS	Quality of Supply
r.m.s.	Root Mean Square

UPS	Uninterruptible Power Supply
VSC	Voltage Source Converter
VSD	Variable Speed Drive

CHAPTER ONE   INTRODUCTION

1.1 Background

In high lightning areas, lightning strokes play an important role in the performance of overhead HV lines. A single stroke, which may terminate on the tower or earth wire can led to back flashovers, provided factors such as the conductor, tower and soil impedance values are favourable. The resultant power surge on the conductor may result in the protective devices operating to extinguish that surge. This operation of the protective devices can lead to consumer interruptions and production losses, which negatively affects the economy. For any power overhead transmission system, the current practise is to have tower footing resistance below a certain value. This would allow the earthing systems to dissipate the lightning surges. The tower footing resistance on 88kV line is required to be within the range of 20 ohms.

The motivation of this study is to evaluate the effect that the different earthing configuration, lightning magnitude, the surge impedances of the line and tower would have on the tower top voltage. Thereafter the quantity of line surge arrestor needed to remove the power surge from the conductor is determined.

The introduction of Vaisala-GAI Fault Analysis and the Lightning Location System ("FALLS") Version 3.2.4, enables one to more accurately determine the magnitude and position of the lightning stroke [1]. Preliminary anaylsis has indicated that only a portion of the strokes can be withstood by the current line design, which includes the Tower Footing Resistance. The remaining potion of the strokes will ulimately lead to poor performance of the line under lightning conditions. The introduction of the FALLS system provided details of the lightning stroke, such as magnitude, time and location. Line Surge Arrestor (LSA), which are a lightning mitigating device can be utilised on existing transmission systems to improve system perfromance. Furthermore surge counters may be attached onto the LSA. This is provide one with information such as the date, time and magnitude of the current that flowed through the LSA.

Analysed data revealed that lightning strokes may result in both the surge arrestor and breaker operating and in some cases only the surge arrestors. This is dependent on the placement of the LSA and various other influential factors such as the associated lightning stroke. EHVDC lines are been increasing used for long distance power transfer and may transverse medium to high lightning areas. Three single pole DC circuit breakers can be used to clear over voltages and to avoid damage to convertor equipment. Furthermore, to improve system performance, the correct placement of LSA in conjunction with proper earthing is would be investigated.

There needs to be proper analysis done as to how surge arrestors, in conjunction with transformer footing resistance can be used to dissipate the energy and improves system performance on shielded AC and DC transmission lines. Furthermore, data measured by surge counters is available. A theoretical model and simulations needs to be undertaken to evaluate this. This would form the core of this thesis.

1.2 Problem statement

Lightning strokes tend to terminate on the tower and/or earthwire. Depending on factors such as the surge impedance of the tower and conductor, the soil impedance and the stroke magnitude, it will result in back flash over across the insulator. The resultant fault surge will propogate along the line until it is extinguished or the protective device operates. This movement of the surge damages and reduces the life span of associated equipment such as breakers and transformers and negatively affects network performance adversely. Should the breaker operate, the resultant short duration outage and/or dips, would impact negatively on customers. Customers with sensitive equipment such as motors would halt and production would stop. This negatively affects production and subsequently loss to that business and economy.

1.3 Aims and objectives

(a.) Aims

- Develop an AC and DC model for overhead HVAC and EHVDC overhead transmission lines, considering parameters such as magnitude of lightning strokes, insulation levels of the line, tower footing resistance, line parameters and position of shield wire.
- Research and propose earthing strategies for HVAC and EHVDC transmission systems.
- Adequately understand the relationship between surge arrestor, lightning stroke and breaker operating.

(b) Objectives

- The developed model would be generic, but will utilise available data for 88kV HVAC and 533kV EHVDC lines. The expected outcome would be to determine the magnitude of lightning stroke that would results in back flash over.
- The model will determine the number and connectivity of line surge arrestors to prevent poor network performance.
- The overall financial benefits and expenditure must be quantifiable.

1.4 Research question/hypothesis

Significant research work on the practical aspects of when or how the LSA dissipates the surge and the current that flows through the LSA needs to be done and forms part of this proposal.

Performance data obtained from HVAC transmission lines need to be correlated to lightning strokes. Furthermore this need to be further enhanced, in terms of number of LSA used and the expected and predicted line performance and a generic model developed for AC lines. This must inform one, that for a given lightning stroke, the number and energy rating of the surge arrestors required, which will prevent outages on that HVAC lines.

EHVDC lines are been increasing used for long distance power transfer and mainly transverse medium to high lightning areas. The placement of LSA in conjunction with proper earthing can be used to enhance the system performance. Alternatively it could be used to degrade the EHVDC system performance. This must be done in conjunction with the design of the earthing systems. Similarly this study must inform us, that for a given lightning stroke, the number and energy rating of the surge arrestors required, which will prevent outages on that particular network.

1.5 Research method

(a.) Literature review

Additional published papers have been reviewed. The theory w.r.t functionality of surge arrestor, configuration of earthing w.r.t towers, soil conditions, system parameters and various calculation methodologies have been re-examined.

(b.) Data

Data, such as lightning and soil parameters, tower and line data has been sourced from industry. This includes data, such as surge arrestor specifications.

(c.) Data measurement

Data, such as that sourced in (b) has been enhanced via further field measurements. These measurements included soil resistivity tests. Critical data, such as the lightning stroke information, tower dimensions and performance data, have been obtained for HVAC and EHVDC lines and utilise in the models. The model of AC and DC systems have been generated using software such as MATLAB.

(d.) Testing of models

The outputs of various model has been tested against expected/published results.

(e.) Analysis of results

(f.) Financial model

These developed models provides a comparison between the expected saving (improved line

performance) versus the capital and operating cost.

(g.) Compilation of report

1.6 Significance of the study

Amongst published work, such as that by "Williamson [2]' highlights the placement of LSA and the improvement of system performance for the AC transmission system. Of concern was the high number of LSA (1500) used to drive lightning related outages down from 28 to 2 over a 6 year period and the low lightning flash density been 4 flashes/km²/year.

The work done by 'Glossip [3]', discusses and compares current and predicted performance of AC and DC lines, and references the 533kV Chora Bassa lines under amongst other parameters, lightning conditions. However, it does not discuss expected or measured results with the placement of LSA.

The research report by 'Ahmeda [4]" entitled – Earthing performance of transmission line towers' discusses and compares different earthing configuration for AC lines. It does not consider DC lines and does not consider the impact LSA would have on the performance of both HVAC and DC system.

Some research has been done and published, such as that by 'Bhavan" [5], entitled 'performance of high voltage direct current (EHVDC) systems with line commutated converters'. This report details the faults and switching on EHVDC lines. The placement of SA is discussed and usage to protect the convertor stations. It does not discuss the use of LSA on EHVDC lines nor is any theoretical simulations undertaken.

The research paper by "He et al" [6], entitled 'Numeral Analysis Model for Shielding Failure of Transmission Line Under Lightning Stroke', is useful in that is highlights shielding failures due to low lightning stroke magnitude. This methodology needs to be adapted for EHVDC lines.

Published specifications documents, such as 'System aspects on insulation levels for EHVDC converter stations' by ABB focuses on the manufacture and characteristics of surge arrestors to withstand lightning over voltage's for both AC and DC systems. For EHVDC systems the emphases is on the surge arrestors to protect the convertor equipment. Opportunity exists to further enhance the DC surge arrestor to be utilised as LSA with the respective surge counters.

Significant research work on the practical aspects of when or how the LSA dissipates the surge and the current that flows through the LSA needs to be done and forms part of this proposal. Performance data obtained from HVAC transmission lines need to be correlated to lightning strokes.

A LSA that would function under lightning conditions needs to be analysed and designed for EHVDC lines. This must be done in conjunction with the design of the earthing systems. EHVDC lines are been increasingly used for long distance power transfer and generally transverse medium to high lightning areas. The placement of LSA in conjunction with proper earthing can be used to enhance the system performance. Alternatively it could be used to degrade the EHVDC system performance.

Both of these models will provide future guidance to power system engineers to ensure that transmission systems are designed to perform at a certain level.

There should be a breakeven point in terms of cost and benefits on the use of transmission line arrestors, in particular the placement of LSA. A financial model needs to be developed, in conjunction with the AC and DC line model to determine *the breakeven point.*

1.7 Expected contributions

(a.) A simulation model comprising the interaction between lightning stoke magnitude, which leads to overvoltages, the tower/soil impedance and the expected performance level of the system has to be developed. This would be done for both HV and DC transmission systems. This would include the model of the tower, calculation of tower top voltage and phase voltages resulting from calculated back flashovers.

(b.) A model proposing different earthing configuration for both the EHVAC and EHVDC lines.

(c.) The integration of LSA into both the HVAC and EHVDC system. The IEEE line arrestor model is to be modelled in simulation packages such as MATLAB.

(d.) The amount of power surge that can be dissipated per surge arrestor is to be determined and hence the number and connectivity of the surge arrestors can be determined. This is to improve system performance. This will be based on current/measured lightning strokes where parameters such as the magnitude is known

(e.) Financial impact – the expected improvement of integrating the surge arrestor into the system vs the financial costs.

1.8 Thesis outline
The thesis report is organised as follows:

Chapter 2 details the literature review of this thesis, which includes review of the HVAC and EHVDC components of overhead lines and the lightning effects on transmission overhead line and towers.

Chapter 3 describes and discusses the methodologies used and the mathematical modelling of soil resistivity and tower footing resistance. The impact and calculation of soil resistivity and tower footing resistance is also presented.

Chapter 4 and 5 discuss the procedure, simulations and analysis of the HVAC and EHVDC systems, respectively. Results and discussion are also included in these chapters

Chapter 6 compares the results of both systems and the thesis is concluded in Chapter 7 with a brief discussion on the conclusion and recommendations.

CHAPTER TWO   LITERATURE REVIEW

This chapter commences by discussing the lightning related performance of overhead power line with emphasis on an 88kV line in South Africa. Thereafter the impact and cost of dips is discussed and after which the focus is on both the EHVDC and HVAC systems. Surge arrestor modelling is also discussed.

2.1 Lightning distribution within a South African Environment

Most power utilities have an abundance of overhead power lines. The voltage levels vary from 11 to 765kV and stretches for many thousands of kilometres. These power line transverse over different terrain, soil and climate conditions. Therefor different performance levels can be expected from these power lines. The climatic conditions that have the most influence on power lines are storms and, in particular, lightning. Figure 2.1 shows the lightning distribution, within the South African environment.
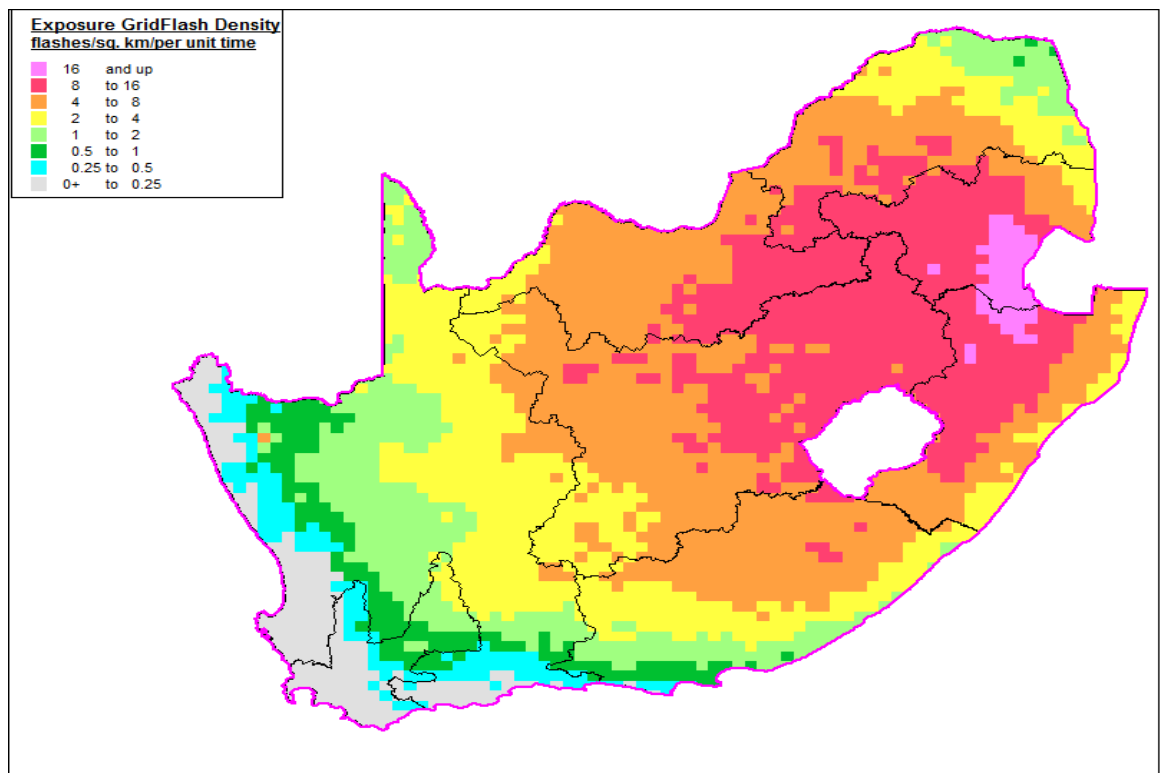
Figure 2.1 Lightning density map of South Africa
Reproduced from reference [1]

Southern Africa has many HVAC and EHVDC lines traversing throughout it. These lines are of different voltage levels. The power lines pass through areas of changing flash density and the lines passing through areas with high flash densities are likely to experience the most lightning strikes. Studies, undertaken by Singh [7], shows the lightning flash density of an 88kV line passing through a high lighting area in South Africa.
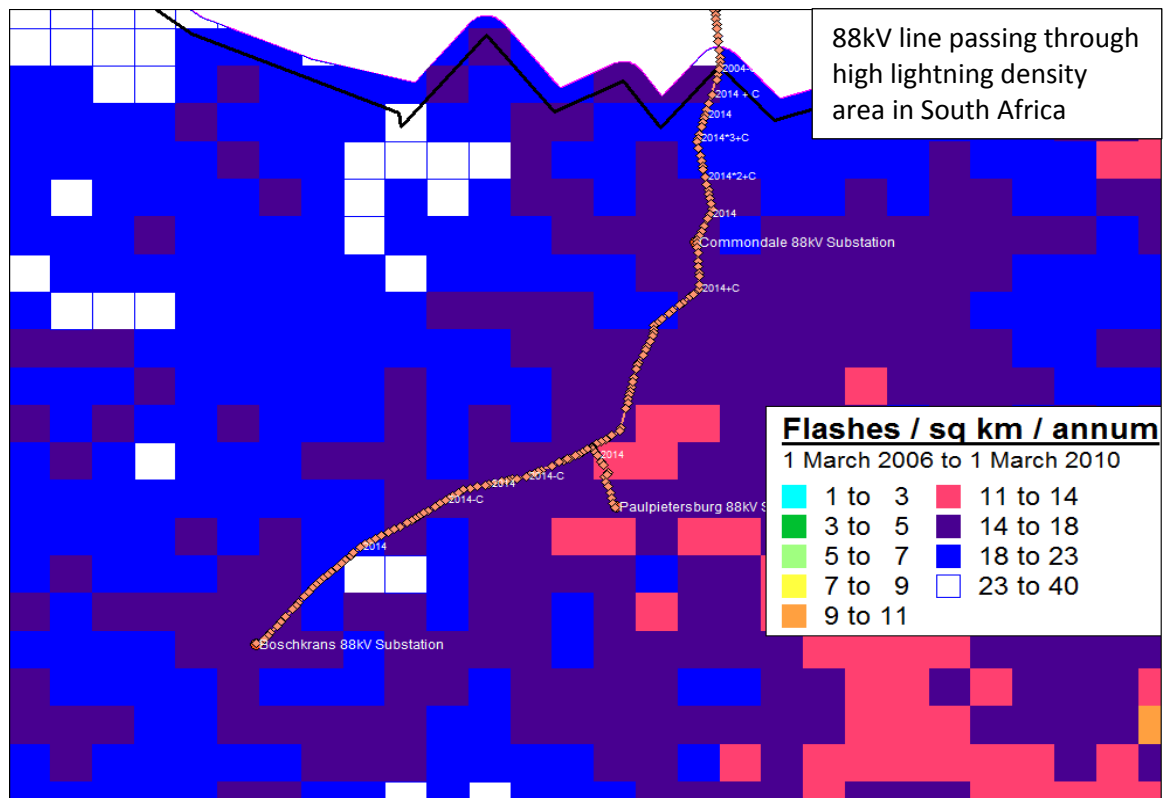
Figure 2.2 Lightning Density for an 88kV line
Reproduced from reference [7]

The highlighted line, shown in figure 2.2, is severely affected by lightning. Research work by *Singh* [7] indicated the following.

1. The line, being 49km long, has been performing poorly over the past 8 years. The average number of breaker trips over a nine year period being 34. These are predormaintly storm related trips as shown in figure 2.3. Storms occurred mainly between the summer months of September and March as shown in figure 2.4.

2. Furthermore on comparison with the FALLS software system, over 73% of these trips are due to lightning on the network.

3. These trips result in small duration interruptions to the customer and play a significant role in generating dips to the customers.
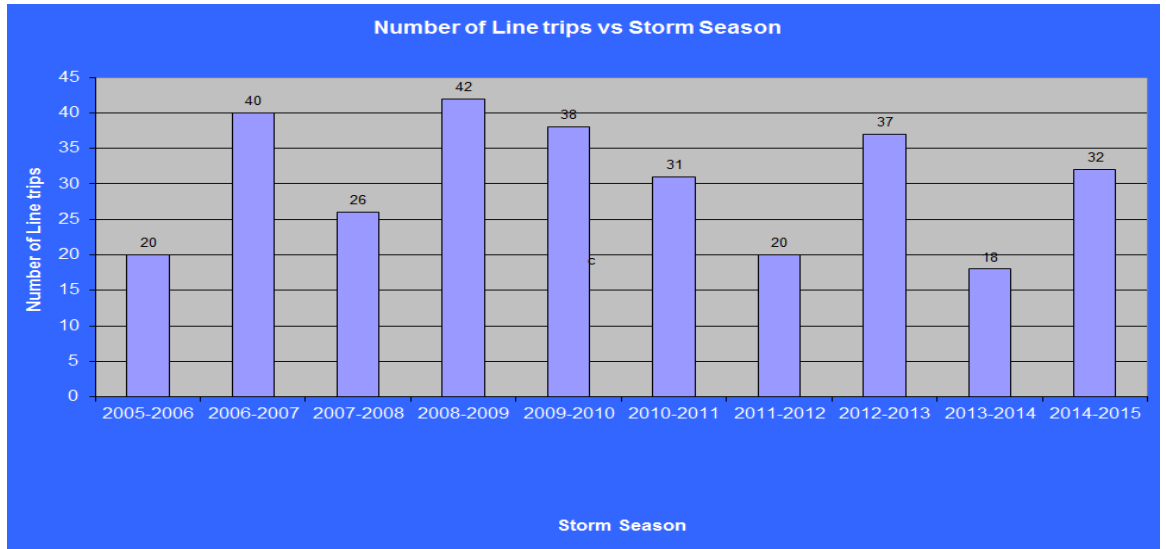
Figure 2.3 Number of line Trips per storm season
Reproduced from reference [7]
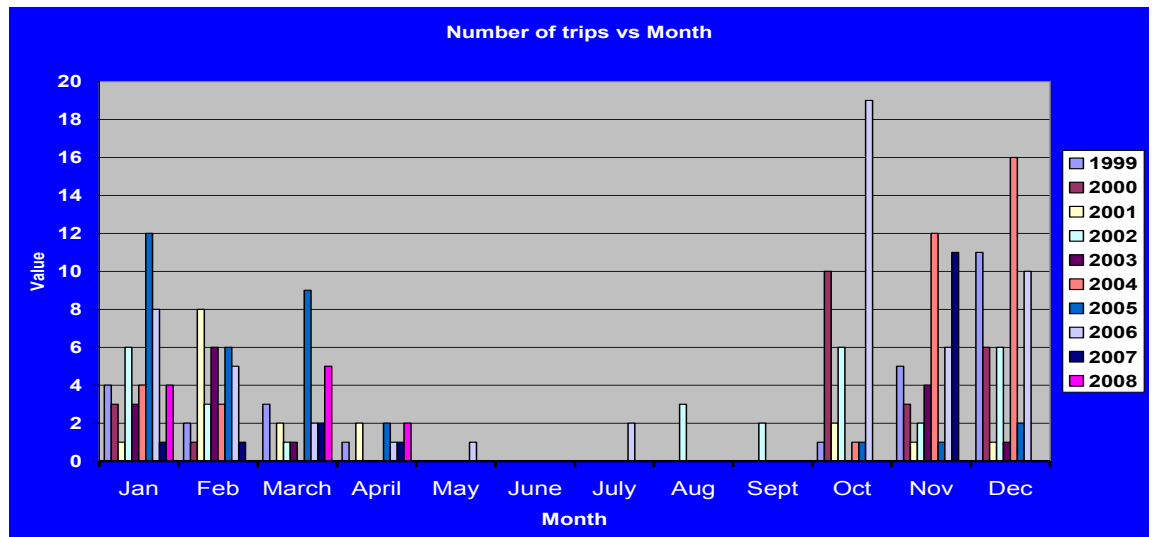
Figure 2.4 Monthly trips per Storm Cycle
Reproduced from reference [7]

The role of dips is fully discussed in the following sections.

2.2 Dip Analysis – Impact of dips

Lightning induced operations of the line breakers of overhead lines, causes voltage depression at the common bus bar. This depression is propagated along adjoining networks and results in various customer experiencing dips at their points of supply. This depth and duration of the dip is depended on the impedance of the line and the protection operation time. Figure 2.5 highlights the dip window as per the NRS 048 [8].
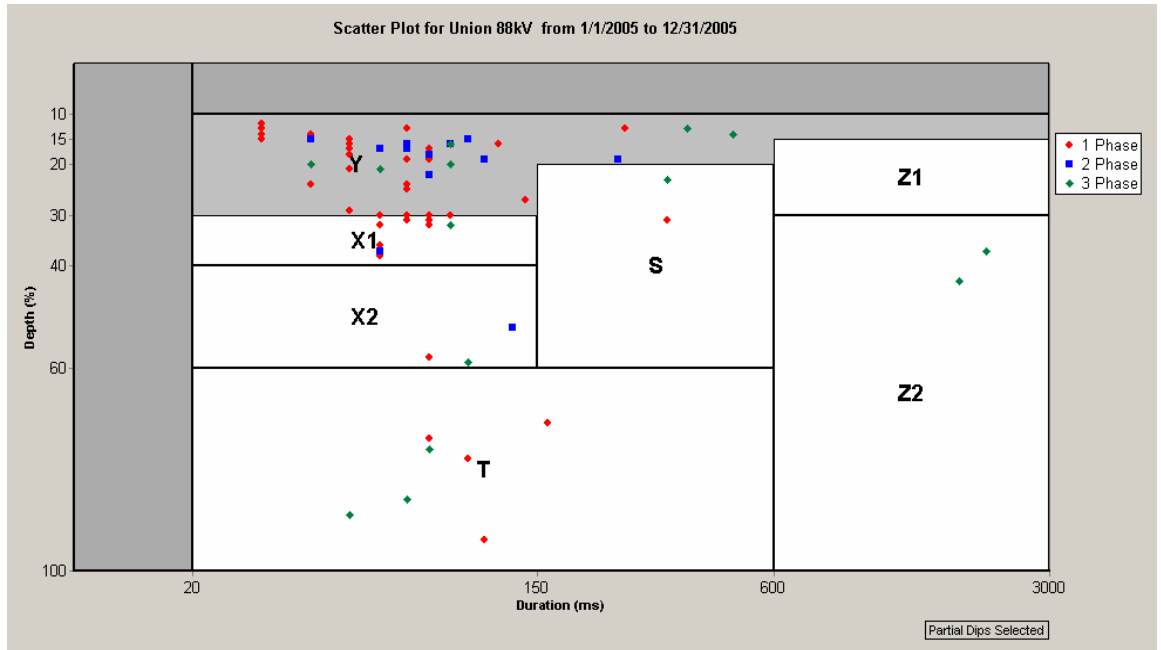
Figure 2.5 Dip window as per NRS 048
Reproduced from reference [8]

2.2.1 Effects of Voltage Dips

The efficiency of electrical equipment is best when the R.M.S. voltage is constant and equal to the required voltage. For individual pieces of industrial equipment, it is possible to determine how long it would continue to function in the presence of a voltage depression or an interruption. Voltage dips can have the following effects on customer equipment:

- Tripping of computers and process-control equipment as a result of operation of over voltage protection.
- Motor contactors can drop out due to lack of voltage to the magnetic coils that keep the contactors connected.
- Variable speed drives can trip due to operation of under voltage protection and overcurrent protection.
- Stalling of directly supplied motors.
- Partial or complete extinguishing of bulbs.

2.2.2. Dip Simulation Methods

Two methods are available for the simulation of voltage dips. These methods are the method of fault positions and that of critical distances. Before discussing the two simulation techniques, a brief discussion on factors that determine dip severity is necessary.

2.2.3. Factors Affecting Severity of Voltage Dips

Voltage dips are influenced by several factors. These factors are briefly discussed.
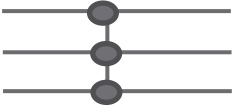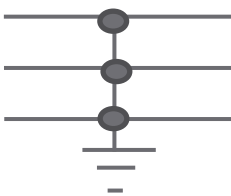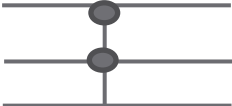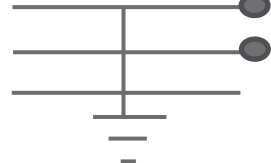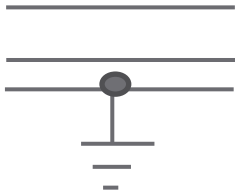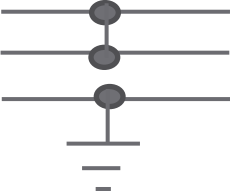
(A) Fault Type

A power system fault generally refers to one of two conditions:

- insulation failure which would result in a short-circuit condition
- failure of the conducting path, which would result in an open-circuit condition.
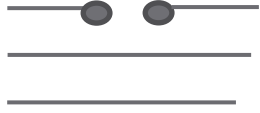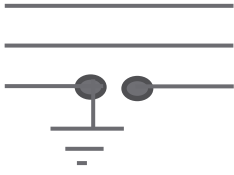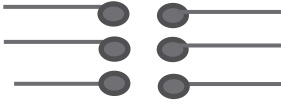
Insulation failures (air) between phase conductors or between phase conductor and earth electrode or both would result in short-circuited conditions. The full range of possible short-circuit conditions is shown in Table 2.1 [9]. The three-phase fault is the only balanced or symmetrical short-circuit condition.

Table 2.1 Short circuit conditions

(a) **Three-phase fault (clear off earth)**	(b) **Three-phase-to-earth fault**
(c) **Phase to phase fault**	**(d)** **Phase to phase to earth fault**
(e) Single phase fault	(f) Single phase and phase to phase

Open-circuit conditions arise when one or more phases fail to conduct. The common causes of this type of failure are broken jumpers on overhead lines and joint failures on cables. Various open-circuit conditions are illustrated in Table 2.2.

Table 2.2 Open circuit conditions

(a) Single-phase open-circuit	(b) Single-phase, open-circuit and single-phase short-circuit
(c) Two-phase open-circuit	(d) Three-phase open-circuit

The effects of a given fault type on customer equipment may be modified considerably by the simultaneous presence of one or more other fault conditions (for example, in a combination of a short-circuit condition and an open-circuit phase condition). Another factor to take into consideration is the fault impedance. The most severe voltage dips result from faults with zero fault impedance.

(A) Source Conditions – alternative mode of supply

Source conditions relate to the amount of all connected generation including on-site generation and interconnections with other systems. Supplying a sensitive load from two or more sources reduces the severity of the voltage dip. Should a fault occur in one source, the resultant voltage dip is mitigated to a certain extent by the infeed from the other sources.

(B) System Configuration

Power system configuration is determined by the items of plant (for example, cables, transformers, overhead lines) being in service at the instant of fault. In interconnected networks, the state of normally-open points determines the impedance between the points of fault and observation, which in turn, affects the magnitude of a fault-induced voltage dip. The system configuration may change during the course of a fault, with consequent changes in the profile of the resultant voltage dip (for instance, sequential tripping of circuit breakers at the two ends of a faulted transmission line).

(C) Fault Position

Faults originating from transmission systems cause dips that can be measured tens of kilometres away, while faults on radial distribution systems may have a more localised effect. Faults that occur close to the substation bus bar causes the most severe dips at equipment terminals, typically Z2-class and T-class dips according to the dip window presented in figure 2.5 [8].

(D) Earthing

The general purpose of the earthing system is to provide protection for plant, equipment and personnel against fault conditions. In electrical supply systems, it is therefore common practice to connect the system to ground at suitable points. The tower earthing methods of overhead power lines have a profound influence on dip performance of the system. In addition, faults which involve the flow of earth current may be affected by the presence of transformer neutral earthing impedance.

(E) Weather Patterns

The occurrence of faults and consequent voltage dips is generally higher during severe weather conditions, in particular lightning. Other weather may include wind, snow, rain or ice. Factors such as soil resistivity, vegetation growth and presence of animals/birds are largely dependent on rainfall patterns [10]. These factors have been proven to affect fault performance of overhead lines.

(F) System Protection

The type of protection system used may have a significant impact on the duration and profile of the voltage dip. Unit protection schemes on transmission systems can clear the fault typically within 80ms to 150ms [8]. In applications where impedance protection schemes are employed, zone 2 clearance time is delayed by several hundreds of milliseconds.

On MV and LV systems, definite time lag (DTL) overcurrent schemes and inverse definite minimum time (IDMT) overcurrent protection schemes are extensively used. In DTL protection schemes, currents above a threshold value are detected in one or more phases and interrupted after a preset time. The trip time is the same irrespective of the magnitude of fault current. IDMT protection schemes respond faster to more severe fault currents. Both DTL and IDMT protection schemes may take several seconds to clear a fault.

(H) Loading

Induction and synchronous motors have the largest current demand during and after a short circuit condition [11]. After a voltage dip, electrical motors re-accelerate until pre-event speed is reached. During re-acceleration, the motor takes a larger current with low power factor, which delays voltage recovery.

2.2.4. The Method of Fault Positions

This method is used to calculate the voltage dip characteristics, i.e magnitude and duration at a monitored site. This would be for a number of faults that could be spread throughout the supply networks. The method of fault positions proceeds as follows:

- Determine the area of the power system in which the short-circuit faults will be considered.
- Select the bus bar of interest (examined site). Select a position for a short-circuit fault (bus bar or point on a line). Specify short-circuit fault characteristics (for example, fault type, fault impedance).
- Calculate dip parameters at the monitored site (magnitude and duration) for the selected fault characteristics. The fault positions are selected, first, close to the monitored site and then further away until the entire area of the power system is covered.

The process is then repeated for different combinations of fault positions and short- circuit fault characteristics to cover all cases.

2.2.5. The Method of Critical Distances

This method does not calculate the voltage dip characteristics for a given fault position, but the fault position (distance from the monitored site) for a given voltage dip magnitude and duration at the monitored site. This method of critical distances works as follows:

- Determine the area of the power system in which short-circuits fault will be considered.
- Select a range of dip magnitudes (for example, 0.2pu to 0.8pu in steps of 0.2pu) and a range of dip durations (for example, 200ms to 3s in steps of 200ms).
- Select short-circuit fault characteristics for each set of selected dip parameters at the monitored site (for instance, magnitude of less than 0.2pu and duration of less than 200ms).

Fault characteristics may include the following:

- Type of fault (single-phase, three-phase etc.).
- Fault impedance at the fault position.
- Method of short-circuit fault calculation.

The next step is to select the monitored site and line segments in the power system where short-circuit fault positions are to be calculated, for the given parameters.

- Repeat the calculations for different combinations of dip parameters (at the monitored site) and short-circuit characteristics.

2.2.6 Dip Influence Zones

The voltage dip influence zone encloses the bus bars and line segments where electrical faults may cause a voltage dip that is more severe than a given value at the monitored node. Voltage dip performance is assessed by performing short-circuit analysis in order to determine dip magnitudes at a particular bus bar as a function of short-circuit locations throughout the system.

2.2.7 Voltage Dip Costs

The research work published by Nzimande [9], indicated that customer surveys have recently been the most effective technique to evaluate the costs of voltage dips to the customer. With this technique, customers are requested to estimate their costs due to dip events of varying duration and magnitude. A disturbance such as a voltage dip can cause customer plant to malfunction or shut down after which a time-dependent restart procedure is needed. Some of these restart procedures may take hours to over a day. Most industrial customers track costs related to voltage dips and interruptions.

The tracking of dip-related plant downtime and dips costs is an important tool in quantifying the impact of voltage dips to the customer. Figure 2.6 is an attempt to quantify the financial impact of voltage dips for the paper plant. The vertical axis represents costs as a direct result of voltage dips (downtime costs excluding consequential costs). The horizontal axis represents circuits contributing to dip costs.

Dip costs were obtained from the paper plant customer. The customer records estimated costs associated with each dip event. Dip data was downloaded from the QOS database. The graph of figure 2.6 can be interpreted as follows [9]:

- Benoni DS/Nevis 1 132kV BKR represents dip costs as a result of faults that occurred on the Benoni DS/Nevis 1 132kV overhead line. Nevis 1 132kV circuit

breaker (installed at Benoni DS) is known to have tripped for these faults.

- Delmas/Nevis 2 132kV HV overhead line represents dip costs as a result of faults (resulting in dips at Enstra) at any part of the second 132kV line between Delmas DS and Nevis transmission station.
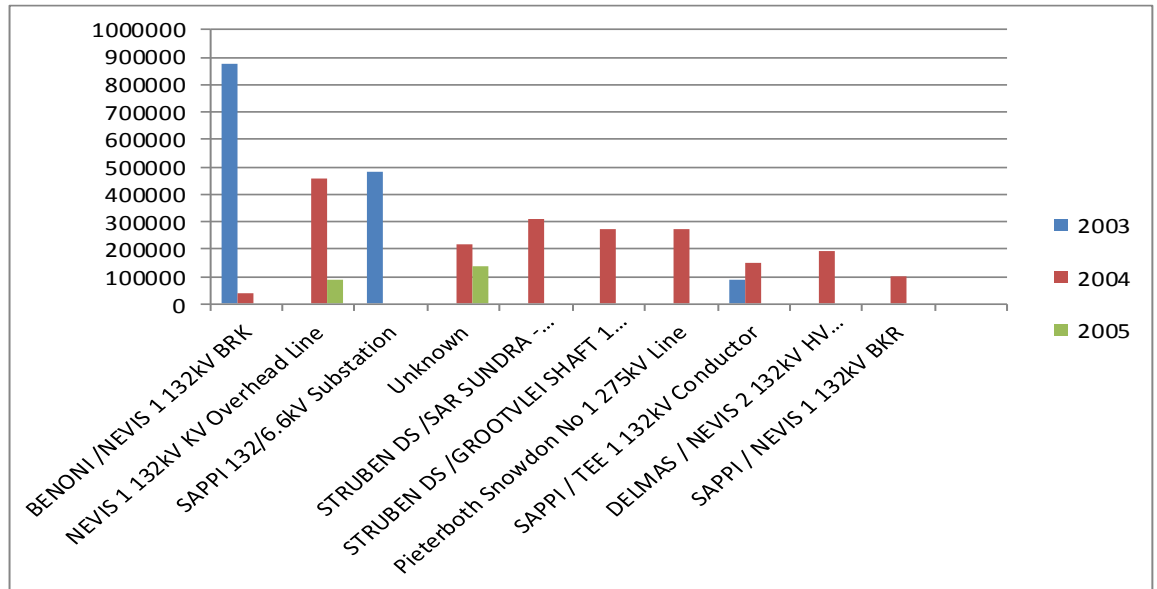
Figure 2.6 Circuits contributing to dip costs – paper plant
Reproduced from reference [9]

Figure 2.6 suggests that faults on the Benoni/Nevis 1 132kV overhead line and SAPPI substation resulted in the highest dip-related financial losses to the paper customer. The highest financial loss was experienced in 2003 [9].   Figure 2.6 enables the customer to identify circuits contributing to dip-related downtime costs. Based on this information, the utility is able to make informed dip performance investment decisions while on the other hand, the customer may decide to investigate other dip mitigation options.

Figure 2.7 shows costs of voltage dips against dip cause categories. Dip data was obtained from Eskom's QOS database, while dip costs were obtained from the customer. The graph was generated using Excel. The vertical axis represents costs as a direct result of voltage dips. The horizontal axis represents dip cause categories.
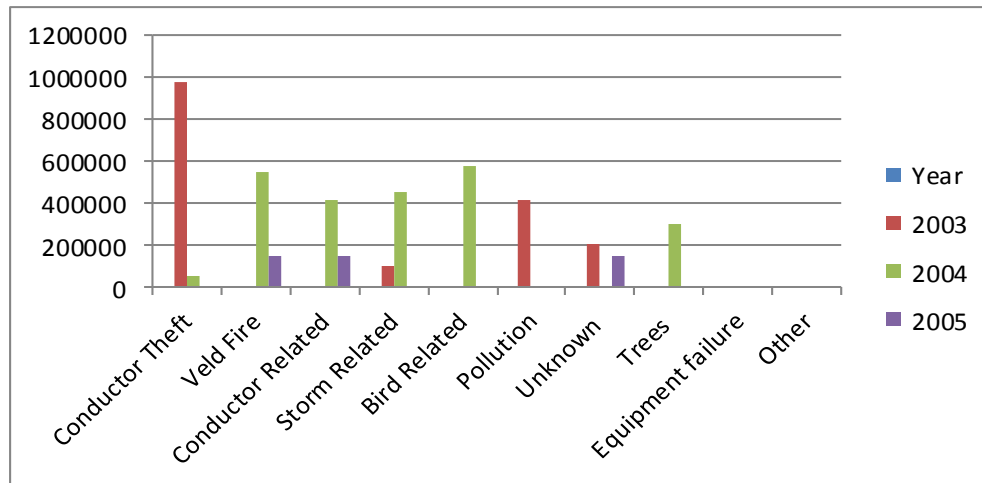
Figure 2.7 Causes of dips and the associated costs – paper plant

Reproduced from reference [9]

Figure 2.7 suggests that dips due to conductor theft incidents resulted in the highest financial losses to the customer. The lowest level of dip-related costs is approximately fifty thousand rands, which suggests that all dip causes categories have a remarkable financial impact on the customer.

Some of the dips are caused by power network tripping due to lightning conditions as discussed in section 2.1. A number of measures can be installed that can prevent these dips. Lightning surge arrestors is one of these measures and is explored in this thesis.

2.3 EHVDC Systems

This section would focus on a brief overview of the EHVDC technology with special emphasis on the comparison of EHVDC and HVAC transmission systems, EHVDC configurations, EHVDC technologies: LCC and VSC, and their advantages and shortcomings. This section then proceeds to discuss the various earthing configurations of the systems and also explores the calculations of resistivity of the multi-layer soil, the step voltages and touching potentials.

2.3.1 Overview of EHVDC Transmission Systems

2.3.1.1 EHVDC Technology

An EHVDC transmission system is a technology that utilises direct current to transmit large amounts of electrical power over long distances efficiently, in contrast with the HVAC transmission networks. The transmission path maybe either overhead lines or underground/submarine cables.

.

A EHVDC transmission network is based on direct current and forms an asynchronous link between the sending and receiving ends of the system. A EHVDC network consists of two converter stations, which are linked by a DC overhead line (OHL) or cable. At the sending end, the AC power is rectified to DC (first converter station). The DC power is transmitted through a DC OHL or cable. At the second convertor station, which is located at the receiving end, the power is inverted to AC. Fig 2.8 shows the main components of an EHVDC system. [12]
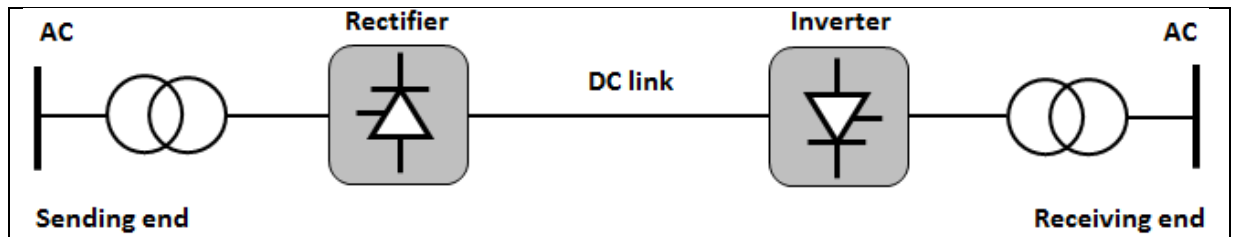
Figure 2.8 EHVDC Systems
Reproduced from reference [12]

The EHVDC technology was developed during the 1930s by ASEA, the Swedish electrical conglomerate. In the 1950s, the research into mercury-arc technology begun, this led to the implementation of the work of Gotland (Sweden) and Sweden via a submarine cable. After a few years, EHVDC transmission systems based LCCs employing thyristor switches commercially known as EHVDC Classic were implemented. However, the technical restriction of Line Commutated Convertors (LCC) limits its use in some transmission and distribution applications. Rapid research and hence development in the field of self-commutated power electronic switches, eg the insulated gate bipolar transistor (IGBT) led to the implementation of EHVDC transmission systems based on Voltage Source Converters (VSC). The VSC technology overcomes the shortcomings of LCC and it is increasingly used more often in transmission and distribution systems. The VSC technology is readily available as EHVDC light and plus systems are been developed by ABB and Siemens respectively.

2.3.1.2 Comparison of EHVDC and HVAC Transmission Systems

In a study, undertaken by [13], showed that the choice between an HVAC and EHVDC system is mainly based on economic and technical factors such as transmission distance and medium; overhead lines or underground/ submarine cable. Over long distance EHVDC transmission is the preferred bulk power transmission system than HVAC transmission system. However, it should be noted that this is only true for distances above a certain distance called the breakeven distance as shown in Figure 2.9.

The breakeven distance for EHVDC systems is in the region of 400-700km and 25-50km, respectively. [13]
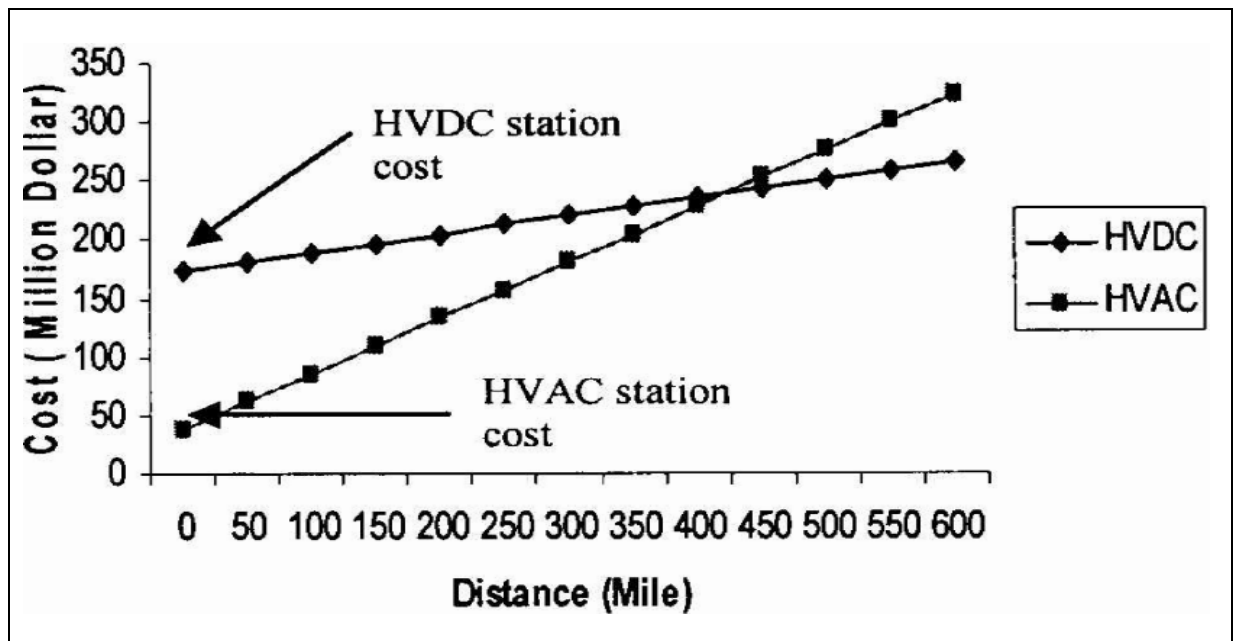
Figure 2.9 Comparison between HVAC and EHVDC systems
Reproduced from reference [13]

2.3.1.3. Advantages of EHVDC transmission systems over HVAC transmission systems

a)   Investment costs:

In accounting for the capital cost for the DC alternative, one should include the capital cost for the converter terminals, AC input/output equipment, filters, the interconnecting transmission line cost. Similarly the capital cost for the step up or step-down transformer, the overhead line, light load compensation if required, reactive power compensation, circuit breaker, building should be evaluated for the AC alternative. Both cases need to consider the control system cost.

The HVAC technology requires three conductors, one for each phase while the EHVDC technology only requires two conductors; this significantly cuts down on the investment cost. The ground return conductor on the EHVDC system can be used for power transfer. The line construction is simpler as well.

b)   Supporting towers:

HVAC transmission systems are associated with massive towers while the EHVDC transmission system requires smaller supporting towers, which reduces the environment impacts. Hence it is often easier to obtain the right-of-way for DC overhead lines and cables.

c) Electromagnetic interferences:

The electric current that flows through a conductor and the distance from the conductor determines the magnetic field around a conductor. The magnetic flux density is inversely
proportional to the distance from the conductor. The Earth's natural magnetic field is 40 µT, while for 450 kV DC transmission line the flux density is about 25 µT [14].

Electric field is created by the potential difference between the overhead conductor, earth and the space charge clouds produced by conductor corona. The space directly under the conductor has the highest electric field, which can be approximately 20 kV/m for a 450 kV transmission line [15]. Weather, seasonal variations and relative humidity can result in the electric field changing. DC has less electric field problems than that of AC because of the lack of steady-state displacement current; thus EHVDC require much less right-of way (ROW) than horizontal AC configuration and less height than the AC delta configuration of HVAC transmission of comparable rating [16].

Step voltage, which is the potential difference between land electrode and line conductor, can result in shock current. Typical the human body resistance is about 1000 ohms. Hence a limit value of 5 mA current can flow through the human body safely and DC has the less electric current density, which is 70 nA/m2 for a 450 kV transmission line [16].

d) Transmission losses:

Considering the fact that there is no skin and proximity effect associated with EHVDC technology, the overall system losses are lower in EHVDC than in HVAC transmission systems.

e) Interconnection of asynchronous networks:

The EHVDC technology makes it possible to interconnect asynchronous networks; power grids operating at difference frequencies. Moreover, the EHVDC system fully decouples the interconnected AC systems and hence prevents the propagation of fault from one AC network to another.

2.3.1.4. Drawbacks of EHVDC transmission systems

a) Inability to use power transformers:

Although the EHVDC technology can be said to be more advantageous and attractive for long distance power transfer, it is impossible to use transformers to alter the voltage level along the transmission path unlike in HVAC technology.

b) **Cost of converter stations:**

The EHVDC system converter stations are more expensive compared to HVAC system converter stations. This is due to the additional AC/DC converter in each substation. Furthermore the convertors require much reactive power and to the harmonic they generate, filters are needed. This increases the cost of the convertor stations [13].

2.3.1.5 EHVDC Transmission System Configurations

EHVDC Transmission links can be categorised into different configurations. This depends on the arrangement of the converter stations, namely: mono-polar, bipolar, multi-terminal and back-to back EHVDC system configurations.

2.3.1.5.1 Mono-polar EHVDC System Configuration

This configuration is made up of two converters connected together using a single pole as shown in figure 2.10. A ground or metallic path can be used as a return path depending on the application.
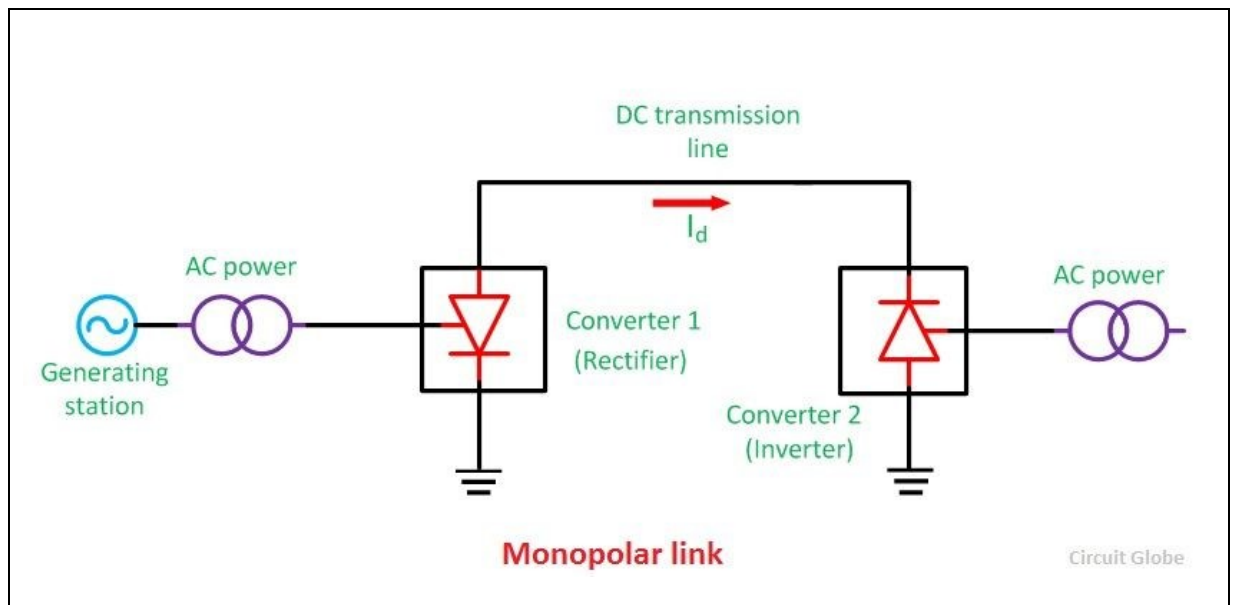
Figure 2.10 Mono-pole EHVDC systems
Reproduced from reference [17]

Although the use of ground return causes environmental concerns due to the use of electrodes and continuous flow of ground current, the use of one high-voltage conductor reduces the cost and transmission losses. Conversely, the use of metallic return means that there is no ground current and the return cable is usually not fully insulated; hence reducing the expenditure on the dc cables. This configuration is applied in most submarine EHVDC transmission systems.

2.3.1.5.2 Bipolar EHVDC System Configuration

In this configuration, two conductors; negative and positive polarity, are used to connect the converter stations. Figure 2.11 shows the bipolar EHVDC system configuration.
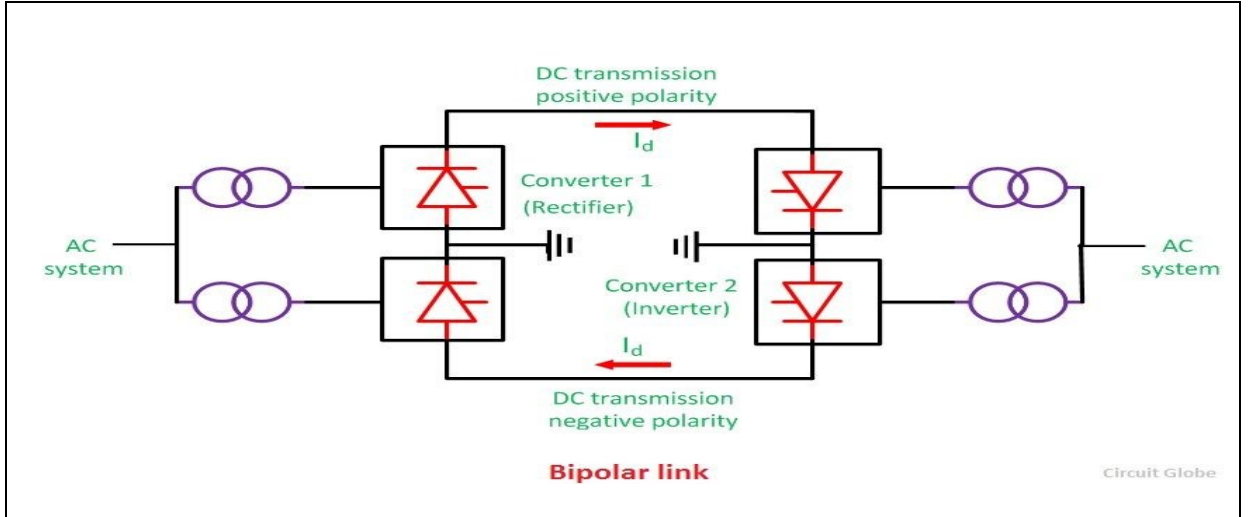
Figure 2.11 Bipolar EHVDC system configuration
Reproduced from reference [17]

A bipolar system is made up of two mono-polar systems. If the neutral point is grounded on both sides, it is possible to use one pole independently making it possible to transmit power even if one pole is out of service.

2.3.1.5.3 EHVDC System Back-to-Back Configuration

The converter stations in this configuration are located at the same site as shown in Figure 2.12. Therefore, the power is not transmitted over long distances.
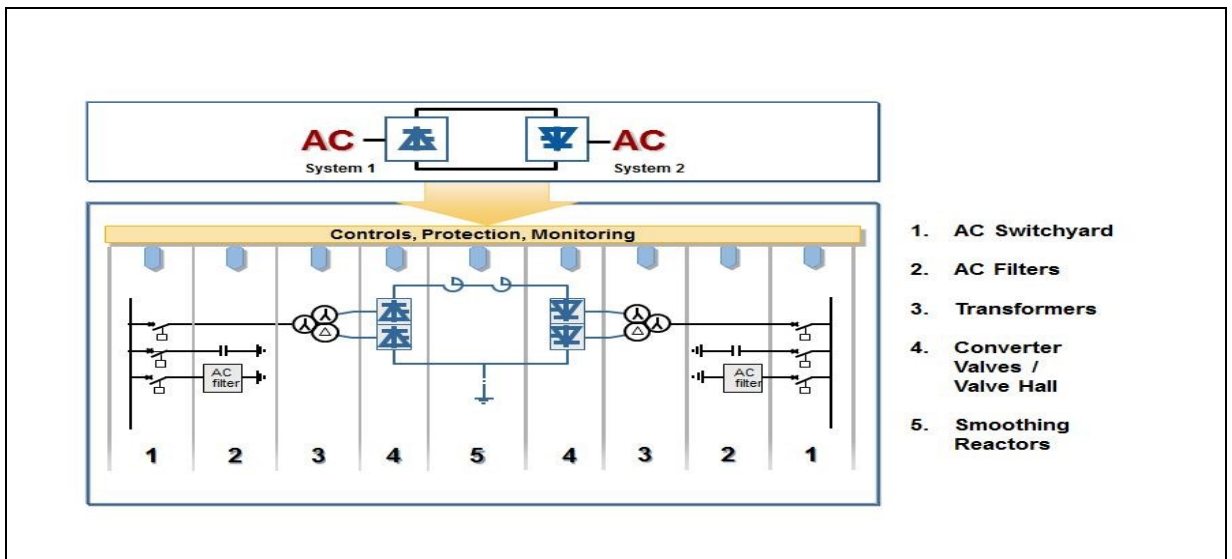
Figure 2.12 EHVDC system back-to-back configuration
Reproduced from Reference [18]

This configuration can be monopolar or bipolar and it is mainly used to interconnect asynchronous systems

2.3.1.5.4 Multi-terminal EHVDC Systems

Multi-terminal EHVDC (MTDC) configurations are made up of three or more converter stations; some converters operating as rectifiers and others operating as inverters. An MTDC network can be of a series or a parallel type. A parallel MTDC network can be further classified to be either of a radial type or a mesh type. Figure 2.13 (a), (b) and (c) shows the series, parallel: radial type and parallel: mesh type multi-terminal DC configurations, respectively.
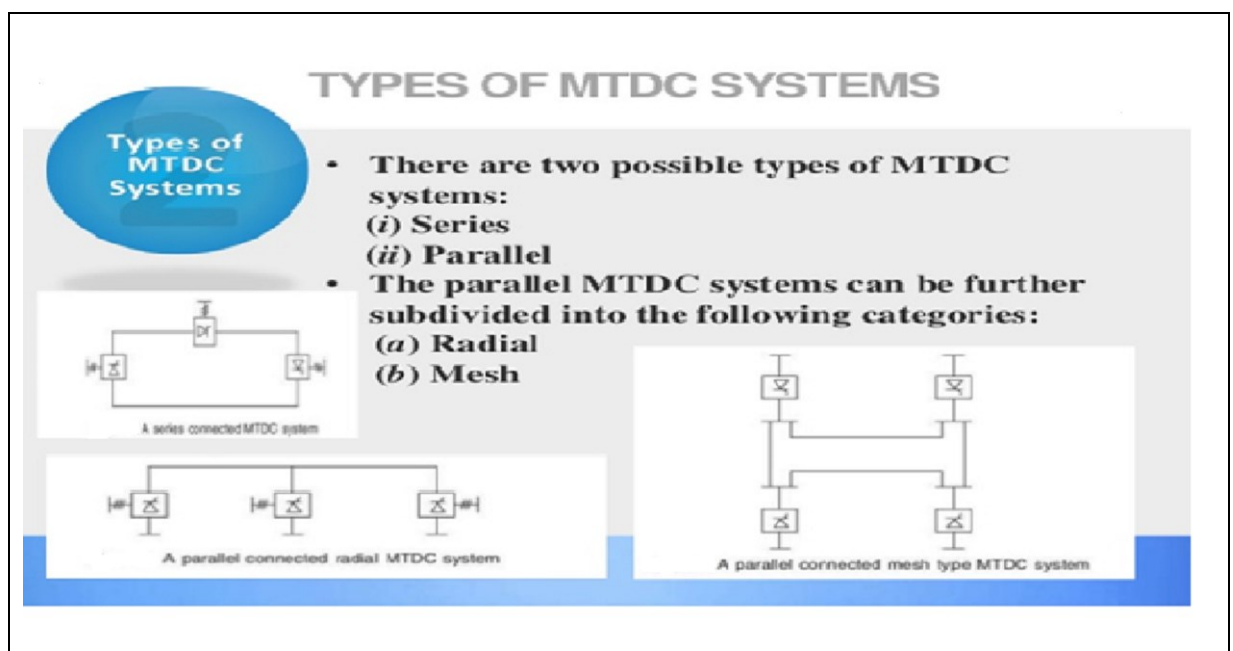
Figure 2.13 Multi-terminal EHVDC system configurations
Reproduced from Reference [19]

When the series and parallel MTDC configurations are combined, they form a hybrid MTDC system. The series and parallel MTDC systems are considered to be cost effective, reliable and are associated with less conversion losses compared to the point-to-point connections. However, the hybrid configuration is not justified from an economic point of view due to the higher number of converter stations.

2.3.2. Soil Resistivity

Soil resistivity, which is expressed in Ohm-metres, maybe defined as the resistance of a cube of soil of 1 m size measured between any two opposite faces. It is one of the main factors in determining the resistance of the charging electrode and the depth level it should be planted to obtain low resistance.
Soil resistivity is a measure of the soils ability to prevent the conduction of the electrical current. Soils conditions that have high moisture contents or increased electrolyte concentration can lower the soil

resistivity. A high electrical resistivity of the soil may increase the galvanic corrosion rate of metallic structures in contact with the soil. The opposite can also be true.

The principle aim of any earthing electrical systems is to establish a common reference potential for systems such as electrical conduits, building structure, power systems, plant steelwork, able ladders & trays and the instrumentation system. This objective requires the resistance connection to earth to be as low as practical possible. The following factors may a key role in achieving this value.

Type of earth (eg, clay, loam, sandstone, granite).
Stratification   ; soil types broken into different layers (eg, loam backfill on a clay base).
Moisture content; As the moisture content is increased the resistivity may fall rapidly,
Temperature : Temperatures above freezing the effect on soil resistivity is practically negligible. Chemical composition and concentration of dissolved salt.

Local surface resistivity variations caused by moisture and weathering has a similar effect on resistivity measurement as the presence of metal and concrete pipes, large slabs, tanks, cable ducts, rail tracks, metal pipes and rugged topography.

Table 2.3 Typical values of soil resistivity of various soil types

Type of soil	Typical Resistivity (ohm/m)
Clay	40
Sand Mix and Clay	100
Slate, Shale and sandstone	120
Mud, Loam and Peat	150
Sand	2000

The soil resistivity value will assist in establishing the conductivity of the ground. This will assist in determining the soil capability to create a simple pathway for the fault or a malfunction in the electrical system. High resistance is known as bad conductor and low resistance is good conductor.

The following equation illustrates that the resistance (R) depends on the resistivity of the conductor.

$$R = \rho \frac{L}{A}$$
(1)

Where ρ = Conductor resistivity

L = Conductor length

A = Cross section area

There are three factors that affect soil resistivity. These are

1.   The number of layers

2.   The refection factor between layers

3.   Each layer thickness

2.3.2.1 Double layer cases of soil resistivity

Soil resistivity can be made up of double layer soil conditions. Here the first layer has resistivity p_1, thickness H and the second layer has soil resistivity p_2 with infinite thickness. Here the ground electrode rods penetrate into the more conductive lower layer. In the case $p_1 > p_2$, the apparent soil resistivity P_a, maybe calculated by the relationship.

$$P_a = I \frac{p_1 p_2}{p_2(H-h) + p_1(I+h-H)} \qquad (2)$$

Where I = average rod length

p_1 and p_2 are the soil resistivity of the upper and bottom layer

H is the thickness of the upper layer

Figure 2.14 shows the relationship between the upper and lower levels and the thickness of the upper layer.
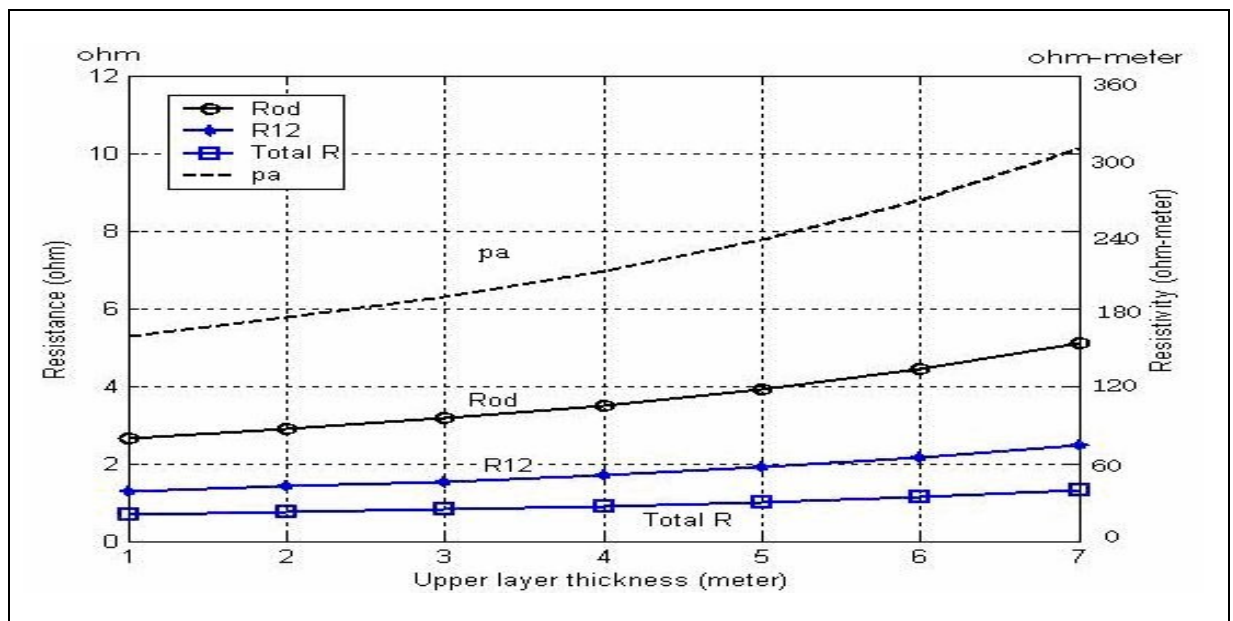
Figure 2.14 : Soil Resistivity vs Upper Layer Soil Thickness
Reproduced from reference [20]

Should there be multi layers (greater than two layers), one then combines the lower layers resulting in a two layer equivalent model. This can be attributed due to the surface potential been closely related to the resistivity of the upper layer, while the grid resistance, which is mainly effected by the deeper layers, is not usually adversely affected by the simplification. Furthermore the top soil layer is subjected to higher current densities and hence would require more accurate modelling.

The reflection factor (K) is given by

$$K = \frac{p_2 - p_1}{p_2 + p_1}$$ (3)

There a number of ways of improving soil resistivity for the different types of soil. Chemical additives such as earth gel may be used. Soil resistance varies from one location to another and fluctuates during the wet and dry seasons. The following factors affect soil resistivity. [20], [21]:

- Closeness of packing and pressure
- Dissolved salts
- Minerals
- Moisture
- Soil Type

Should the soil resistivity be high, more electrodes required to achieve the required earth resistance value. The thickness of the soil layer also play an important role in determining the soil resistivity. Research has shown that the soil environment may be modelled as an upper and a more conductive lower layer [20], with the electrode or the electrode been buried in the upper layer. To determine the the soil resistivity for multi-layer and depth of soil would required detailed modelling.

As mention above an important requirement for low resistance is moisture. When defining earthing system evaluation, it is more suitable to use the two layer model. This standard two-layer model is sufficient for conducting a suitable design according to IEEE 80 [22]. Figure 2.15 shows the Wenner Method, which has been found to be the most efficient method to determine the soil resistivity value [13] [22].

a)   **Wenner Method**
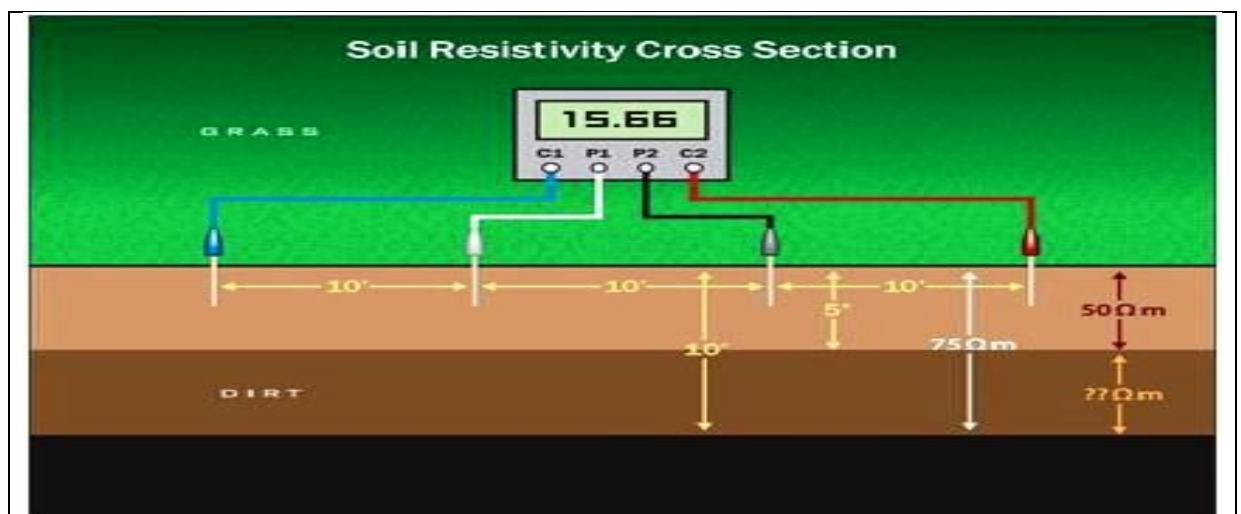
Figure 2.15 Wenner Four Electrode Method
Reproduced from Reference [23]

Below are the various steps performed during Wenner Method

- On the centre of the assessment location, placed the soil resistivity measure equipment
- Install the two potential electrodes on the left and right side point of view. This would depend on the distance test needed. Based on the soil conditions, the electrode can be planted up to 10 cm in the ground.
- The electrodes cables should be connected with the soil resistivity measuring equipment's.
- Power the electrode from soil resistance measuring equipment.
- Ensure that no human contact is made with the energised electrode.
- The soil resistivity measuring equipment's LCD or monitor will display the value of the soil resistivity.

a) **Schlumberger Array**

The properties of Schlumberger array are as follows:

- Since the outer electrodes are moved 4 or 5 times for each move of the inner electrodes, economy of manpower is gained with the Schlumberger array
- The effect of lateral variation on test results is reduces due to the reduction in the number of electrode moves.
- By using the reciprocity theorem with the Schlumberger array when contact resistance is a problem, considerable time saving can be achieved.
- Contact resistance normally affects the current electrodes more than the potential electrodes, hence the inner fixed pair may be used as the current electrodes. This configuration called the 'Inverse Schlumberger Array'. It should be noted that use of the inverse Schlumberger array can increases personal safety when a large current is injected.
- Should the magnitude of the current be large, thicker current cables may be needed. The inverse schlumberger array decreases the length of the bulkier cable and more time is required to move the electrodes.
- For a 0.5m inner spacing, the minimum spacing accessible is in the order of 10 m. This necessitates the use of the Wenner configuration for smaller spacing
- When using Schlumberger arrays, reduced voltage readings are attained.

b) **Driven Rod Method**

This method or Three Pin or Fall-of-Potential Method are generally used on overhead transmission line structure earths or on places that have with difficult terrain. This is because of

the restricted measurement area, the insubstantial penetration that is obtained in practical situations and the imprecision confronted in 2 layer soil situations.

2.3.2.2 Benefits of Testing Soil Resistivity

- A properly designed and installed system would adequately fulfil the key role in obtaining and sustaining a professional and well-protected facility.
- This would ensure that hard-line business competition companies stay entirely reliable in the fast paced competitive business world.
- The grounding system is an important part of the planned site and must be treated equally as all the other critical components. To achieve this conventional methods and/or an enhanced system with electrolytic electrodes with carbon backfill and checking soil resistivity must be undertaken.

The resistivity in any given locality would change over time. The measured resistivity is a estimation, pertaining to the existing conditions at the instant of measurement. The two reasons for the variation are natural causes and human intervention. Some examples of the natural causes include formation of perma frost, seasonal variations of temperature and changes in the availability of ground water.

Pollution, chemical treatment of soil and installation of large underground structure are some of the human intervention causes.

Information on resistivity is gathered and stored in data banks. Data banks are maintained by universities and government agencies also store other pertinent geological data such as porosity, mineral content, moisture, etc.

Research work undertaken by Malanda [24] shows that the soil resistivity tended to saturate as the depth increased. Furthermore, the soil resistivity for dry soil for certain soil types is at least doubles that of the wet soil. Also as the depth increases the resistance of the soil tend to migrate toward each other.

2.3.3. Earth Electrode

There are a number of configurations available to design an earth electrode. The simplest configurations include a single horizontal straight wire, the single driven vertical rod and horizontal disc. Other arrangements such as wires connected in star formation, wires in the form of a square loop

and a group of driven rods are more complicated. For these simple arrangements, there are approximate analytical solutions. [25], [26].

Some research has been conducted to consider the effects of earth nonhomogeneity. It must be noted that the analytical analysis is complicated and the solution is only possible with very simple and well-defined configurations. The earth resistance calculation was initially worked on by H.B. Dwight, in his paper titled 'Calculation of Resistance to Ground' [25]. Erling Sunde, [26], who authored a text titled 'Earth Conduction Effects in Transmission systems' also tackled the calculation of earth resistance. The text 'Earth Resistances' [27] authored by G.F. Tagg, has a collection of references and information etc. This, representing the efforts of earlier researchers, including Sunde and Dwight.

2.3.4. Type of electrodes

EHVDC system requirements differ from one system to another. This is due to the large variations in geographical, geophysical and technical properties of electrode sites. This has resulted in a variety of configuration and electrode shapes been developed. Generally, complete symmetrical shapes are seldom realized as some degree of adaptation to the site is always needed.

2.3.4.1. Land Electrodes

Depending on the depth of burial and the configurations, land electrodes are categorized into three types as described below.

a). Shallow horizontal electrodes

Generally these are installed in the ground within trenches with coke ground beds. This is shown in Figure 2.16 [28]. The contact between the earth and electrode elements needs to be as uniform as possible to prevent non-uniform current sharing.

The electrode elements that are in direct contact with water will carry more current initially than those that are not in contact or only partially in contact with water. Some examples are: electrodes in shallow earth, shoreline, or even in deep vertical construction. More corrosion or electroplating of earth materials will be experienced by those elements leading to eventual overloading of other elements **as** the current distribution between elements changes.
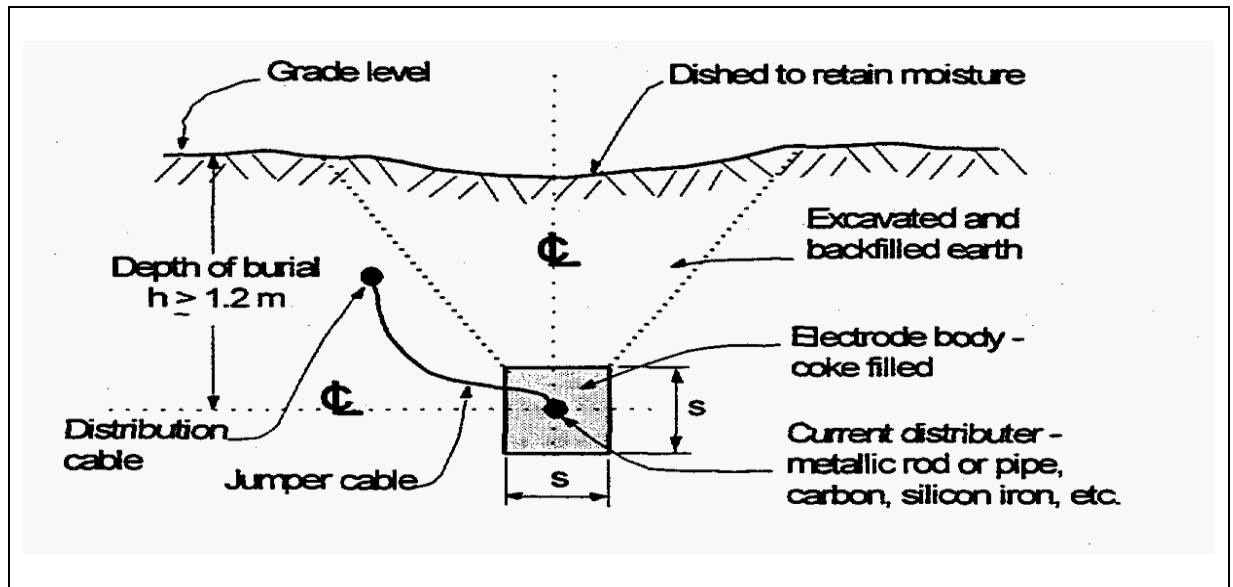
Figure 2.16 Shallow Horizontal Electrode
Reproduced from reference [28]

b). Horizontal (Linear, Ring, Star)

The horizontal electrodes are usually set at or very near the ground surface. They may be configured in many geometric forms such as linear rings, double ring and stars, (see Figure 2.17). Depending on the site constraints and the desired effect that is to be accomplished other horizontal configuration can be considered.

The horizontal electrodes are generally placed in a dug trench below or in close proximity to the ground water table. These electrodes are surrounded by coke breeze. The desired current densities and step potential determine the size of the horizontal array. The size of the tract of land may also determine the configuration although this is usually a secondary consideration.

Due to uniform current distribution, a circular ring configuration is preferred, although irregularly shaped or linear electrodes can also be made. One may branch a linear electrode in order to adjust to the site and to utilise the site area in an optimal way. These electrodes type (linear and branched) need a bigger volume of coke and also a larger metallic element size in the outer ends. This is due to increased current density.
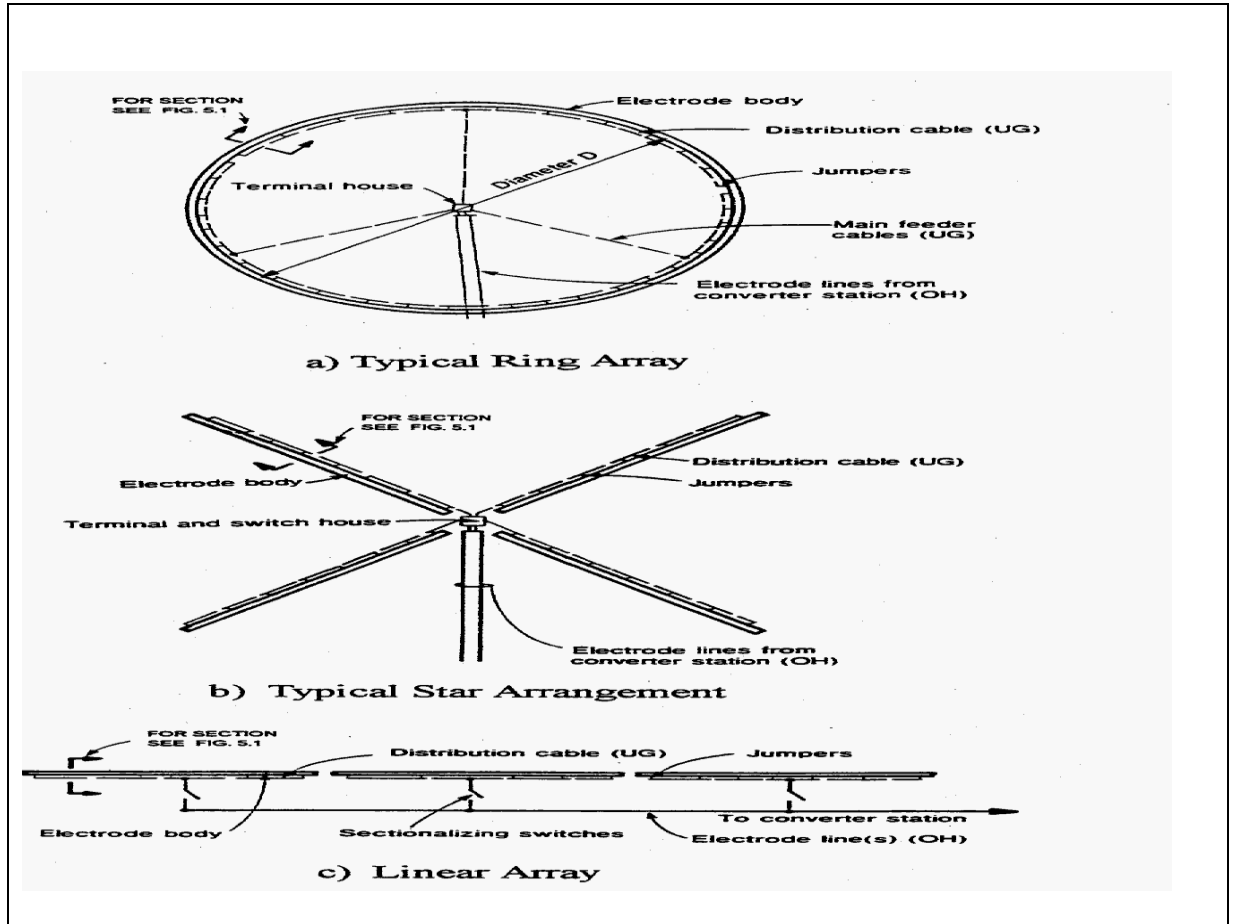
Figure 2.17 Horizontal Electrode Arrangement (Linear, Ring, Star)
Reproduced from reference [28]

c). **Vertical electrodes**

These types of electrodes have been installed in the ground upto 200m deep. At depths of this magnitude layers of lower resistivity and higher moisture content are found. Also the risk of interference at the site area as shown in Figure 2.18 is decreased. The vertical elements may be constructed in several geometric patterns such as circular, rectangular, linear and grid. This is similar as the shallow electrodes. Coke is normally used to backfill the electrode wells, see Figure 2.18. In dry conditions a mixture of graphite and bitumen may be utilised to make contact to low resistivity structures such as graphite deposits.
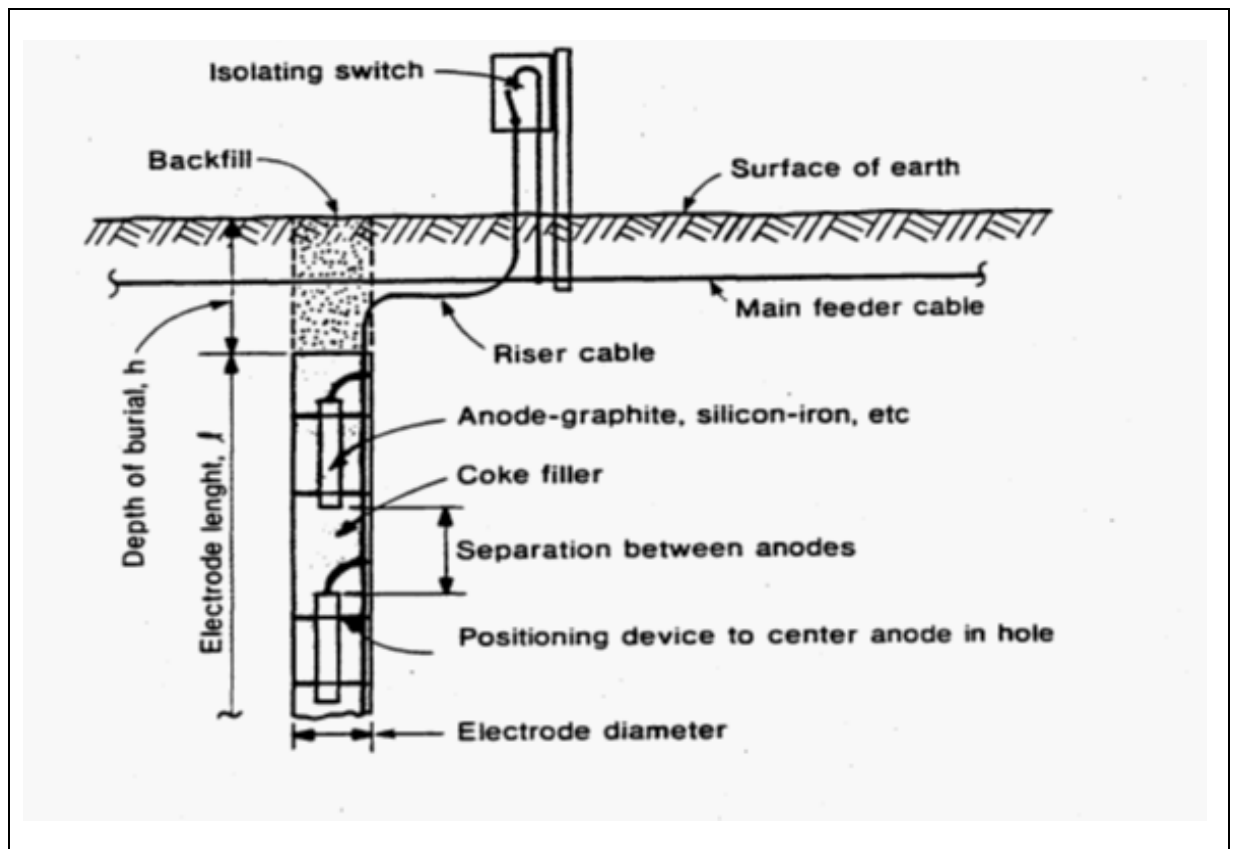
Figure 2.18 Typical Vertical Configuration
Reproduced from reference [28]

Vertical arrays are those installed in wells or boreholes and their selection is usually determined by the terrain, which would include ground water considerations and/or any land restrictions that might exist [28]. Typically a vertical arrangement would have several arrays of electrode elements, which can be suspended in wells or boreholes and surrounded by compacted coke breeze filler. An example of the vertical array is the Lisbon electrode in northern New Hampshire. The number of elements per borehole/well will fluctuate depending upon the layout and other physical and chemical aspect of the site. The number of electrode wells is determined by the contact area required to limit the current densities to acceptable levels for a given electrode current.

d). Deep well electrode – This technologies would be applicable provided the geological conditions indicate that there is a soil structure in which the upper layers have relatively high resistivity, but the lower or deeper soil structure has low to very low resistivity. The current drilling technology can result that wells can be drilled to a depth of 1000m. At these deeps, the low resistivity would result in the rapid current dispersion deep underground. Furthermore it would reduce electric potential and gradients at the surface. Hence the risk of corrosion due to exchange of current between the soil and buried facilities is reduced.

Normally 3 to 5 deep-well electrodes would be arranged in either a linear or polygonal configuration. The current carry capacity of individual wells over 1000m deep can be up to 1000A. Wells arranged in a regular polygonal shape would assist to reduce the imbalance current between the deep well electrodes. However, if the soil resistivity is not similar for each well, the overall effect may be reduced. Feeder cables may be utilised to distribute the current to the metallic electrode elements at different well depths.

One can use petroleum coke to provide the electrical interface between the metallic elements and the soil. This would reduce the corrosion of the metallic elements and reduce the current density at the soil-electrode interface. The gas, which can be produced by heat or electrolysis, may prevent current from flowing through the coke and should to be vented using a perforated pipe. This pipe should run the full length of the electrode.

2.3.5. Selection of electrode type [29]

It is crucial to selection the correct ground electrode type during the design stage. This process can be complicated. In general, many electrode types should be placed close to the converter station. The different options needs to be technical and economic feasible and the most suited chosen option must also be safe, reliable and environmentally friendly. The designer in selecting the electrode type, should consider the following

- How far apart the converter station and the prospective electrode site would be.
- Soil resistivity in the vicinity of the converter station.
- The electrode operational duties.
- Any permitted operating duration limitations.
- Philosophy regarding operations and maintenance.
- Expected cost.
- Any land use limitations.
- Safety
- The number of infrastructure elements that may be adversely affected

For converter stations are placed close to the sea and should the expected electrode operational duty is high or continuous, then the preferred technical option is to utilise the sea or beach electrodes. This is as a result of the low resistivity of seawater when compared to soil. A land electrode would be required, should the distance between the converter station and the sea be long. Should the geological conditions consist mainly of high resistivity bedrock and no part of the lower strata consists of some

type of low resistivity material, then the only possible option would be to construct a long electrode line to the seashore.

In some countries there may be local regulations or laws which could restrict the maximum permitted duration or Ampere Hours of electrode operation. This could be one possible differentiating factor in favour of land electrodes. For electrodes that have a low duty and have no requirement for continuous or long-time operation with high ground current, or have the operational time legal restricted, land electrodes may be preferred due to lower cost.

Should the surface soil is not suitable for shallow electrodes on land than there is merit is using the vertical types of land electrodes. This is because the active part of the vertical electrode would be at a depth below that of the ground water table and/or in a layer of moist soil. Normally the vertical borehole or well is drilled into the ground to take advantage of the low resistivity soil or brackish water conditions. The depth of the well will cause the hydraulic pressure of water increases (greater depth greater pressure) and hence the risk of electro-osmosis decreases. This causes boiling point of water to increases, which allows a higher current density to be used when compared with a horizontal type of electrode placed only a few meters down in the ground. Generally a vertical electrode will result in lower surface potential gradients and usually the resistance of the electrode to remote earth would be lower for the same length of active element. Unfortuntely the drilling and casing cost is considerably higher than the digging costs for shallow electrodes.

2.3.6 Electrode Design Aspects [29]

2.3.6.1 General Design Consideration

The ground electrode has to be the path to transfer the EHVDC system current from the insulated or metallic overhead conductor into ground. Furthermore, the purpose of the ground electrode should not be a protective ground for the EHVDC scheme or for any other equipment. The following aspects should be addressed by the ground electrode design:

- Safety
- Physical design constraints and criteria.
- Future environmental impact
- Potential influence of electrode operation on other facilities
- Physical constraints of building an electrode at the site

a) Safety Requirements for Animals and Humans

The safety requirements of a ground electrode can be summarized in a single objective as follows: "The design and hence operation of the electrodes must not endanger or create an unsafe condition for people or animals either in publicly accessible, within a controlled area".

There are two categories into which the operational conditions considered for safety can fall into. These are:

a) Continuous conditions which can occur for a duration of 10 seconds or longer

b) transient conditions which can last for a duration of less than 10 seconds. Should a DC transient line fault occur, the overcurrent protection should clear the fault in approximately 50 ms. which will reduce the fault current to zero.

The tolerance of the human body to dc current is time dependent as shown in Table 2.4.

Table 2.4 Continuous Exposure Limit (5mA) Transient Exposure Limit (30mA)

BODILY EFFECT	MEN/WOMEN	DIRECT CURRENT (DC)	60 HZ AC	100 KHZ AC
Slight sensation felt at hand(s)				
	Men	1.0 mA	0.4 mA	7 mA
	Women	0.6 mA	0.3 mA	5 mA
Threshold of pain				
	Men	5.2 mA	1.1 mA	12 mA
	Women	3.5 mA	0.7 mA	8 mA
Painful, but voluntary muscle control maintained				
	Men	62 mA	9 mA	55 mA
	Women	41 mA	6 mA	37 mA
Painful, unable to let go of wires				
	Men	76 mA	16 mA	75 mA
	Women	60 mA	15 mA	63 mA
Sever pain, difficulty breathing				
	Men	90 mA	23 mA	94 mA
	Women	60 mA	15 mA	63 mA
Possible heart fibrilation after 3 seconds				
	Men and Women		500 mA	100 mA

Reproduced from [30]

The human body tolerance levels of current are those that above the threshold of perception but are those currents that are well below the current that would result in fibrillation of the heart and also below that of the let-go current level. These current magnitudes may cause some irritation to the person, but would not be high enough to endanger life or cause injury. Hence by using the acceptable levels of dc current within the body the safety criteria for electrodes can are defined. An exception to this the maximum transient electrode fault current. This has a short duration and may be characterized as an ac current or pulse current superimposed on a dc level.

Substantial research and testing has been done to determine that sensitivity of adults to dc current. However there is very little data concerning minors, i.e children. In women the threshold of perception and let-go currents are lower compared to men. Therefore for children the threshold of perception and let-go currents should be lower than that for women [31]. In most cases 6mA is the acceptable level of current that a body threshold used to design the electrode.

b)   Safety Metrics and Criteria

Humans and animals safety at any electrode site is of concern primarily within the area where the associated surface potential gradients resulting from electrode operation and surface potential rise are high. This is applicable to areas where there are bodies of water and the currents that can enter the human and animals are present in the water.

Safety can be defined in terms of the following quantities (using the definitions from IEEE Std. 80 [32] and modifying them to reflect the special character and operating characteristics of EHVDC ground electrodes).

- Touch Voltage
- Step Voltage
- Transferred Voltage or Transferred Potential
- Potential gradient in water
- Metal-to-Metal Touch Voltage

When considering the safety of the earth electrode installation, the above quantities must be addressed. Note: As discussed previously the acceptable values within the human and animal bodies are based on acceptable levels of currents and is not based on voltage.

However as one can easily calculate and verify voltages or potential gradients by measurements it is usually desirable to be able to work with these parameter for convenience in electrode design. The safe or acceptable voltages and potential gradients values can be ascertained by working backwards from the acceptable levels of current in the body using assumed conservative values of contact resistance and body resistance.

From the criteria listed, only the transferred potential and voltage gradient in water can be extended for significant distances into publicly accessible areas. It is advised that the areas of the earth electrode sites be located behind locked fences as the general public cannot be protected from the effects of the step voltages approaching the limits.

Assumptions are required, when the acceptable voltage criteria for electrode design is calculated, with respect to resistance of the body and the contact resistance between the body and the earth or energized object. In this regard there are some differences between IEC 60479 and IEEE 80. However the IEEE calculation methodology is simpler to apply for body resistance and contact resistances in series with the body resistance as follows:

- The resistance between the hand and foot or skin contact to metallic structures should be zero.
- The resistance of the glove and shoe resistances must be zero.
- The human body resistance can be approximated by a single resistance value of 1000 Ω. This value is equal to the resistance of a human body from hand-to-hand, hand-to-feet or from one foot to the other foot. (i.e. RB = 1000 Ω)
- In determining the contact resistance of a foot to ground, one may make the assumption of a metallic disc or a circular plate with a radius "b" of 0.08 m representing the foot. The resistance from each foot to ground (Rf) is given as

$$Rf = \rho s / 4b = 3.125 * \rho s \qquad (4)$$

These assumptions are consistent with that made in IEEE Std. 80 relating to safety in substation design.

Animals have a different body resistance value compared to humans. The tolerable levels of current may also be different for the various animal species. However, the calculation methods are exactly the same.

The following nomenclature is used in this section:

IBc – body current in continuous conditions (A)

IBt – body current in transient conditions (A)

RB – body resistance (Ω)

Rf – contact resistance between foot and soil (Ω)

Es – step voltage (V)

Esc – step voltage in continuous conditions (V)

Est – step voltage in transient conditions (V)

Et – touch voltage (V)

Etc – touch voltage in continuous conditions (V)

Ett - touch voltage in transient conditions (V)

Ewc – continuous voltage in water (V)

Ewt –voltage in water under transient conditions (V)

ρs – surface resistivity at the electrode site (Ωm)

Generally the distances used in determining acceptable conditions for step, touch, metal to metal and water safety are 1m, 1.25m, 2m and 2m respectively. This is illustrated in figure 2.19.
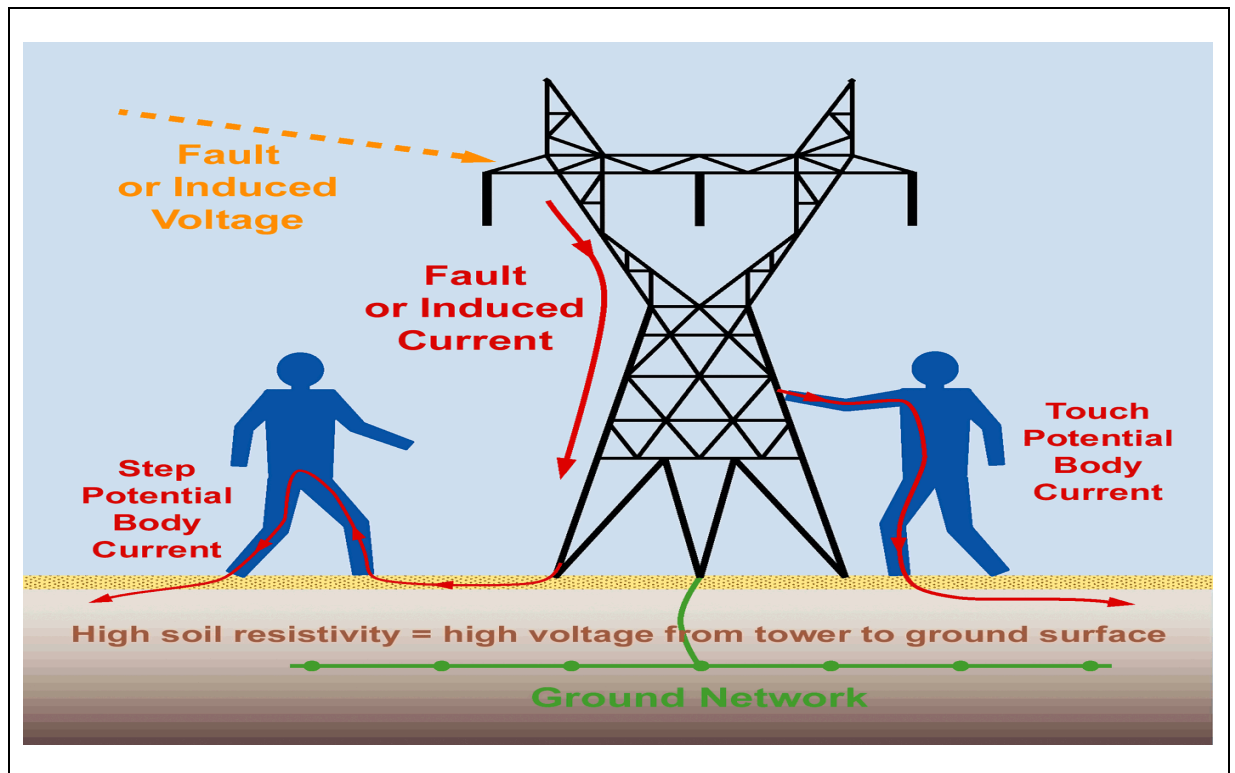
Figure 2.19 Graph displaying the step and touch potential body current
Reproduced from reference [23]

Step Voltage, Touch Voltage, Metal To Metal Touch Voltage

Step voltages values should be limited and should not exceed the following criteria:

a) In public accessible areas under continuous operating conditions, the step/touch voltage must not exceed a value that would result in body currents been above the threshold of perception. This current should be less than 6 mA.

b) During short time, transient operating conditions and transient faults, the step touch voltage must not exceed a value that would result in body currents been greater than the lowest threshold of let-go-current. This current is less than 30 mA.

c) Transferred potential can be viewed as a special case of touch voltage. Hence the same associated continuous, body current limits and transient voltage limits would apply to transfer potential. The distance however can be any unspecified value. This type of potential may be present on cable or

metallic objects that are on the site and could become grounded at one point and floating at another point. Figure 2.20 illustrates concept of transferred potential.
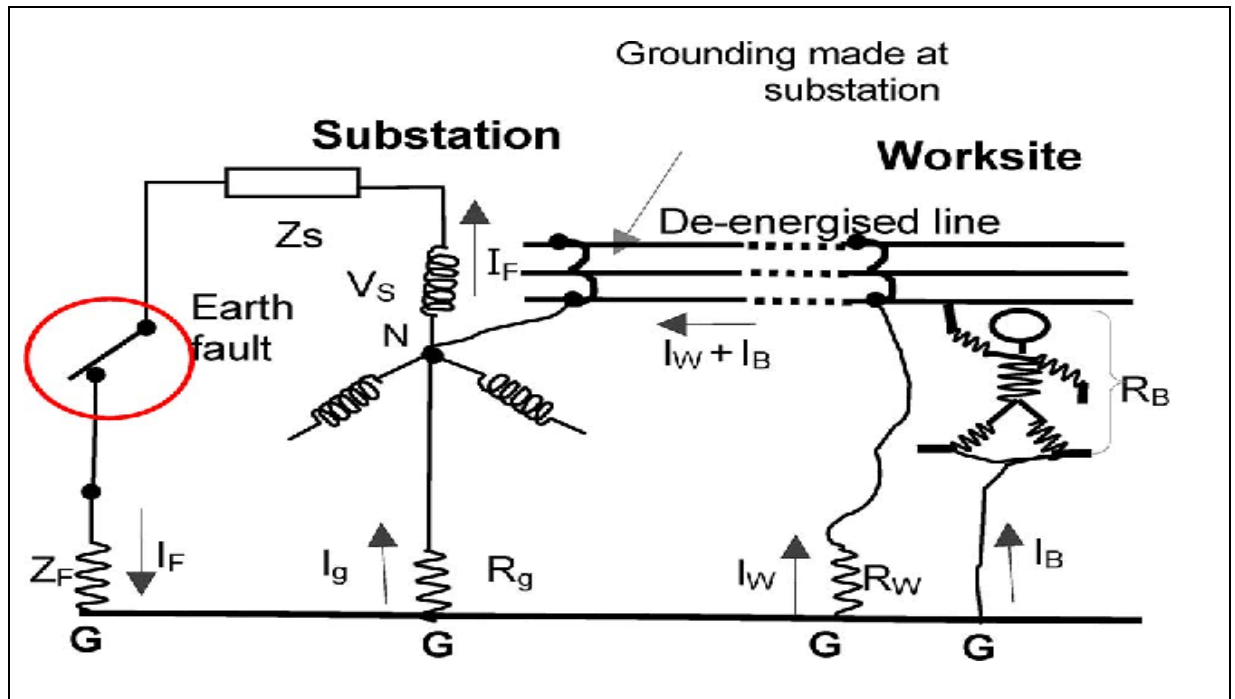
Figure 2.20 Conceptual Illustration of Transferred Potential
Reproduced from reference [33]

One of the risks of transferred potential is that of metallic cables entering or leaving the site and metallic fences near the site. The resistance of the metallic object and the connection from the object to ground is assumed to be much higher than the resistance of the body (i.e. effectively zero). For wooden fence posts the resistance is assumed to be infinite.

The movement of transferred potentials on fences can be accomplished by sectionalizing the fence to limit the transferred voltage to safe levels. Should there be impractically small lengths of fence close the electrode, than the transferred potential criterion should not be selected based on the threshold of perception but rather on the transient current limit. Design cannot entirely eliminate the risk of transferred potentials, but the risk can be reduced by adopting the suitable design measures and procedures.

d)   Current density

The electrode element surface current density should be selected with a view to avoid electro-osmosis for land electrodes. Furthermore, this selection would reduce chlorine selectivity for elements that are in contact with saline water for sea electrodes and beaches. To avoid electro-osmosis, the maximum average current density recommended for land electrodes, should be in the range of 0.5 A/m2 to 1

A/m2 for beach. For sea electrodes the maximum average current density should be 6 A/m2 to 10 A/ to reduce chlorine selectivity for elements in contact with saline water.

e)   **Ground Potential Rise (GPR)**

The GPR would occur at the electrode relative to the surrounding area [29] , when the dc current injected into the earth (anodic operation) or collected from the earth (cathodic operation). The current and the resistance of the electrode to the remote earth would determine the magnitude and distribution of the GPR. At or near the grounding site the main determining factors of the GPR are the resistivity of the local soil or body of water and the grounding element configuration.

A lower maximum GPR would result from grounding elements within a large contact area as well as having a EHVDC ground electrode installed in seawater or in a low resistivity soil or seawater. This would result in a smaller potential gradients or step voltages.

It must be note that at a significant distance from the electrode outside the zone of influence, the local soil conditions or element arrangement at the grounding site would not affect the GPR distribution. Outside of the zone of influence the GPR distribution is determined by the remote earth resistivity. At the ground electrode location the GPR distribution determines the step potentials and consequently safety. The surrounding infrastructure can be affected by the electric fields resulting from electrode operation. These are predominantly electrical interference (eg wye-grounded transformers and machines) and electrolytic corrosion (eg buried and immersed metallic infrastructure).

The difference between the maximum and minimum values of ground potential on the site would equal to the highest transfer potentials that can occur on that site.

2.3.7. Over voltages in EHVDC systems

The horizontal clearances between tower member and pole conductors are governed mainly by the maximum expected overvoltage [34]. Over voltages in overhead transmission lines are mainly categorized into temporary, slow-front and fast-front over voltages according to the rise time and duration of the overvoltage [35].

Temporary over voltages may occur due to mal-operation of the controller system in the EHVDC converter station, line energization and reclosing. However, normally energising a line, the dc voltage is smoothly ramped up from zero, and for reclosing the line, the trapped charge will be eliminated through the line de-energization process to limit the over voltages.

Slow-front over voltages on dc transmission lines generally happen due to ac or dc side fault occurrence and clearing process. However, the most significant slow-front over voltages come from single pole to ground faults and occurs on the un-faulted conductor.

The magnitude and duration of the slow-front over voltages depends on converter technology, system configuration, line length, fault location, and smoothing reactor. Fast front over voltages are mainly caused by lightning surges directly striking the conductor, or the tower and shield wires that may result in insulator back flashover. The crest times of the fast front over voltages are from 0.1–20 µs. The over voltages caused by lightning depend also on the tower geometry and footing resistance of the towers [36], [37].

In order to determine the tower top minimum air clearances for EHVDC voltage levels, continuous operating voltage and temporary over voltages have negligible impact because the required voltage withstand strength is mainly affected by slow front and fast front over voltages [34].

As mentioned earlier, most VSC EHVDC projects use either grounded bipole or symmetrical monopoles configurations. LCC EHVDC is a mature technology and all dc over voltages associated with it are well known; studies show that lightning and fault over voltages on the dc side of LCC systems are between 1.8 to 2.3 pu, when the maximum overvoltage happens for an earth fault in the middle of the line. Faults in other locations produce smaller over voltages.

However there is no corresponding experience base for dc overhead lines which use modern Modular Multilevel Converters (MMC). Controllers that are proper designed for MMCs, eg the full-bridge converters, may reduce the slow front overvoltage levels. This overvoltage level is formerly associated with LCC cases, thus reducing clearance requirements and facilitating compaction.

2.3.8. Back flashover (BFO)

This phenomenon [34] occurs between the dc pole conductor with opposite polarity as the lightning current and the tower. A polarity reversal at the overhead system will occur due to BFO. In cases of long overhead/cable length of 50km and above the BFO can lead to a polarity reversal of 2.34p.u. of the system rated voltage. As the cable length decreases the maximum voltage along the cable increases.

The maximum voltage along the cable (approximately 2km) can differ by as much as 300 kV compared to the maxima at the sending end. One must note that the BFO analysis was performed for a worse-case tower grounding conditions and extremely rare lightning impulse currents (150 kA).

Lightning incidences can cause over voltages caused by back flashovers as well as over voltages resulting from shielding failures. Over voltages resulting from back flashovers (BFO) may occur the shield wire or the tower top is struck by a lightning stroke current, who's magnitude is current high enough to cause a tower-to-conductor short circuit.

The BFO should result in the dc pole operating voltage of the opposite polarity as the lightning stroke, been superimposed with the lightning surge voltage. BFO's would occur in cases where the lightning stroke crest is high and poor tower grounding conditions.

2.3.9. Shielding Failure

Shielding failures (SFO) [38] would occur when the lightning stroke bypasses the shield wire and stroke terminates directly on the dc pole conductor. This phenomenon would occur for low magnitude lightning current. As the magnitude of the lightning stroke increases, the protection effect of the shield wires would improve, reducing the probability of shielding failure.

The ground wire shielding effectiveness can be evaluated on the basis of an electro geometrical model. The critical lightning stroke current magnitude that can result in a SFO would be within the range of 7 - 31 kA. This would depend on the different parameters used to calculate the striking distance.

Should the dc pole be struck by direct lightning strokes, the polarity would be the same as the lightning current. The constructive superposition of the dc pole operating voltage and the imposed lightning surge voltage can lead to severe over voltages.

Should the dc pole be struck by direct lightning strokes with the opposite polarity, destructive superposition of the imposed lightning surge voltage and dc operating voltage will occur. For high lighting current, this may yield to a polarity reversal.

2.4 HVAC Systems

This chapter deals with the different components on transmission lines and the effect lightning strokes would have on these lines. The tower footing resistance and soil resistivity are discussed. Thereafter the affects that lightning has is explored, Furthermore this section discusses induced lightning strokes calculations and the tower top voltages based on tower footing resistances, condcutor reistances and the magnitude of the lightning strokes. Thereafter the surge arrestor models are examined.

Soil resistivity has been discussed in 2.1.1. and is not repeated in this sections

2.4.1 Tower earthing and performance under high impulse current

Should lightning strike a transmission line or tower then the tower potential would raise above the insulator voltage withstand level. This would result in a flashover from the tower to a phase conductor. This could result in outages to that particular overhead EHVAC line. This flashover type is known as a back flashover. The tower footing electrical resistance is an important parameter affecting back flashover voltage in transmission systems (IEEE Std. 1313.2-1999) [34]. The IEEE Std. 1243-1997 [37], furthermore states *"the overall performance of an entire transmission line is influenced by the individual performance of the towers rather than by the average performance of all the towers together''* [34] .

A study was carried out by Whitehead [34], to investigate the effect of the average tower footing resistance on the lightning outage rate, on a 500 kV transmission line. The results were that the line outage rate was approximately proportional to the average tower footing resistance. The lightning outage rate was 1.0 per 100 km per year, for an average tower footing resistance of 30 Ω. This can be seen in Figure 2.21. Research done by Chisholm and Chow [35] confirmed these results.

Tomohiro et al. [39] studied the influence of the tower footing resistance on the lightning fault rate. Their results are shown figure 2.21, where it is shown that with the increase in tower footing resistance, the lightning fault rate increased.
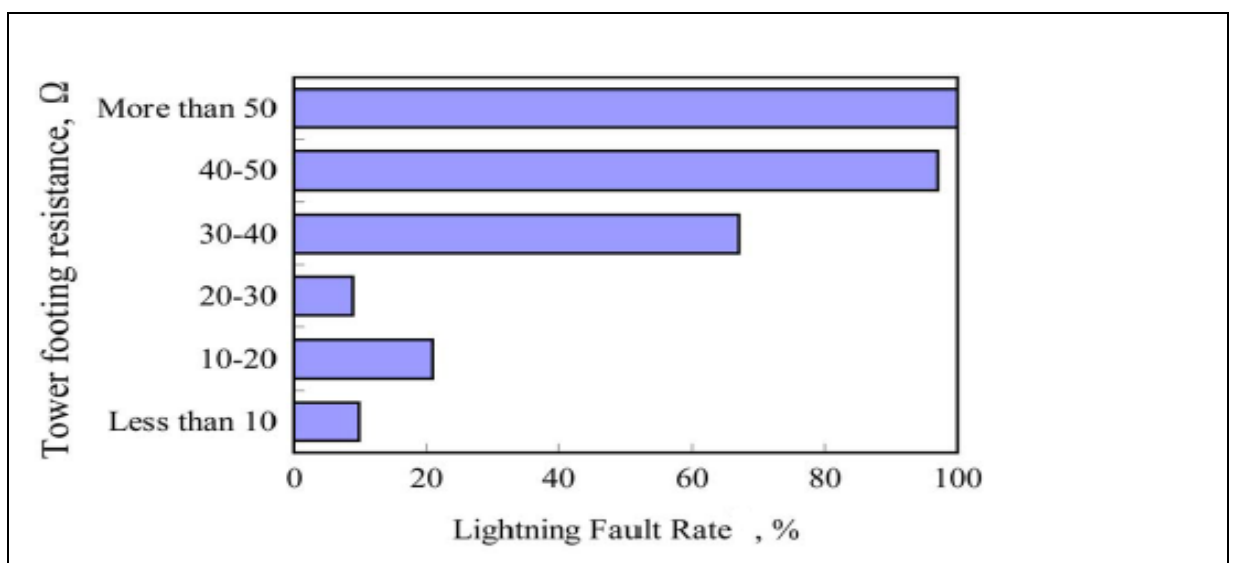
Figure 2.21 Tower footing resistance vs. lightning fault rate

Reproduced from reference [39]

A Japanese power company [39] published a standard design for footing resistance against isokeraunic level, system voltage, and line importance. This is shown in Table 2.5. The important effect that the tower footing resistance has on the lightning performance of transmissions lines is once again highlighted. ,

Table 2.5 Design values of the system voltage, isokeraunic level and tower footing resistance

System voltage, kV	Design value of tower footing resistance, Ω		
	I	II	III
500	13		
275	13		
154	15		20
77	13		20
33	20		

IKL: Isokeraunic level, thunder storm days per year
I : IKL more than 30 and important lines.
II : IKL from 20 to 30.
III : IKL less than 20.

Reproduced from reference [39]

Most countries design and try and maintain the target level of 10Ω or less for the tower footing resistance. This is to provide sufficient protection against back flashover. Having a TFR of less than 10Ω is considered more economically beneficial than increasing the insulation level of the line to withstand lightning strikes. However, should the TFR be high, for example 50Ω, the outage rate of the shielded transmission line may be higher than that of the unshielded lines. This can be seen in figure 2.22.
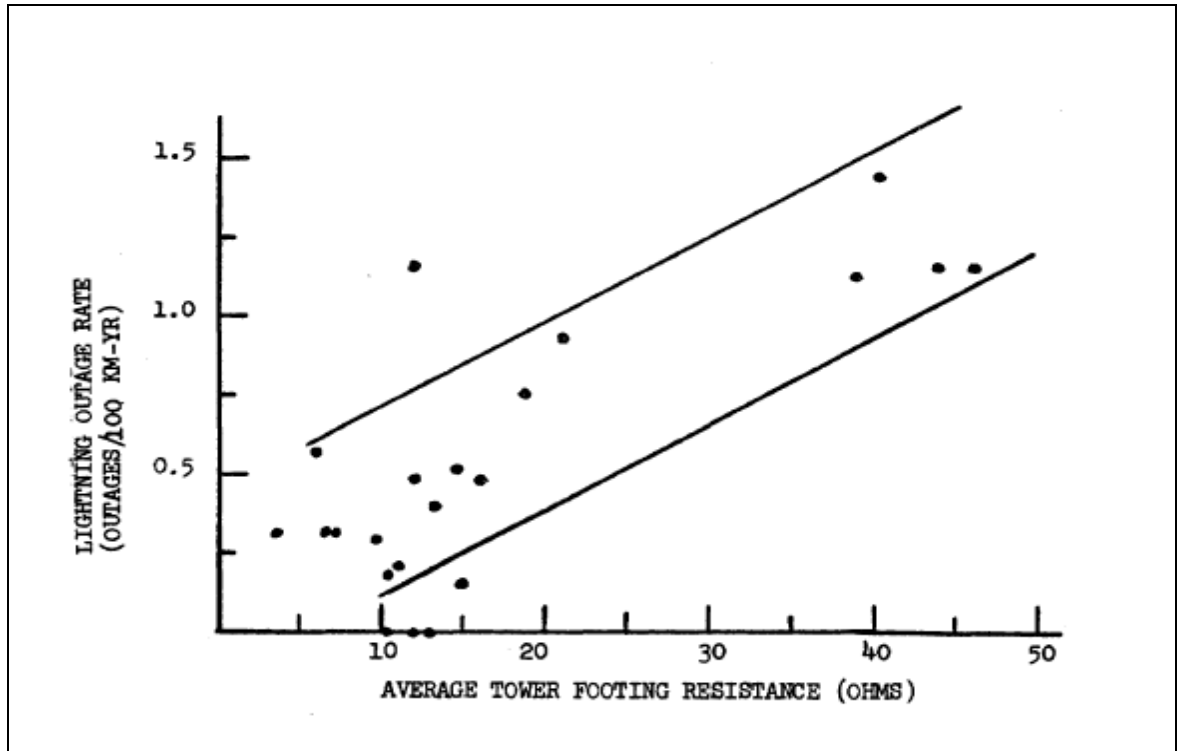
Figure 2.22 Lightning outage rate vs tower footing resistance for a 500 kV line
Reproduced from reference [34]

Literature research indicates that there are very limited numbers of experimental field studies on tower footing impulse resistance under high impulse currents. Also a few numbers of investigations have been undertaken on a full scale tower footing and tower base.

A series of field tests to determine the transient behaviour of tower footing earthing resistances was undertaken by Kosztaluk et al. The test comprised of injecting a current of 24 kA with rise time in the range between 3 and 12us into the tower footing. Equation (5) defined dynamic resistance:

$$Ri = v(t)/I(t) \tag{5}$$

The measured dynamic resistance as a function of the impulse current is shown in Figure 2.23. The numbers on the curves refer to the time in μs. As the current first starts to rise at 1μs, the resistance is close to low frequency resistance. After approximately 1us (current exceeds 2 kA), which corresponds to a current density on the electrode of 0.3 A/cm², it was noticeable that the impulse resistance decreased. This was attributed to soil ionization. When the current reached the maximum value, there was a slight decrease in the resistance. This observed can attributed to the tail of the current.
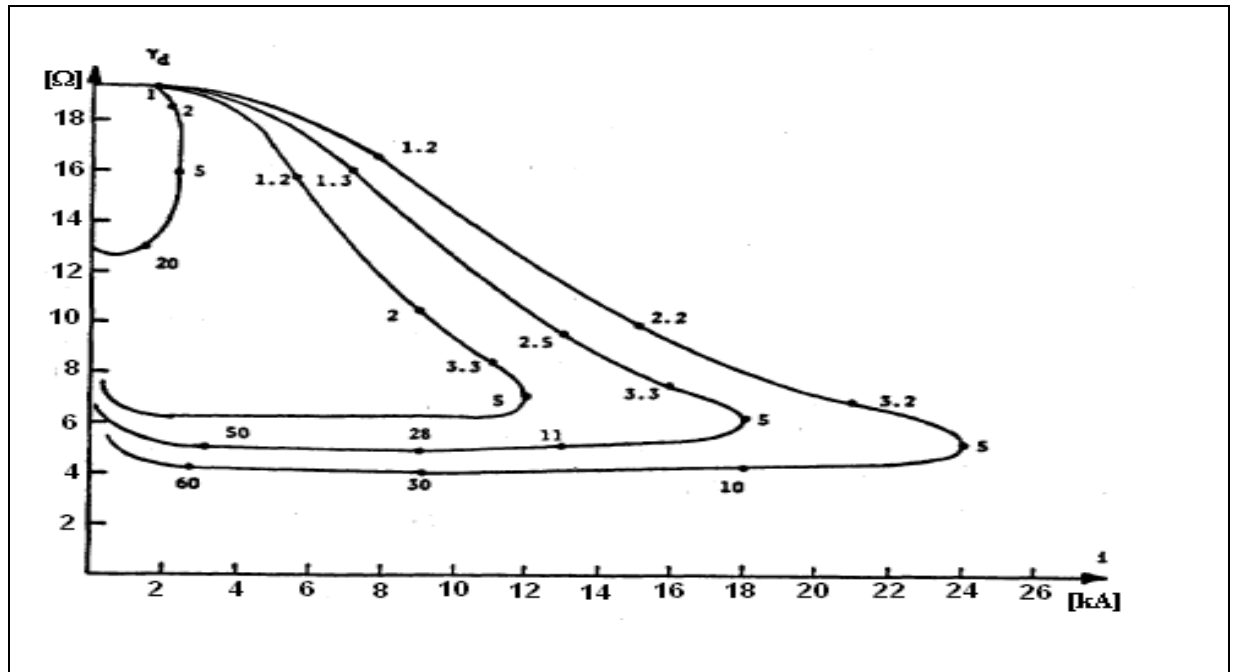
Figure 2.23 Dynamic resistances against impulse current
Reproduced from Reference [34]

Makoto et al. [40] performed similar tests. They investigated the impulse impedance of a tower footing base and other electrodes. These electrodes included rods, a grounding sheet, and crow's foot electrode under high impulse current. Furthermore a tower footing base was erected in soil that had a resistivity of 250 Ohms meter. A high impulse current, 30 kA with front time 3.5μs, was injected into the test electrodes.

The two cases considered in this investigation are

i) Current was applied to the independent earthing system and there was no additional earthing arrangements installed.
(ii) The tower footing was connected one at a time to different auxiliary electrode systems

The test results on the individual electrodes are shown in Figure 2.24. Basically as the impulse current increases, the impulse resistance decreases. This is evident for the short rod. With respect the case of the tower base, the decrease is small. By adding electrodes to the tower base reduces the impulse resistance as shown in figure 2.25. The combined systems indicate that the resistance is practically constant with impulse current. This was explained by the fact that the critical ionization level of the soil is more than the current density on the lateral surface of the tower footing base.
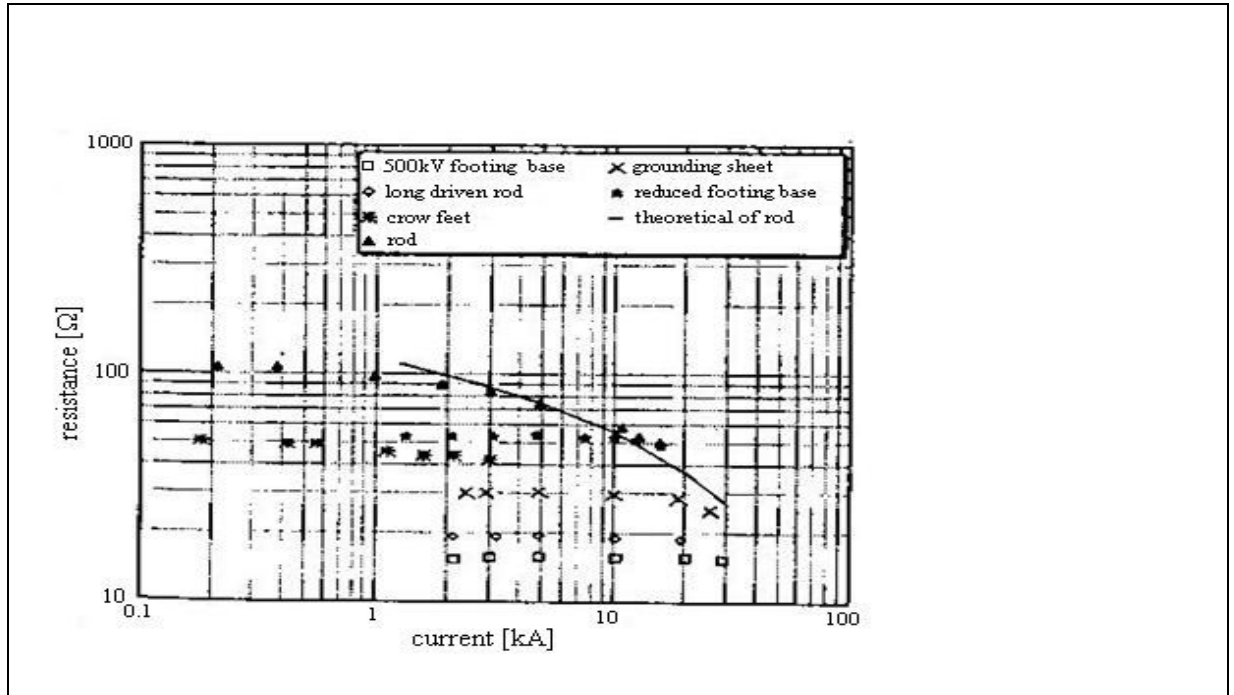
Figure 2.24 Current-dependent characteristics of resistances for various earthing electrodes.
Reproduced from reference [34]
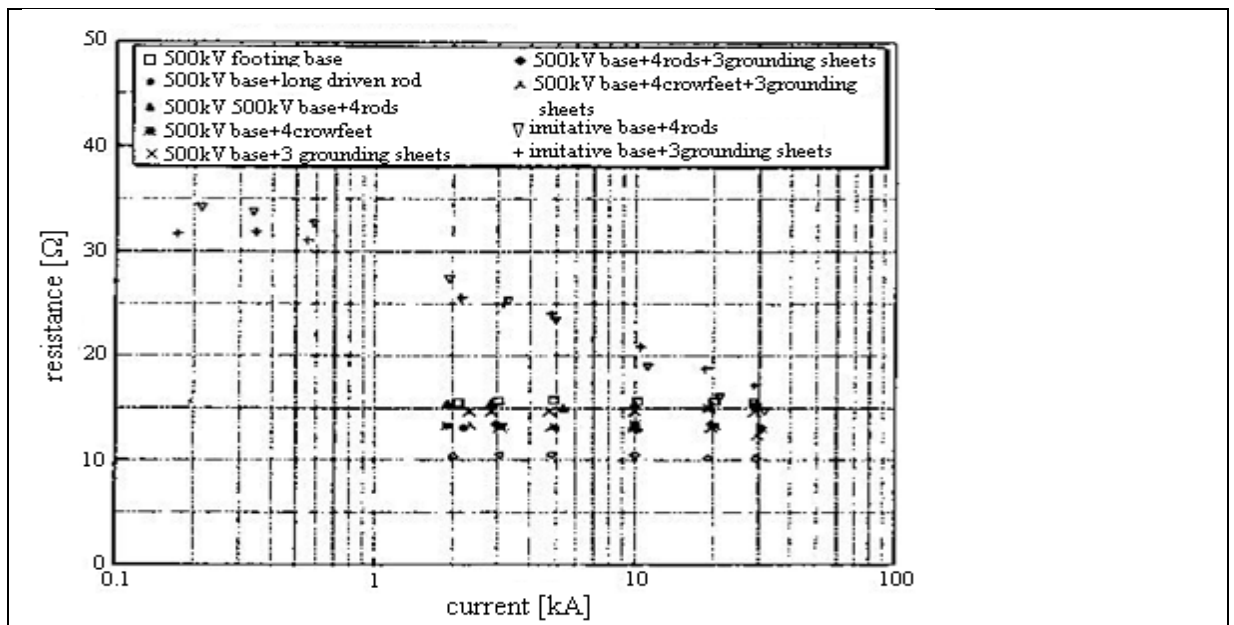
Figure 2.25 Current-dependent characteristics of resistances for composite grounding systems.
Reproduced from reference [34]

2.4.2 Tower Footing Resistance

The resistance offered by the metal parts of a tower, combined with the ground resistance to the dissipation of current is called the tower footing resistance. Should the the tower footing resistance value be low there would be less voltage stresses across the line insulation. Lightning strokes to the tower would result in high currents that would flow into the ground via the tower footing, giving rise

to thermal effects and soil ionisation. This would cause the ground resistance of the tower base to decreases by an amount, which would depend on the current magnitude, soil resistivity and tower footing construction [20], [41], [42], [43]. Hence to prevent line back flashover and maintain the ground potential rise within safety tolerance, the tower footing resistance value should be as low as practically possible. The lower the tower footing resistance, the more negative reflections are produced from the tower base travelling towards the tower top and would assist in lowering the peak voltage at the tower top.

Tower footing resistances are affected by the following two key factors.

(a.)   Electrode configuration
(b.)   Soil Resistivity

2.4.3 Electrode Configuration

An earth electrode can be a pipe, metal plate, or conductor connected electrically to earth and may be made of aluminium, copper, mild or galvanized steel. The following factors influence the earthing are [20], [44]:

(a.)   Electrode resistance – individual or group of electrodes.
(b.)   Soil composition in the immediate neighbourhood.
(c.)   Soil temperature
(d.)   Soil moisture content
(e.)   Electrode depth

2.4.4. Soil Resistivity

Resistance of a cube of soil of 1 m size measured between any two opposite faces is define as soil resistivity and is expressed in Ohm-metres. Soil Resistivity is a key factor in determining the resistance of the charging electrode and the depth level it should be planted to obtain low resistance. Soil resistance fluctuates seasonally and changes from place to please. The following factors affect soil resistivity. [20], [21]:

(i.)   Minerals
(ii.)   Dissolved salts
(iii.)   Moisture

In obtaining the desired earth resistance value, one can either increase or decrease the number of electrodes required. Furthermore the thickness of the oil layer is an additional factor that needs to be considered. The soil environment is noted for having an upper layer and a more conductive lower layer.

2.4.5 Earthing method and configuration

Different types of earthing methods and configuration are available for improving tower footing resistance and are shown below [21].

1.   Vertical electrode (Driven rod)

2.   Horizontal electrode

3.   Earthing grid

4.   Ring electrode

2.4.5.1. Vertical electrode/Driven Rod – Figure 2.26

Generally the driven rod (vertical earth electrode) is the more utilised type of earthing electrode and the most economical one to install. There are two ways to obtain the desired earth resistance using the vertical electrode method. One way is to use long vertical rods. This is suitable for ground conditions with high soil resistivity. The other way is to connect a number of rods is parallel. This is sometimes called "array of rod electrode".
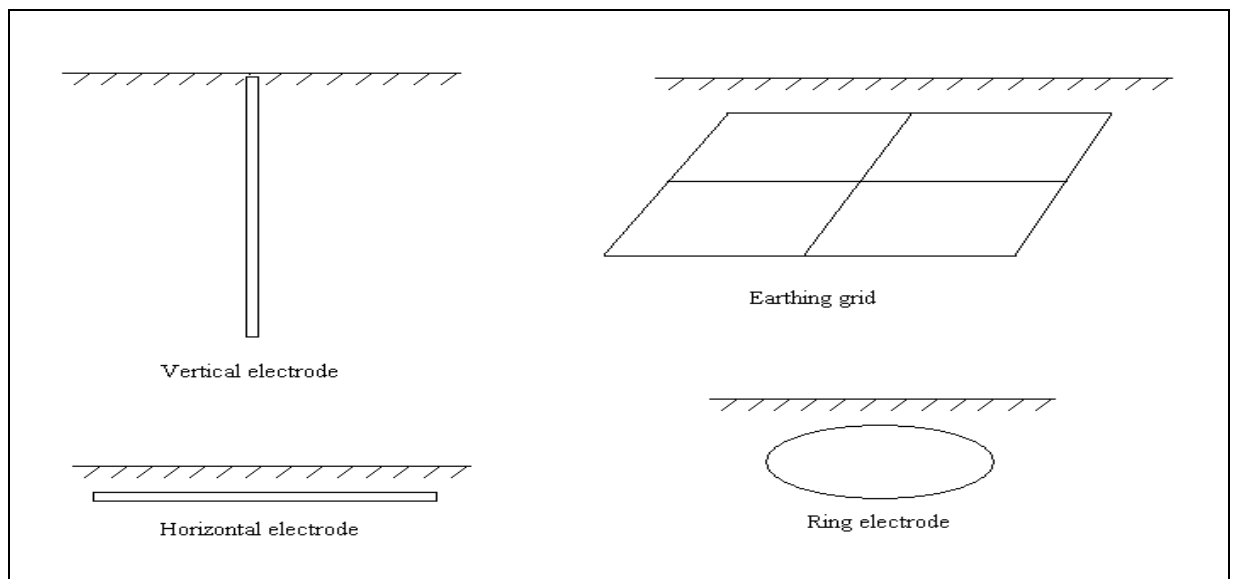
Figure 2.26 Various electrode configurations
Reproduced from Reference [45]

The parallel electrode combined resistance a function of several factors. These factors are:

1.   The configuration and number of the electrode

2.   The distance between the electrode

3.   The electrode configuration and the soil resistivity.

2.4.5.2. Horizontal Electrodes – refer to figure 2.26

These types of electrodes are installed horizontally under the ground surface and makes good connections to ground. Should the down conductor be jointed to a location near the middle of the

trench electrode, two parallel transmission probes are created, which results in the surge impedance been halved.

This type of earth electrode, when applied to tower lines, may be continuous or non-continuous. They may lay parallel to the line conductors and between towers. The conductors can also be laid perpendicular to the transmission line and enhanced arrangements using 4 point, 6 point or 8 point star can be used.

2.4.5.3. Earthing Grid

This type of earthing requires the conductors to be laid under the earth surface. The earthing grid are mostly utilised to support driven rod method. It can also be used separately when deep driven rod method is unpractical due to terrain and soil considerations. When multiple injection points are required, earthng grid method should be used. In these cases electrodes can be connected to the grid at various locations. This should result in the mesh providing a good earth regardless of the location of the fault current injection point. Furthermore increasing the grid coverage area would reduce the earth resistances

2.4.6 Induced Voltage

When the lightning stroke terminates on the ground close to the overhead line, induced voltage occurs. The field radiated by the lightning stroke and the line conductor causes an electromagnetic coupling between them. Hence the return phase stroke would be the trigger for the induced voltage. However should the lightning stroke terminate very close to the line; the preceding leader also can cause significant induced voltage. There are three models that could be used to evaluate the electromagnetic coupling. These are:

1.   Rusak

2.   Chowhuri

3.   Agrawal et al.

For induced voltage to occur, the distance from the stroke termination and line, should be 200 meters or less. Furthermore the probability of a flashover would depend on the soil, stroke magnitude, and line parameters. Nucci and Rachidi [46] evaluated all three models. In all cases the experimental data followed that of the measured data. Further work undertaken by Nucci and Rachidi are revealed in the following figure 2.27.
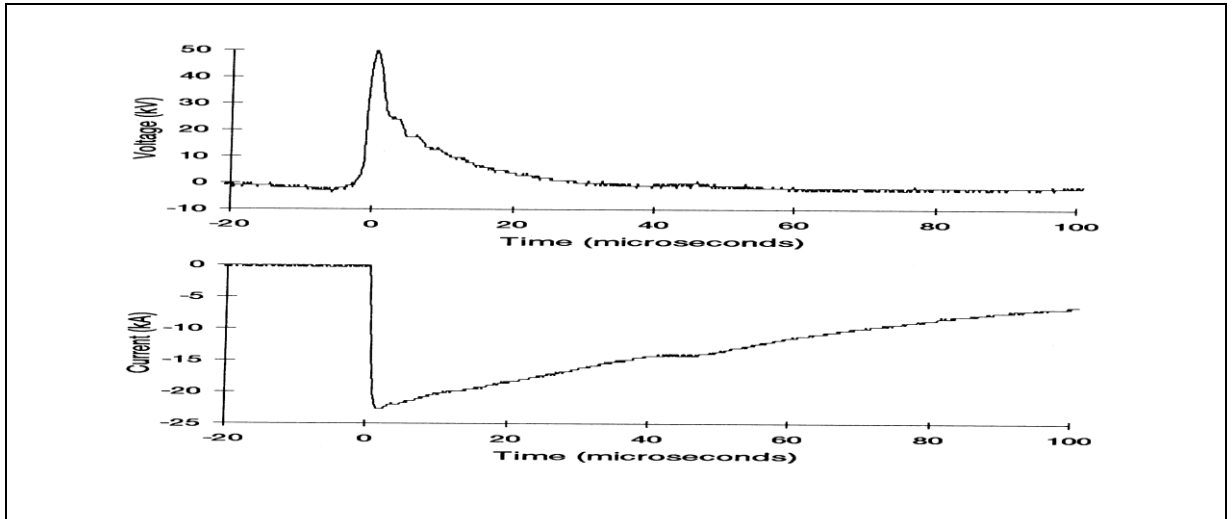
Figure 2.27 Graph of current vs time
Reproduced from reference [46]
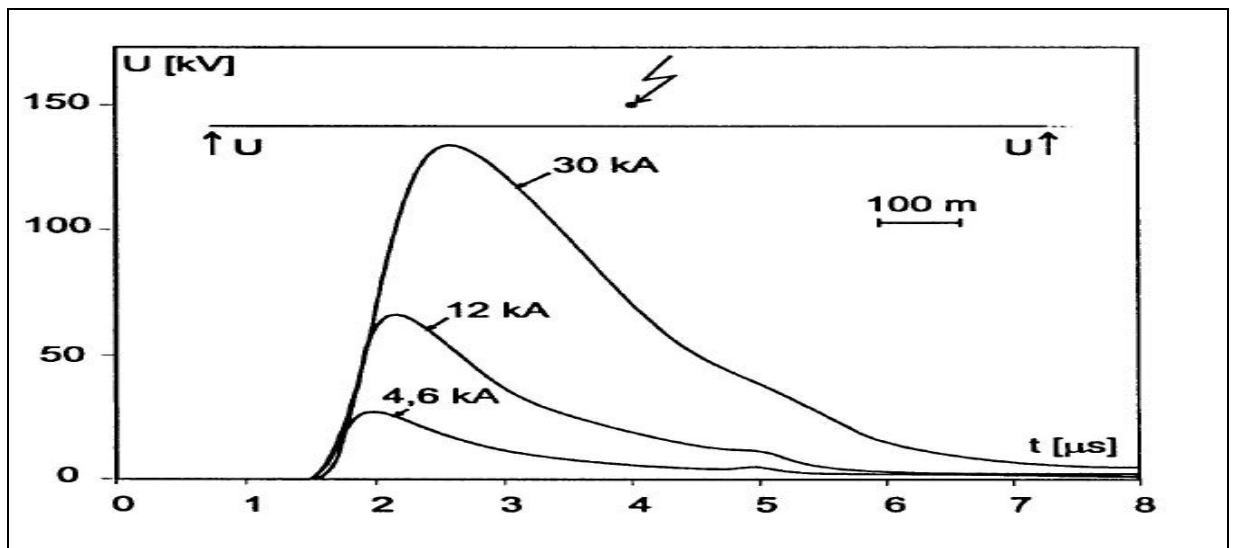
Figure 2.28 Graph of voltage vs time
Reproduced from reference [46]

Figure 2.28 shows for a given current stroke magnitude, a corresponding overvoltage may be recorded. Hence it was concluded that for a perfectly conducting ground and infinite long wire, the overvoltage on a structure by be determine using the following simplified Rusak formula.

$$U_{Max} = \frac{Z_0 * I_{Max}}{d} \qquad (6)$$

d = Distance from structure

Imax – Maximum lightning stroke

Umax – Maximum flashover voltage

Zo = Ground Impedance

It must be advised that this is generally for lightning strokes within 200meters for the structures.

2.4.7 Insulator flashover voltage

Insulators serve two critical functions: They provide a means by which power line conductors are suspended and they insulate energized poles from the suspension point, i.e. the grounded tower. Proper insulation design of an EHVDC transmission lines is essential for a reliable operation over the lifetime of the circuit [47]. Dc voltage subjects insulators to much more unfavourable conditions than does ac voltage. This is due, in part, to a higher collection of insulation surface contamination with unidirectional electric fields. Moreover dc and ac arc propagation across the insulator surface is different due to the natural zero crossing of the ac arc. Selection of insulator type, material, and string configuration for EHVDC is complex and site-dependent.

Insulators for high voltage power transmission may be made from ceramics (glass or porcelain) or of polymer composite configurations [27]. Two basic insulator configurations have proven useful for EHVDC: One of which is comprised of individual cap and pin "discs" which are used in sufficient number to accommodate the voltage for which they are selected; the other being "long rod" insulators consisting of a central glass core for mechanical support surrounded by a moulded polymer core with "skirts" to accommodate contamination [27].

The cap and pin insulator types are made of a ceramic shell to which metal cap and pin components are cemented to provide a means of attaching insulators to each other and to the tower and the line hardware. This configuration provides flexibility within the insulator string. Cap and pin insulators have good mechanical strength and a long term track record. However, they are heavy and expensive. Long-rod insulators can be adapted in length to the applied voltage or connected in series for higher dc voltage applications. There are two popular long-rod insulator options:

Long-rod ceramic insulators are one-piece units of varying length made of glass or porcelain. They have a long term track record of almost 40 years and have demonstrated moderately satisfactory performance.

A newer insulator technology consists of an interior rod for mechanical strength, surrounded by a molded polymer outer surface with skirts optimally contoured for dc applications. They are significantly lighter and their performance in contaminated environments is considerably better than ceramic insulators of equal length. Furthermore the hydrophobic property of the exterior surface material discourages wetting, thus increasing electrical withstand strength per unit length in comparison with disc insulators. However, this is relatively a new technology with a limited

experience base on which to base life expectancy.

The line insulators joining the conductors to the tower may be modelled as a capacitor. The insulator transient-voltage withstands level can vary, in that it may withstand a short duration high transient voltage, and it may fail to withstand a long duration lower transient voltage. This is often referred to the volt-time characteristic of the insulation. The insulator specifications also prescribe the withstand voltage of that insulator [48]. The insulator voltage withstands capability can be calculated using the expression shown in (7).

$$V_{flashover} = K_1 \ + \frac{K_2}{t^{0.75}} \tag{7}$$

where

K_1 = 400L

K_2 = 710L

L = Length of insulator (meters)

t = elapsed time after lightning stoke (us)

The volt-time curves can represent the back flashover mechanism of the insulators. Whenever back flashover occurs, a parallel switch is applied and also if the voltage across the insulator exceeds the insulator voltage withstand capability, the back flashover occurs. The back flashover is simulated by closing the parallel switch. Once the back flashover occurs, the voltage across the insulator goes down to zero.

Figure 2.29 shows the insulator flashover voltage for different insulator lengths.
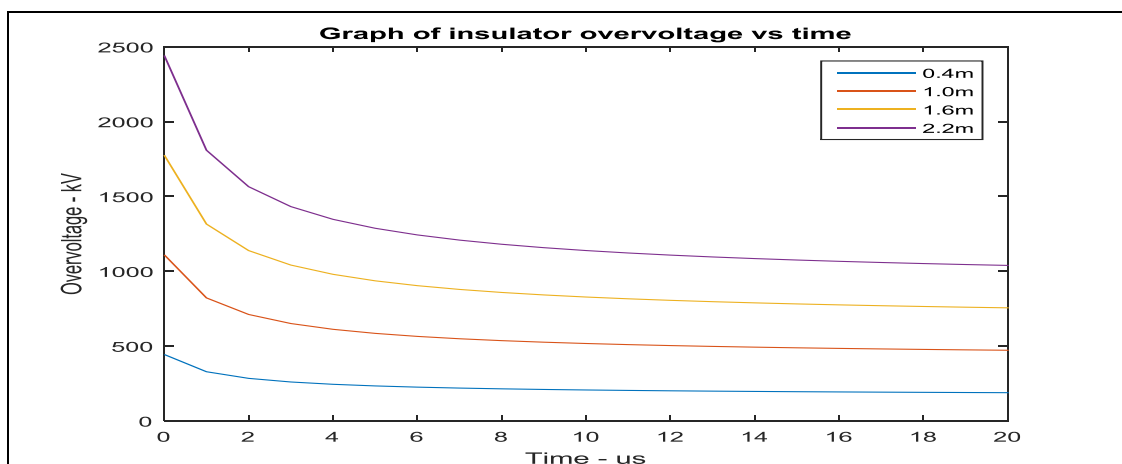
Figure 2.29 Graph of insulator overvoltage vs time

Reproduced from reference [49]

The calculated insulator flashover voltages increases as the insulator length increases.. Using a lightning waveform of 8/20 microsecond, the calculated flashover voltage for a 1.6 meter insulator (132kV) is 1770kV.

2.4.8 Tower Top Voltage

Most lightning stroke that terminate on the earth wire, tower or directly onto the phase conductor would cause current to flow through the tower to ground. The tower resistance and the ground resistance would provide a voltage at the tower top with respect to earth. There will be a flashover across the insulator if the tower top voltage is greater than the insulator flashover voltage. One can use conventional traveling-wave theory to calculate the voltage produced by the current and charge fed into the tower and ground wires. Proper surge impedances values must be used.

Various literatures publish a wide range of tower surge impedances; hence it is important that a specific equation justified by theory be obtained. The estimation of voltage at the tower top (Vt) can be performed with reference to figure 2.30. [50].

$$V_t = Z_I I - Z_w \left(\frac{I}{(1-\omega)} - \frac{\Delta I}{(1-\omega)^2} \right) \tag{8}$$

Where

$$Z_I = \frac{Z_S Z_T}{Z_S + 2Z_T} \tag{9}$$

$$Z_w = \left(\frac{Z_S^2 Z_T}{Z_S + 2 Z_T^2} \right) \left(\frac{Z_T - R}{Z_T + R} \right) \tag{10}$$

$$\omega = \left(\frac{2Z_T - Z_S}{2Z_T + Z_S} \right) \left(\frac{Z_T - R}{Z_T + R} \right) \tag{11}$$

$$\Delta I = \left(\frac{2T_t}{T_0} \right) I \tag{12}$$

Z_I = Tower top intrinsic impedance (Ω)

Z_S = Line surge impedance (Ω)

Z_T = Tower surge impedance (Ω)

Z_w = Wave impedance of the tower (Ω)

R = Tower footing resistance (Ω)

ω = Damping constant for all the travelling waves

T_t = Wave travel time on the tower (ms)
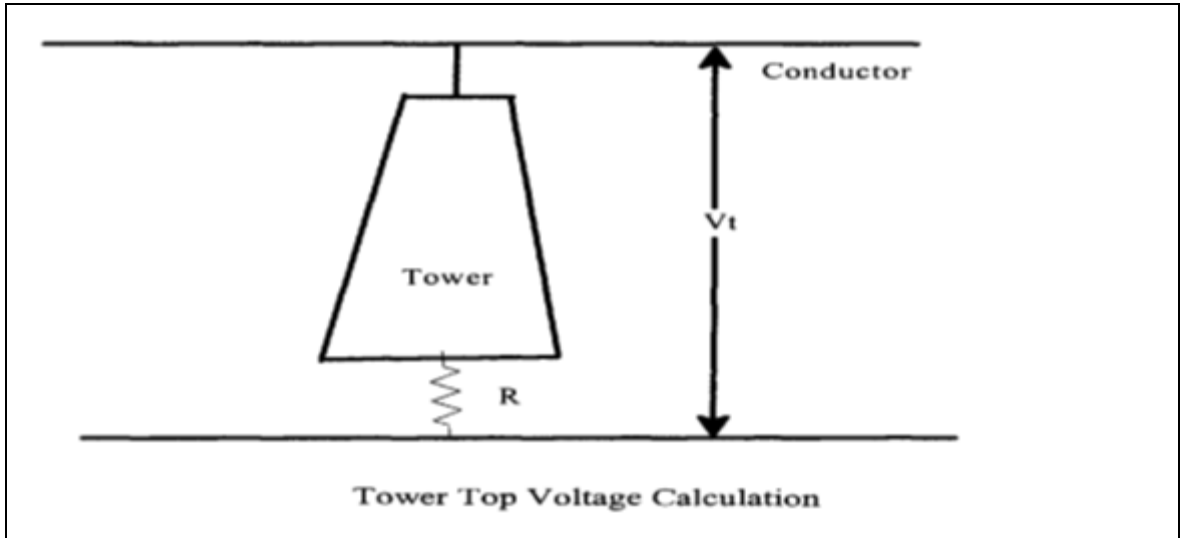
Figure 2.30 Tower Top Voltage Calculation
Reproduced from reference [50]

2.4.8.1 Analysis and computer simulations

Dekker [50] illustrates the use of the above equations to calculate the voltage at the tower top of a 230kV tower. The following parameters were used:

R = 10ohms

T0 = 2micro seconds

Tt = 0.3microseconds

Zs = 350ohms

Zt = 200ohms

The current through the tower is 10kA.

Using equations 9 – 12, we obtain Z_I = 93.3ohms, Z_w = 275.9ohms, ω = 0.0603 and $\Delta I = 3kA$. Substituting this in equation 8 gives a tower top voltage of 1065kV.

2.4.9 Line Surge Impedance

The line surge impedance may be given by [51]:

$$Z_g = 60 \ln \frac{2h}{r_i} \tag{13}$$

Where h is the ground-wire height,

r_i = radius of conductor

2.4.10. Tower Model

The transmission tower configuration depends on:

(a) The insulator assembly length.

(b) The minimum clearances to be maintained between conductor and tower and between the conductors.

(c) The location of earth wire/s in relation to the outermost conductor.

(d) The mid span clearance required from considerations of the dynamic behaviour of the conductors and lightning protection of the line.

(e) The minimum distance between the lower conductor and ground level.

From a safety perspective, transmission power conductors must maintain clearances to earth along the route they pass through. This would include open country, national highway, rivers, railway tracks, tele-communication lines, other power lines etc. as laid down in the Indian Electricity Rule and other various standards or code of practice. Under loading conditions, the maximum working tension should not be greater than 50% of the ultimate tensile strength of the conductor.

By ignoring the tower resistance and permitting low precision, the tower model may be equivalent to one inductance, which is called lumped inductance model [48]. The lumped inductance model formula is:

$$Z_T = 60\ln\left(\cot\left[0.5\tan^{-1}\left(\frac{r_{avg}}{H_t}\right)\right]\right) \tag{14}$$

$$\text{where } r_{avg} = \frac{r_1 h_1 + r_{2(h_1 + h_2)} + r_{3h_1}}{h_1 + h_2} \tag{15}$$

Z_T = average tower surge impedance

r_1 = tower top radius

r_2 = tower mid-section radius

r_3 = tower base radius

h_1 = height from base of tower to mid-span

h_2 = height of mid span to top

This is the recommended formula as per the IEEE and CIGRE and can be based on figure 2.31.
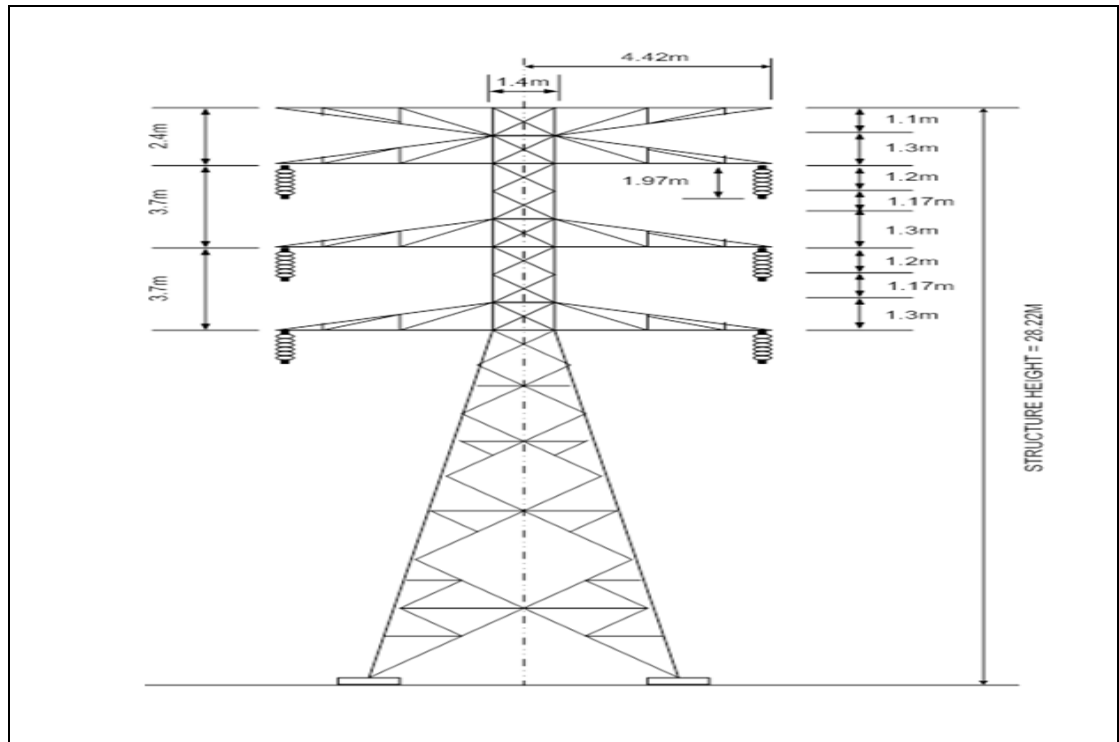
Figure 2.31 Tower Structure
Reproduced from reference [48]

The tower surge impedance model can be views as a transient wave process. In the surge impedance models, the superposition of the lightning overvoltage and the reflected voltage wave from the bottom of the tower equates to the tower overvoltage. The *calculation* principle of the tower surge impedance occurs when the tower is most regarded as a cone [48].

2.4.11 Peak lightning current

When a lightning stroke hits an overhead line earth wire [52], the injected current is divided equally between the earthwire ends that connect the towers. Hence the impedance Z. as viewed from the lightning stroke becomes a parallel circuit of earth wires Z_{ew}, the tower impedances Z_t and the ground impedance Z_e as shown in figure 2.32.
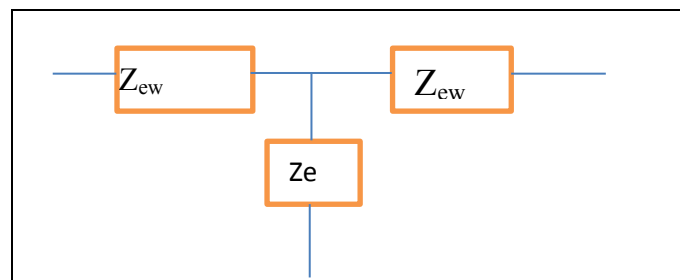

Figure 2.32 Three way current split based on impedance
Reproduce from reference [49]

The lightning channel impedance can be assumed to be 3000Ω, the earth wire impedance 500Ω, tower impedances 200Ω and ground impedance 50Ω, then the equivalent impedance as seen by the lightning strike would be approximately 334Ω. This means that approximately 90% of the stroke current is injected at the strike point.

Hence if the earth wire experiences a 30 kA stroke, there will be a 14 kA surge going in opposite direction to each other. The surge will travel to a tower top (point of impedance change) where there would be a reflected and transmitted component. The junction at the pole top has several current routes available and the surge would split according to the inverse ratio of the surge impedances of the available routes – say ~200Ω down the tower and ~500Ω for the continuing earth wire. This would result in the 14 kA surge split been approximately 5/7 down the tower i.e. 10 kA.

2.4.12 Back flashover

Most lightning strokes have the capacity to discharge hundreds of kilo - Ampere along with low-rise time [52]. Should these strokes strike overhead earth wires, towers or even phase conductors, they may produce over-voltages of sufficient magnitude to cause a flash over across the insulators. Back-flashover would occur when the difference between the tower top voltage and cross-arm voltage exceeds the phase insulator flashover voltage.

Most of the stroke current flows to the ground during a flashover, hence the tower footing resistance plays a major part on the over voltages generated. Normally the line to ground fault caused by the back flashover would be cleared by a protective device resulting in a line outage, which would last for a few milli-seconds. This time is depended on the speed of the protection devices. The surge generated by the back flashover has a very sharp wave front. This is as a result of the arc, which cause the phase wire to increase in less than 1µs from an induced voltage level (surge along the earth wire) to virtually the full lightning surge voltage.

2.4.13 Surge Arrestor Models

In power electrical systems, metal oxide surge arresters (MOSA) are commonly used as protective devices against lightning over voltages and switching. The Electromagnetic Transient Program (EMTP) is a powerful simulation program, which can be used to evaluate insulation coordination in these types of devices.

Suitable mathematical and/or circuitous models for these arresters are extremely important as assess their behaviour under voltage stresses conditions. However in attempting to create a unique model for

MOSA to evaluate all the possible transient permutation in power systems would be unpractical. This is because the model would be extremely complicated and would require a lot of simulation resources. Therefore, by identifying an appropriated model for a MOSA, the type of transient overvoltage can be evaluated. Switching surge studies could be performed by representing the MOSA only with their non-linear V-I characteristics [48].

The dynamic characteristics that MOSA have are significant for lightning and other fast wave front surges. Current surges that have front times faster than about 10 μs, the arrestor residual voltage increases as the time to crest of the arrester discharge current decreases. The arrester residual voltage normally reaches a peak before the arrester discharge current reaches its peak. The residual voltage increase may reach about 6% when the front time of the discharge current is reduced from 8 to 1.3 μs.

The voltage across the arrester is a function of the discharge current, and the rate of its rise. These characteristics are referred as frequency-dependent behaviour and would need a more sophisticated model than the simple static non-linear resistance one. There are a number of models, which have been proposed to simulate these dynamic characteristics. These models do have an acceptable accuracy; however difficulties arise in the calculation and adjustment of their parameters: eg iterative procedures are required. Also the manufacturer's datasheets do not have the necessary data. The IEEE WG.3.4.11 [53] [52] has recommended a simplified model for zinc oxide surge arresters [54], which has already been developed, on the basis of the frequency-dependent model.

Should the arrester discharge currents with time-to-crest be less than 4 μs, then voltage spikes may appear on the front of the arrester residual voltage waveform. Should the time-to-crest be more than 4 μs then voltage spikes do not exceed the residual voltage. Therefor these spikes are not within the proposed model´s scope and cannot be considered for the adjustment procedure.

2.4.14. The Frequency – Dependent Model

Figure 2.33 shows the frequency-dependent model, such as proposed by IEEE [52]. The RL filter separates the two non-linear resistors A0 and A1. The influence of the filter is negligible as arrester discharge currents has slow rising time. Hence the two non-linear resistors are essentially in parallel and characterize the static behaviour of the MOSA. The impedance of the filter becomes more significant for fast rising surge currents. This results in the inductance L1 obtaining more current from the non-linear branch A0. The resistor A0 has a higher voltage for a given current than A1; hence the model would generate a higher voltage between its input terminals, what matches the dynamic characteristics of MOSAs.
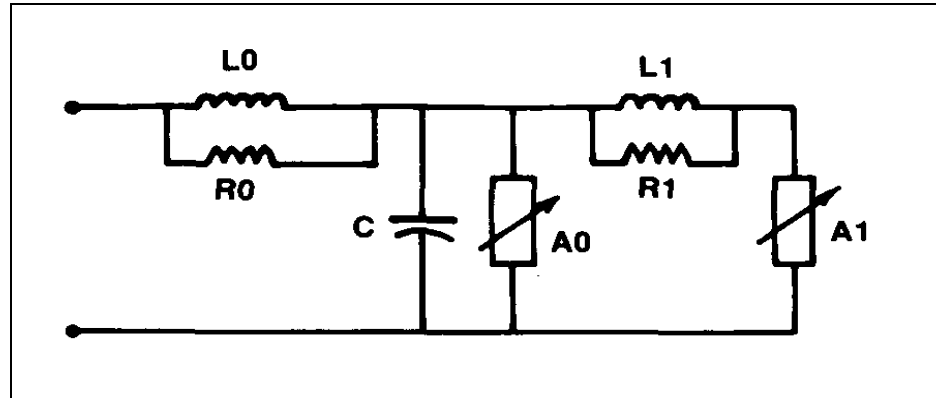
Figure 2.33 IEEE frequency-dependent model line arrester
Reproduced from reference [48]

In the model the inductance associated with magnetic fields in the immediate vicinity of the arrester is represented by the inductor L0. When the model is implemented on a digital computer program, then the numerical integration is stabilised by the resister R0. The terminal-to-terminal capacitance of the arrester is represented by capacitor C.

The resister R1 and the inductance L1 make up the filter between two non-linear resisters of the model. Starting from the physical dimensions of the arrester, the following formulae can be used to calculate L0, R0, C and R1.

L1 = 15d/n (μH)
R1 = 65d/n (Ω)
L0 = 0.2d /n (μH)
R0 = 100d/n (Ω)
C = 100n/d (pF)

where,

d= surge arrestor estimated height as per data sheet in meters

n= number of parallel columns of metal oxide in the arrester

The proposed curves for A0 and A1 are shown in Fig 2.34. These curves are the result of research undertaken by Radhika, Suryakalavathi and Soujanya [52]. This work is based on an arrestor height of 1.45 meters.
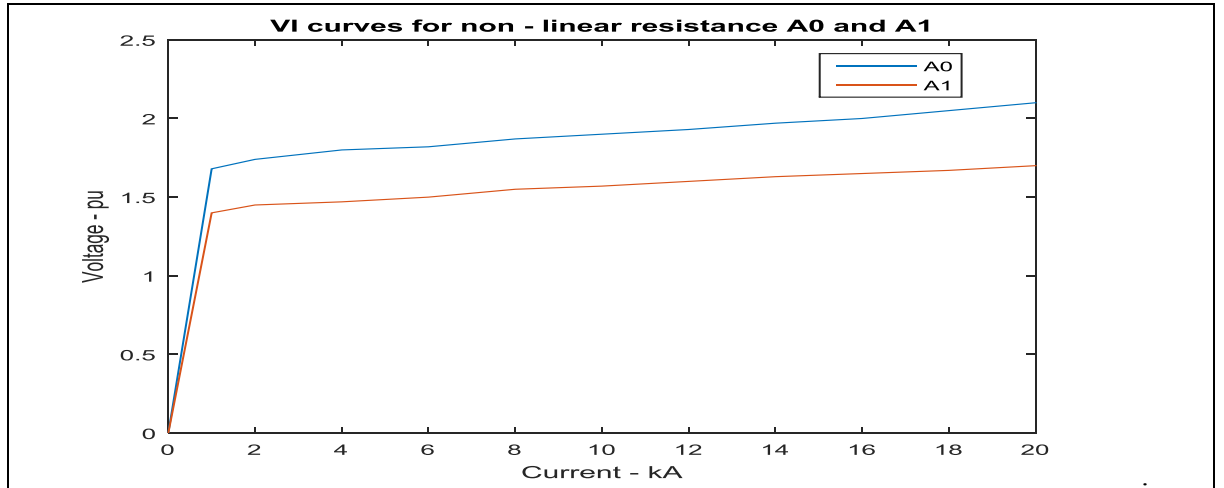
Figure 2.34 Non-linear characteristic for A0 and A1
Reproduced from reference [52]

Notes : The per-unit values are referred to the residual voltage peak value that was measured during a discharge test. This test was conducted with 10kA lightning current impulse (Ur 8/20). In order to get a good fit with the published residual voltages for switching surge discharge currents, these curves have to be adjusted. The inductance associated with the magnetic fields in the immediate vicinity of the arrester is represented by the inductance L0.

Radhika, Suryakalavathi and Soujanya determined that the parameter L1 has the most influence on the result and suggested a formula, starting from the physical dimensions. This constitutes an initial value only and L1 needs to be adjusted by a try- and error process to match the residual voltages for lightning discharge currents. These are published in manufacture's catalogue. Satisfactory results for discharge currents are within a range of times to crest for 0.5 μs to 45 μs are obtained from this model A alternative approach to determine L1, utilising the electrical data of the arrester, is also proposed in [52] [55]. Here the authors reported relative errors between the measured and calculated residual voltages as been lower than 4.5% for discharge currents with time-to-crest ranging from 1 μs to 30 μs.

Figure 2.35 can be used to determine the initial characteristics of both the nonlinear resistors. Each of the V-I points for the nonlinear resistors is found by selecting a current point and then reading the relative IR in pu from the plot. This value is then multiplied by $\frac{V_{10}}{1.6}$ to determine the model discharge voltage in kV for the associated current. This scaling from pu to actual voltage is done by the application of the following formula to the "Relative IR" pu voltage found for that current as shown in Figure 2.35:

For A0,

$$V_d = B_o \frac{V_{10}}{1.6} \tag{16}$$

Likewise, for A1

$$V_d = B_1 \frac{V_{10}}{1.6} \qquad (17)$$

where V_d = Discharge voltage
B_o = Relative IR in pu for A_0
B_1= Relative IR in pu for A_1

The associated V-I voltage for a l0kA current for the nonlinear resistor, A_0 is determined by reading the "Relative IR" for a 10kA current from Figure 2.34. Examination of the plot shows that the "Relative IR" for a 10 kA current is 1.9 pu. Hence the 10kA surge arrestor would have a discharge voltage of 296kV

$$Discharge\ voltage = \frac{1.9*248}{1.6}kV \qquad (18)$$

Furthermore the recommended IEC Triangular waveform is shown as follows
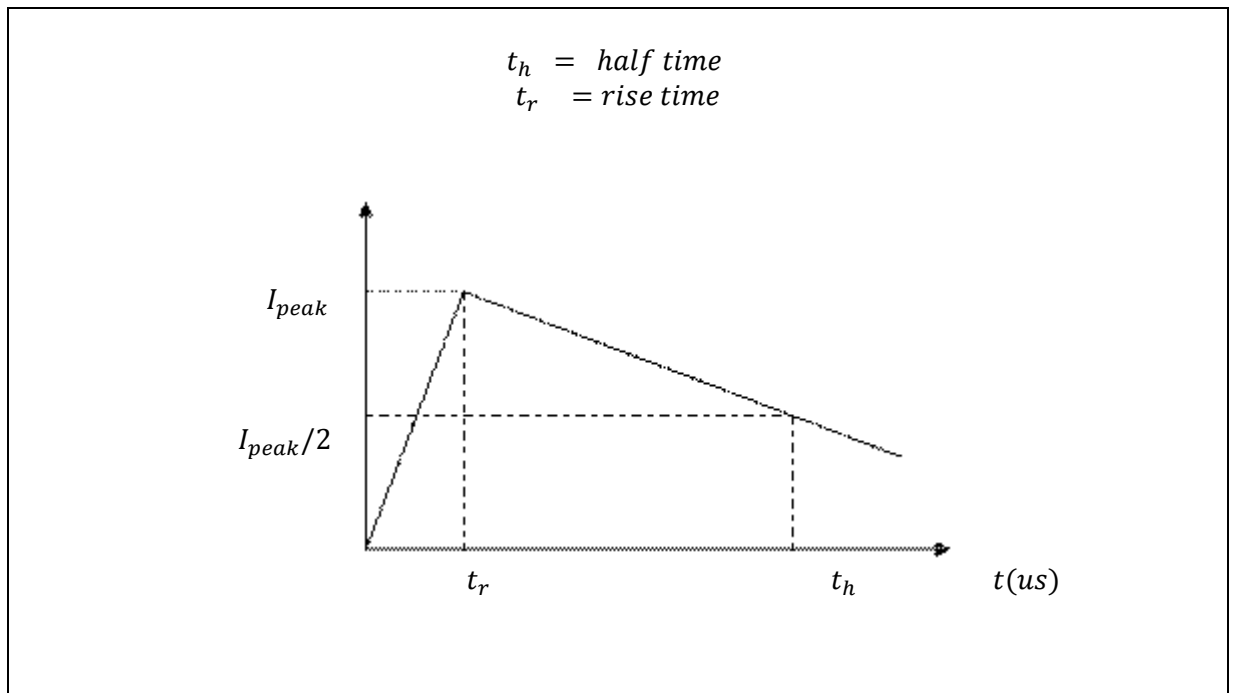
Figure 2.35 Recommended IEC Triangular waveform
Reproduced from reference [48]

2.4.15. Surge Arrestor Energy

Simulation Studies concluded by *Hassan, Et al* [48], *determined the energy obtained from l*ightning strokes that terminate on the tower/ /shield wire and conductors. This energy would provide an indication if the surge arrestor is suitably sized to withstand the stroke.

2.4.15.1 Lightning stroke to Ground Wire or Tower

During a back flash over, the energy discharged by the line arrestor, W_a can be estimated by: [52]

$$= I_a \times E_A \times \tau \quad \dots\dots\dots\dots\dots\dots\dots\dots\dots\dots\dots\dots\dots.(19)$$

Where,
I_a = arrestor current in Amps
E_A = Arrestor discharge voltage in Volts
τ = time constant in second

The time constant of the arrestor current τ is estimated by [48];

$$\tau = \frac{Z_g}{R_i} T_s \qquad\qquad \dots\dots\dots\dots\dots\dots..(20)$$

Where,
Z_g = ground wire impedance, Ω
R_i = footing resistance, Ω
T_s = span length divided by speed of light,

Results obtained by *Hassan, Et al* revealed that for lightning strokes between 20 to 200kA the calculated and simulated energy is below that of the surge arrestor rating. This is shown in table 2.6.

Table 2.6. Energy rating for an 88kv surge arrestor for different current rating

Stroke Current (kA)	Calculated Energy (kJ/kV)	Simulated Energy (kJ/kV)
35	0.06	0.07
80	0.15	0.24
100	0.25	0.31
150	0.50	0.52
180	0.65	0.64
200	0.76	0.73

The surge arrestor rating used on 88 and 132kV lines is 5.1kJ/kV. Hence both the calculated and simulated values are within this value.

CHAPTER THREE   SOIL RESISTIVITY AND TOWER FOOTING RESISTANCE

Chapter 3 deals with the soil resistivity analysis and its impact on the grounding system design. It is proposed that line surge arrestors be installed on power line that is affected by lightning to improve its performance level. There are a number of factors that contribute towards performance level of the line. These factors include soil resistivity, line and tower surge impedance, lightning stroke magnitude, tower footing resistance etc. These factors combined together will determine the flash over voltage that would result from a particular lightning stroke. Should this voltage exceed that of the insulator withstand voltage, a back flash over would occur.

The flash over would result a surge current on the conductor, can be extinguished by the breaker operation. This breaker operation would result in dips and small duration outage to customers, leading to loss of productivity. The following flow chart, figure 1, indicates a process that can be followed to determine the end stage (number of require LSA to prevent outages on power networks). Tower footing resistance and soil resistivity and are two key parameters, which effects the entire process, ending with possible consumer interruptions.
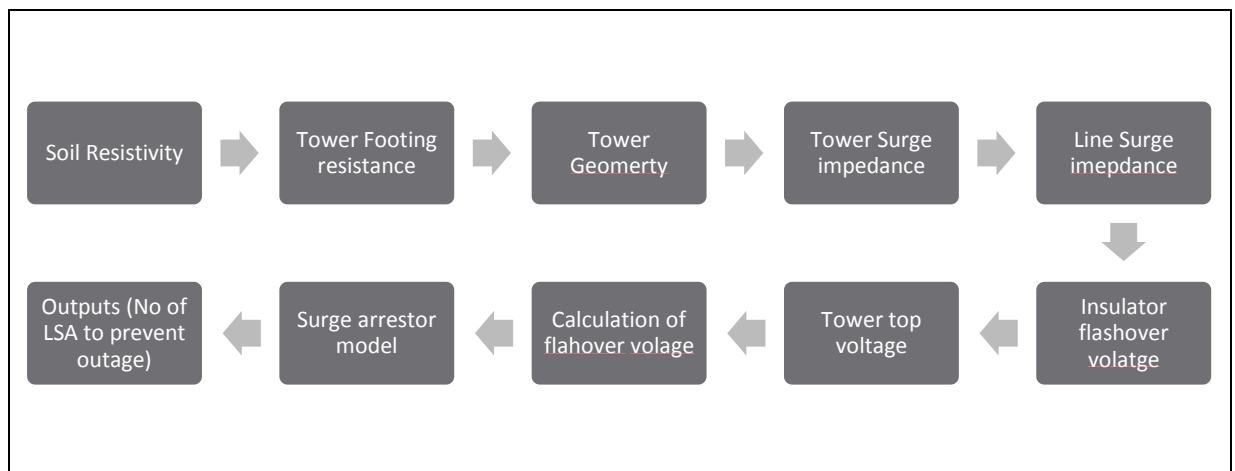

Figure 3.1 Flowchart to determine Phase Voltage resulting from Back Flash Over

3.1 Soil Resistivity

3.1.1 Background

Resistance of a cube of soil of 1 m size measured between any two opposite faces is define as soil resistivity and is expressed in Ohm-metres. Soil Resistivity is one of the main factors in determining the charging electrode resistance and the required depth, it should be planted to obtain low resistance. Any proper earthing system design has to ensure the following :

- Safety of people, animals and equipment.

- Limit voltage elevation to a minimum.

- Ensure that the power system is reliable.

If incorrect soil resistivity values are used, then this may result in the incorrect design of the earthing system, which ultimately can increase the number of consumer interruptions, under lightning conditions. Soil resistance also fluctuates depending on terrain. This fluctuation determines on the type of soil, the soil depth, existence of moisture on the top level and temperature. One of the main objectives of earthing electrical systems would be to establish a common reference potential for that system, building structure, plant steelwork, electrical conduits, cable ladders & trays and the instrumentation system. To achieve this objective, a suitable low resistance connection to earth is needed, which can be difficult to achieve and can depends on the following factors:

Type of earth (clay, loam, sandstone, granite etc).

- Stratification: different layers of soil

- Moisture content: As the moisture content is increased, resistivity should fall.

- Temperature

- Chemical composition and concentration of dissolved salt.

- Presence of tanks, large slabs, metal and concrete pipes, cable ducts, rail tracks. etc

- Topography: the rugged topography would have a similar effect on resistivity measurement as local surface resistivity variation caused by weathering and moisture.

3.1.2 Soil resistivity values for various soil types

Table 3.1 displays the soil resistivity values for different soil types.

Table 3.1 Soil Resistivity for different Soil Types

Soil Type	Resistivity (ohm m)
Clay	40
Clay and Sand Mix	100
Shale, slate and sandstone	120
Peat, Loam and Mud	150
Sand	2000

3.1.3 Factors effecting soil resistivity

3.1.2.1. Stratification

There are three factors under stratification that could affect soil resistivity. These are

1. The number of layers

2. Each layer thickness

3. The refection factor between each layer

3.1.2 2. The effect of different layers on soil resistivity [20]

Earth can be made up of various soil layers of different thickness. The first layer has soil resistivity ρ_1, thickness H and the second layer has soil resistivity ρ_2 with infinite thickness. If $\rho_1 > \rho_2$, the apparent soil resistivity ρ can be calculated by the relationship.

$$P_a = I \frac{p_1 p_2}{p_2(H-h) + p_1(I+h-H)} \tag{1}$$

Where

L = average length of the rod

ρ_1 = upper layer soil resistivity

ρ_2 = bottom layer soil resistivity

H = upper layer thickness

A sub-routine was development in MATLAB and is based on equation 1. Refer to Appendix A. The following two figures 3.2 and 3.3 were generated. This shows the relationship between the upper layer thickness and the soil resistivity. H, ρ_1 and ρ_2 are variables and inputs to the program.
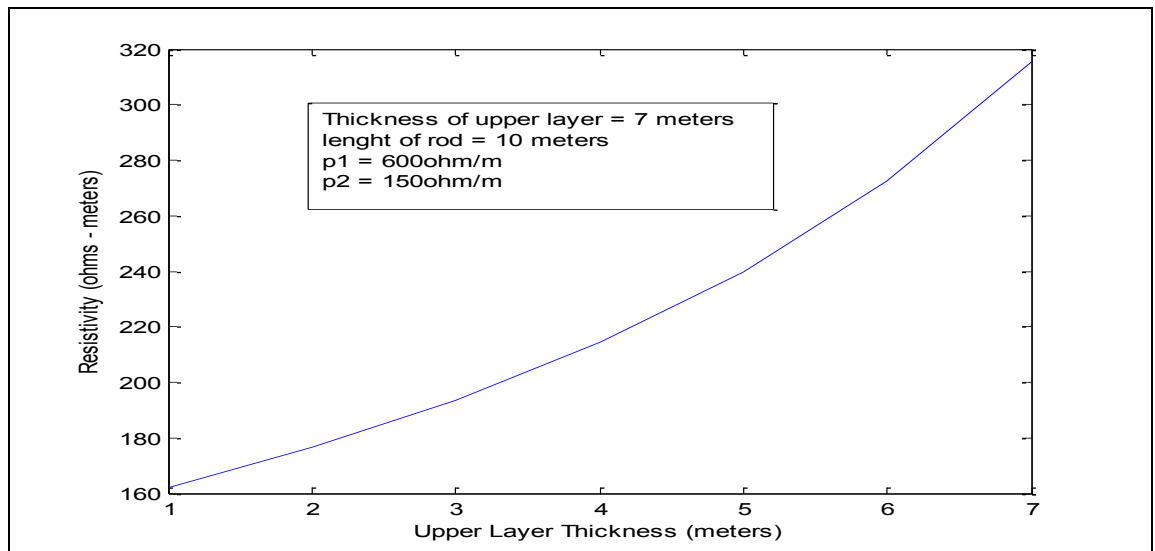

Figure 3.2 Relationship between upper layer soil thickness and resistivity

Upon increasing the thickness of the upper layer, the soil resistivity increases accordingly. This is because the soil resistivity of upper layer is much greater then that of the lower layer. Should the soil resistivity of the upper level be much less then that of the lower level, the soil resistivity decreases accordingly as shown in figure 3.3.
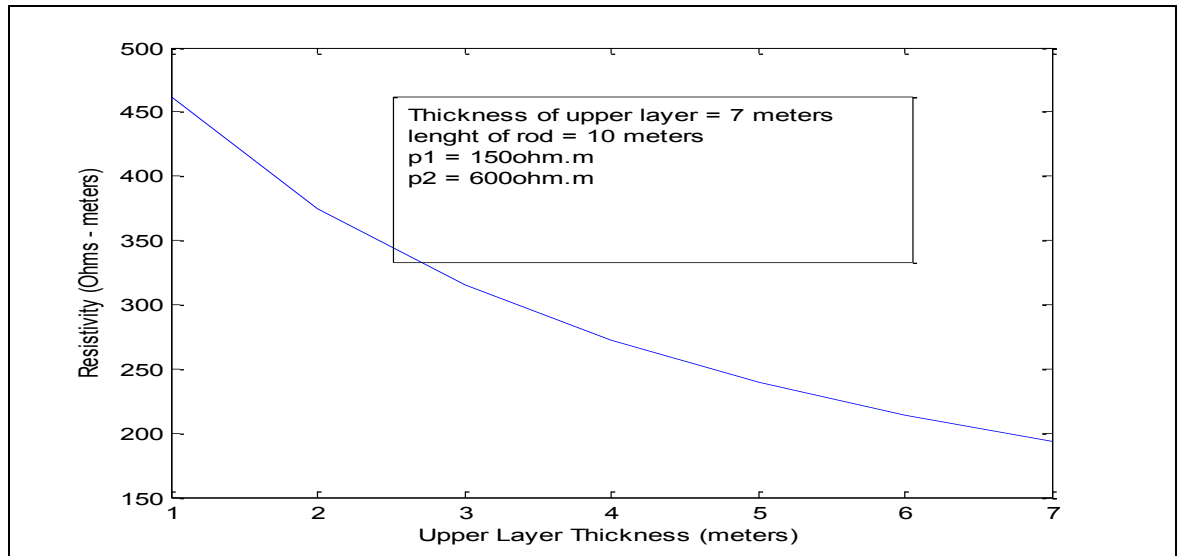
Figure 3.3 Relationship between upper layer thickness and soil resistivity

If there are more than two soil layers, one can combine the lower layers to form a two layer equivalent model. The model can be done because the upper layer resistivity is closely related to the surface potential, while the resistance of the grid, which is mainly effected by the deeper layers, is not usually adversely affected by the simplification. One can conclude that to achieve low soil resistivity, the electrodes need to be embedded in the layer with lower soil resistivity.

3.1.4 Effect of structure, moisture and temperature on soil resistivity

The differences in soil type and seasonally changes due to variations in the soil's electrolyte content and temperature would result in different soil resistivity for different regions. It is therefore recommended that these variations be considered when assessing soil resistivity. The two ways to measure soil moisture are.

1. Soil Moisture Tension
2. Soil Moisture Content

3.1.4.1 Soil moisture tension

Soil moisture tension indicates the difficulty in extracting water from soil, i.e the force per unit area required to separate soil from water. A soil that is saturated means that there is a lot of water in the pore spaces and coating the soil particles. This results in the soil moisture tension been low and the moisture makes it very easy for plant roots to get water

When the soil tension reaches a certain threshold, plants can no longer extract water from the soil even though water is present. The water is stuck to the soil particles and they won't release it. At this point the plant will become stressed, wilt and eventually die if water is not replenished.
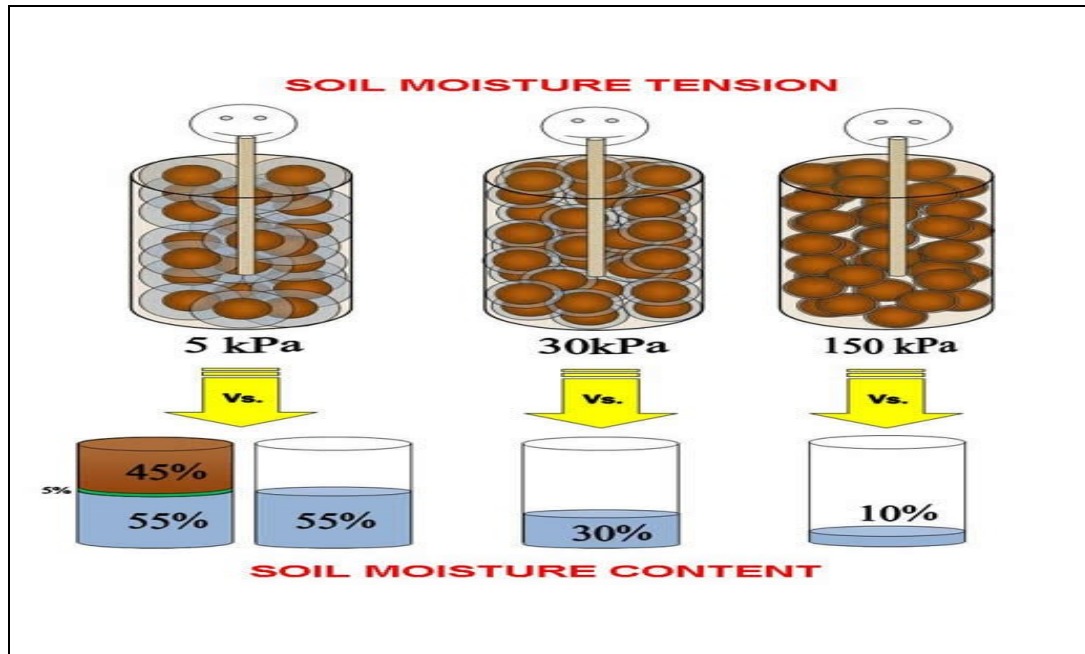

Figure 3.4 Soil moisture tension vs content
Reproduced from Reference [56]

Figure 3.4 shows that the greater the tension the less water will be present. This would have the effect of dry soil and increase resistivity as shown in Figure 3.5. Resistivity can be seen to be directly proportional to the Tower footing resistance. This would have the net effect of increased power outages.

3.1.3.4 Soil moisture content

Soil moisture content is a measure of the amount of water in the soil and is expressed as a percentage. What percentage of the total 'volume' of soil is moisture? Take a cubic metre of top soil. Remove the soil particles and then compact to remove all gaps between them (assume that it squashes down to about 40% of its original volume). Undertake a similar exercise for the organic matter. This should occupy about 5% of the volume. The volume that is left is made up of pore spaces which can be occupied by either air or water.

Hence, the water component, in a totally saturated sample of this soil as shown in Figure 3.4, would be 55% of the original cubic meter. The remaining 45% is soil. The soil holds onto a layer of water that is inaccessible to plants. This results in the value of the "dry" soil, (occurs when roots cannot get any

more moisture and plants become stressed, wilt and die), will not be 0% but something slightly more [57].
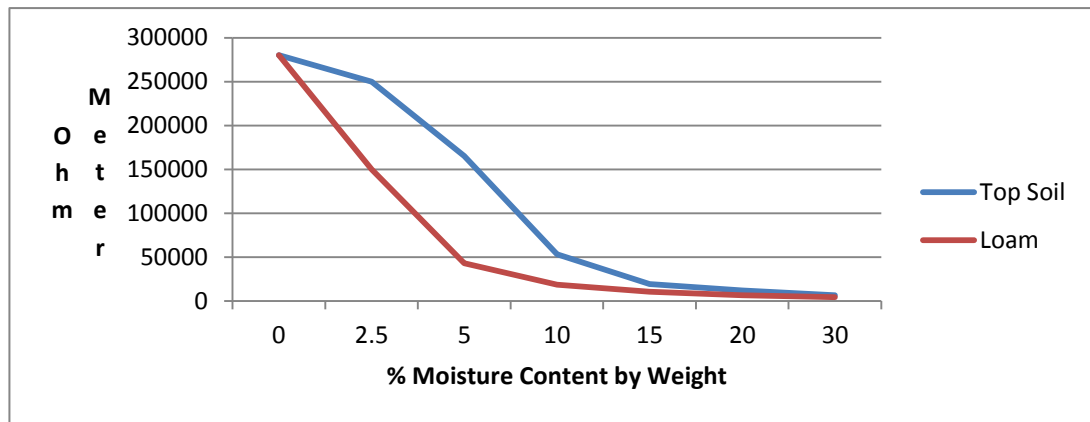

Figure 3.5 Soil Moisture content vs Soil Resistivity

The soil moisture content can be expressed by volume as ratio of volume of water to the total volume of the soil sample. It can also be expressed by weight as the ratio of the mass of water present to the dry weight of the soil sample.

The soil moisture content ratios for a particular soil sample may be determined by :
- The water mass must be determined by drying the soil to constant weight
- Measure the soil sample mass before and after drying. The difference between the weights of the wet and oven dry samples water mass (or weight) is the water mass.
  Note: The criterion for a dry soil sample is the soil sample that has been dried to constant weight in oven at temperature between 100 – 110C (105 C is typical).

3.1.5 Techniques available to measure the content of soil moisture
Listed below are some of the techniques that can be utilised to measure soil moisture content [58].
- There is classic gravimetric moisture determination, which is a simple direct method.
- There is lysimetry, which is a non-destructive variant of gravimetric measurement. In this method, the container filled with soil and is weighed either continuously or occasionally. This would determine the changes in total mass in the container. These changes may be in part or totally due to changes in soil moisture
- Various radiological techniques, such as neutron scattering and gamma absorption, can indirectly determine the water content.
- Water content can also be derived from the dielectric properties of soil, for example, by using time-domain reflectometry.

- Soil moisture can be measured inferred on a global scale from remotely sensed measurements of the earth's thermal or reflective properties.

The measurement by the gravimetric method will be discussed in 3.1.6.

3.1.6 Procedure to measure soil moisture content using the gravimetric method

- Weigh and record the weight of the aluminium tin [59]
- In the tin, a soil sample of about 10g should be placed and the weight recorded (wet soil + tare).
- The sample should be placed in the oven, which should be set for 105C. Dry for 24 hours. The weight of the sample must be recorded (dry soil and tare).
- The sample should be replaced in the oven and dried for several hours, Thereafter the weight must be recorded (dry soil and tare).
- Repeat point 5 until there is no difference between any two consecutive measurements of the weight (dry soil and tare).

3.1.7 Effect of temperature on soil resistivity

The effect temperature has on soil resistivity is predominant at or near 0ºC. At this temperature the resistivity increases sharply. In general, soil resistivity decreases as temperature increase and vices verse. This phenomenon is highlighted in Figure 3.6. Also the greatest rate of change in soil resistivity is at the point where moisture in the soil freezes. The following table and graph illustrates the effect of temperature on soil resistivity [60] .

Table 3.2 Effect of temperature on soil resistivity

| Temperature (Celsius)	Resistivity (Ohm-meter)
-5	700
0 (ice)	300
0 (water)	100
10	80
20	70
30	60
40	50
50	40

Reproduced from reference [60]
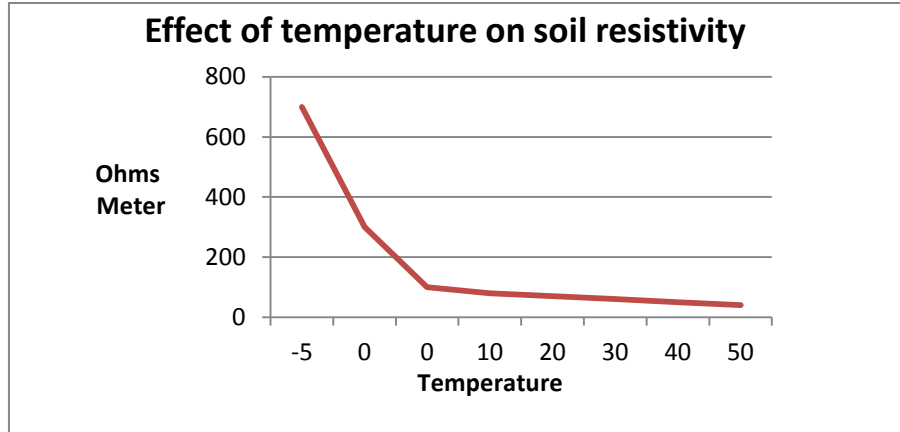
Figure 3.6 Effect of temperature on Soil Resistivity

3.1.7 Measuring soil resistivity

The three common test methods for measuring soil resistivity, the Wenner 4 pin, Schlumberger Array and the driven rod method are discussed in the following sections.

3.1.7.1 Wenner 4 Pin Method

From an operational perspective, the Wenner method is the least efficient. It requires the longest cable layout and largest electrode spacing. The large spacing's requires one person per electrode to complete the survey timeously. The Wenner Array is most susceptible to lateral variation effects. This is because all four electrodes have to be moved after each reading.

In terms of the ratio of received voltage per unit of transmitted current, the Wenner array is the most efficient. If unfavourable conditions, like very dry or frozen soil, are present, considerable time would have to be spent trying to improve the contact resistance between the electrode and the soil. The schematic system used for the Wenner test is shown in Figure 3.7.
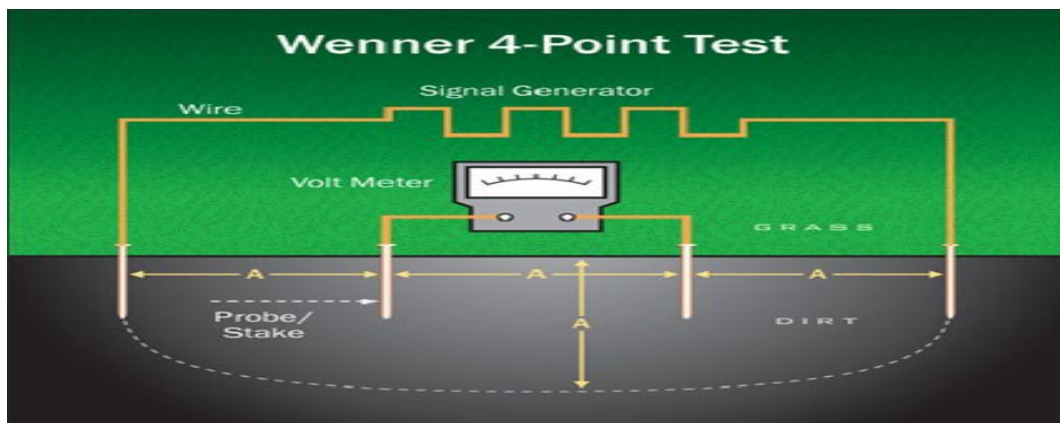
Figure 3.7 Wenner 4 point test method
Reproduced from reference [23]

The Wenner 4 point test is commonly performed during the design and planning of grounding systems at the raw land sites.

The A - spacing should be changed to get the resistivity as a function of depth. The A spacing can be logarithmically increased with a 5-7 values per decade. The maximum value of A -spacing should be at least 3-5 times the maximum depth of investigation.

3.1.8 Schlumberger Array

- Since the outer electrodes are moved 4 or 5 times for each move of the inner electrodes, economy of manpower is gained with the Schlumberger array
- The effect of lateral variation on test results is reduces due to the reduction in the number of electrode moves.
- By using the reciprocity theorem with the Schlumberger array when contact resistance is a problem, considerable time saving can be achieved.
- Contact resistance normally affects the current electrodes more than the potential electrodes, hence the inner fixed pair may be used as the current electrodes. This configuration called the 'Inverse Schlumberger Array'. It should be noted that use of the inverse Schlumberger array can increases personal safety when a large current is injected.
- Should the magnitude of the current be large, thicker current cables may be needed. The inverse schlumberger array decreases the length of the bulkier cable and more time is required to move the electrodes.
- For a 0.5m inner spacing, the minimum spacing accessible is in the order of 10 m. This necessitates the use of the Wenner configuration for smaller spacing
- When using Schlumberger arrays, reduced voltage readings are obtained.

Figure 3.8 shows the schematic system for the Schlumberger Array.


Figure 3.8 Schlumberger Array
Reproduced from reference [61]

3.1.8.1 Field procedure

• The potential electrodes (P) are kept stationary and the current electrodes (C) are moved out.

• This array is symmetric with the current electrodes placed at a distance L from the centre.

• The distance indicated by MN separates the potential electrodes.

• Moving the current electrodes out would result ΔV becomes smaller and smaller until it becomes to small too small to measure. The current electrodes are then moved out and the measurements continues.

• The apparent resistivity requires a more complicated formula.

• The a - spacing is logarithmically increased by 5-7 values per decade.

• The maximum value of L in a Schlumberger array should be at least 3-5 times the maximum depth of investigation.

3.1.9 Fall of Potential Technique

Figure 3.9 shows the connectivity for the Fall of Potential Technique
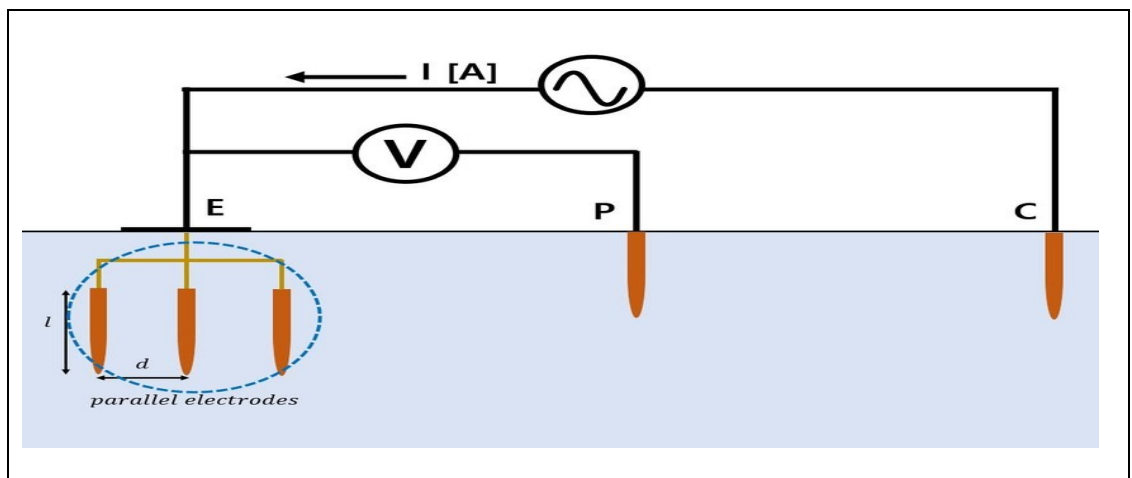
Figure 3.9 Fall of Potential Technique
Reproduced from reference [12]

This technique requires three points of ground contact. One of these points is the earth electrode under test (COM). A current probe (C) is placed at some distance from the ground system under test and a voltage probe (P) is inserted at various distances between the system under test and the current probe. The Megger meter is then used to inject current into the tower footing earth electrode under test [12].

A voltage drop was created, when the current flows through earth, which is the resistive material. This voltage drop, which is measured by a voltage probe (P), is proportional to the amount of current flow and the resistance of the earth electrode to earth. The meter shows the amount of current flow and the

voltage drop. By moving the voltage probe (P) at regular intervals, the resistance at several locations can be measured. The intervals should equal to 10% distance of COM and C.

During measurement, the current probe (C) position should be moved far enough away from the earth electrode under test so that the voltage probe (P) can lie outside the effective resistance areas of both the test and earth electrode. This is because there may be overlapping of the resistance areas which can cause a steep variation in the measured resistance

3.1.10 Soil Resistivity Test

Two locations were identified for soil resistivity measurements and analysis. These areas are Kwa - Makhutha Comprehensive High School (KCHS), with coordinates: 30.0210°S and 30.8665°E and Durban University of Technology (DUT), with coordinates: 29°51'09″S and 31°0'13″E. Both these site are located within Durban area of South Africa. The wet and dry soil conditions were tested on both locations. The Wenner Method was utilised and a series of measurements were taken at the two respective locations.

1. Location 1

The Durban University of Technology premise in Kwa Zulu Natal was the first test location chosen for this work. The type of soil found at this site is the red loamy soil.

a. Location 1 - wet soil conditions

These measurements were taken on the 28th of October 2017, between 7 am and 12 pm. This was a day after the occurrence of a light rain of approximately 4 mm/hr, which should increase the moisture content of the soil. The light rain lasted for duration of approximately 8 hours at the measurement site. Furthermore the recorded temperature at the time of observation was 22 degrees celsius.

b. Location 1 - dry soil condition

These resistance measurements were taken on the 4th of November 2017, between 7 am and 12 pm. This is eight days after the site experienced rainfall. Hence the soil moisture content was very low at this observation time. Furthermore the recorded temperature at the time of observation was 25 degrees celsius.

2. Location 2

The Kwa-Makhutha Comprehensive High School premise was the second test location.. The type of soil found at this site was gravel soil.

a. Location 2 - wet soil conditions

These resistance measurements were taken on the 28th of October 2017, between 1pm and 6pm. This was a day after widespread rains of about 7 mm/hr occurred, which should result in the soil moisture content of the soil been high. The rain last for a duration of 12 hours at this site and temperature recorded was approximately 21 degrees celsius.

b. Location 2 - dry soil condition

These resistance measurements were taken on the 4th of November 2017, between 1pm and 6pm. This was 5 days after the occurrence of rain at this site. Hence the soil moisture content was very low and the recorded temperature was approximately 25 degrees celsius.

B. Step Wise Method of Measurements

Probes were equally spaced and placed in a straight line. Also for each measurement the probes were placed at different soil depth. The soil depth ranged from 0.5m to 2.5m. The wire conductors were connected to the probes and meter. The probes were driven to the earth to establish electrical contacts. The two outer probes C1 and C2, which are connected to the meter, would inject constant current to the ground. The current would flows through the earth (resistive material) and develop a potential difference or voltage. The inner probes P1 and P2 measure the voltage drop. The depth of the test electrodes was calculated from equation (2).

$$b = 0.1a \tag{2}$$

a is the distance between the electrodes

b is the depth of the electrode

3.1.11 Results and discussions

Generally the soil resistivity values for the two locations DUT and KCHS follows the expected variation with different depth. Both location measurements were analysed and discussed in the several graphs shown in table 3.3.

A. Location 1 - DUT wet soil conditions

Table 3.3 shows the relationship between soil depth and resistivity and that of soil resistance and depth respectively under both dry wet conditions. Upon increasing the spacing the resistivity decreases. This indicates that the top layer has a higher resistivity compared to the bottom layer.

B. Location 1 - DUT dry soil conditions

The heat generated during the hot days would dry the soil and increases the resistivity of the soil. The upper layer is most affected and will show the greater resistivity change. There is a change of about 400 ohms-meter as the depth is increased.
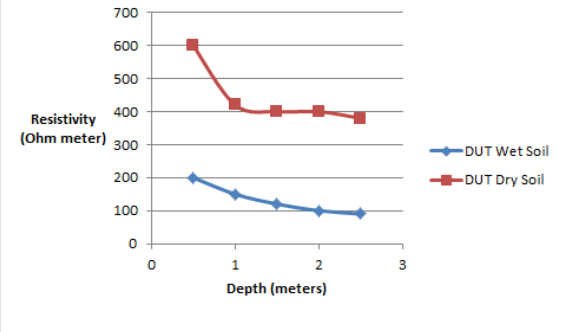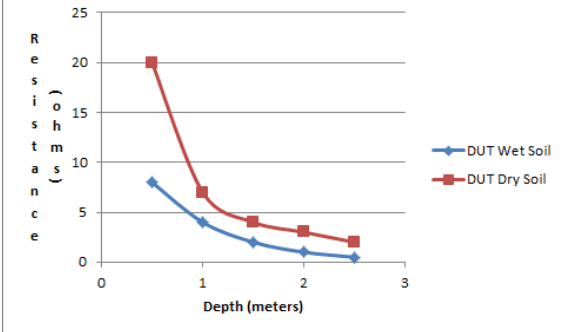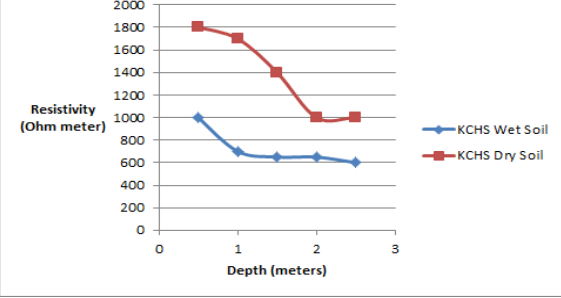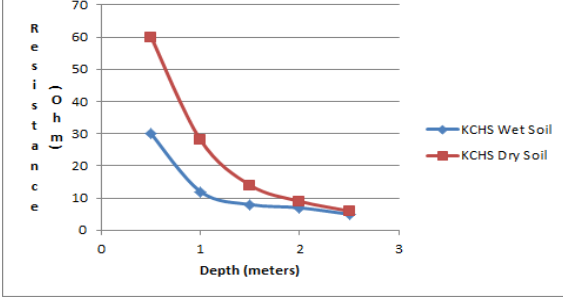
C. Location 2: KCHS wet soil conditions

The results obtained from the Kwa-Makhutha site, shows that resistivity also depends o the soil type encountered at the site. The soil type at DUT is loam, which gave a lower resistivity value that the gravel soil at the Kwa-Makhutha site. Also as expected the resistivity decreased as the soil depth was increased.

D. Location 2: KCHS dry soil conditions

The heat generated during the hot days would dry the soil and increases the resistivity of the soil. The upper layer is most affected and will show the greater resistivity change. At a depth of 0.5 m the resistivity was 1826 ohm-meter. This changes to 1000 ohm-meter as the depth was increased to 2m. This shows that the upper level has a higher resistivity then the lower levels

Table 3.3 Soil Resistivity/Soil Reistance vs Soil Depth for DUT and KCHS

Fig 3.3.a Relationship between soil resistivity and depth for DUT under wet and dry soil conditions.

Fig. 3.3b Relationship between soil resistance and soil depth for DUT under dry and wet soil conditions

Fig. 3.3c Relationship between soil resistivity and depth for KCHS under dry and wet soil conditions

Fig. 3.3d. Relationship between soil resistance and depth for KCHS under wet and dry soil conditions.

It is recommended to use extreme soil parameters as worse case scenarios for grounding system design. This would provide maximum protection against external influence such as lightning strokes. The higher the soil resistivity is, the more the number of electrodes required to achieve the desired earth resistance value. The layer thickness also places a role in determine the resistance values and the soil layers. Normally, the grid or the electrode is buried in the upper layer.

3.1.12 Conclusion

1. The investigation indicates the soil resistivity for dry soil conditions is greater than that of wet conditions. The depth at which the readings was taken remain consistent.

2. Relating this into South Africa weather patterns, one would expect high soil resisance at the onset of the summers season, hence a higher amout of back flash overs and consumer outages.

3. The Resistance curve offer the same trend.

3.2. Tower Footing Resistance

3.2.1 Modelling of Soil Resistivity

Currently there are four types of configuration and earthing methods and configuration available for improving tower footing resistance. These are:

1. Horizontal electrode
2. Driven rod (Vertical electrode)
3. Ring electrode
4. Earthing grid

3.2.2 Vertical electrode (Driven rod)

The vertical electrode method is the more common method of earthing towers. This method results in an electrode is driven vertically into the ground. If the desired resistance is still high then additional electrodes should installed/driven into the ground. The vertical electrodes would thus be installed in parallel. Utilising the MATLAB program, a genetic model was created. This model was developed based on the following formula (3) [11, 12].

$$R = \rho \frac{\left[\ln\left(\left(\frac{L}{\alpha}\right)+((r-1)\times D)\right)\right]}{2\times r\times L\times \rho} \tag{3}$$

Where:

R = Tower footing resistance

r = Number of electrodes

ρ = Soil resistivity

L = Conductor length (meters)

a = Conductor radius (meters)

D = distance between rods (meters)
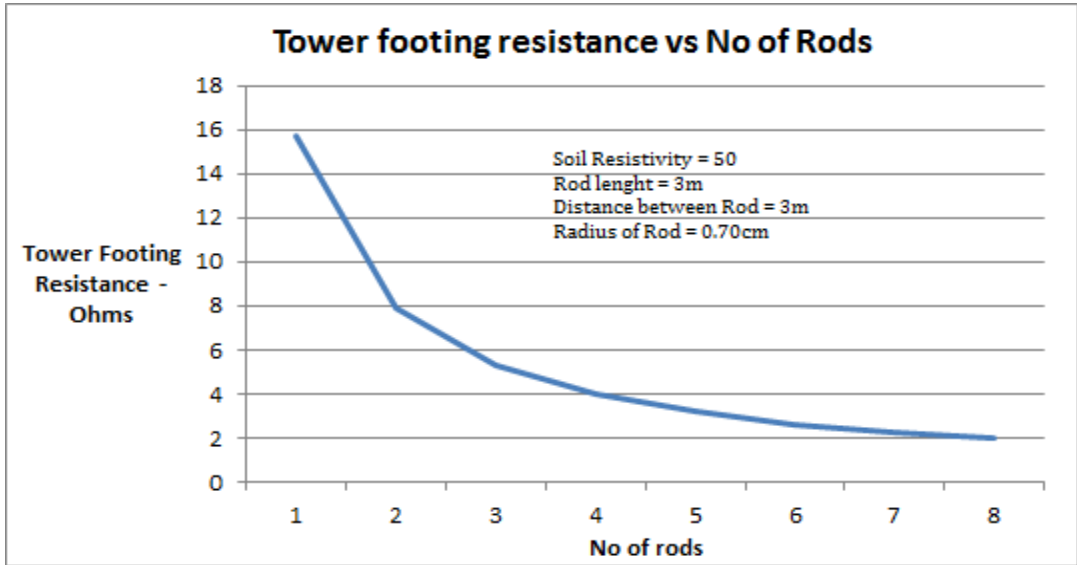
Figure 3.10 Decrease in earth resistance as the conductor length increases.

The sub-routine was created using the variables as inputs to the program and the outpt been the tower footing resistance values. The soil resistivity is considered to be uniform. From figure 3.10, it can be deduced that upon increasing the number of electrodes, the tower footing resistance tends to converge towards a particular number. Hence it is not economically viable to increase the number of electrodes beyond this 'saturation' number.

3.2.3 Horizontal electrode (crows foot)

This type of earthing method is more suited and effective when the down wire is connected to a point in the middle of the electrode. This creates a parallel transmission path, which would half the surge impedance. Crows foot can be more effective should they be used in combination with spike electrodes, which can be located close to the junction of the down conductor. The following formula (4) can be used to calculate the resistance [11, 12]:

$$Rg = \rho(ln\left(\frac{4L}{\sqrt{dh}}\right) - 1)/\pi L \tag{4}$$

Where:

ρ = soil resistivity (ohm-meter)

L = Buried electrode length (meters)

d = Electrode diameter (meter)

h = buried electrode depth (meter)

The tower footing resistance was calculated by developing a genetic model in MATLAB based on equation 4. The following parameters are used:

$\rho = 90$ ohm-meters

$h = 0.5$ meters

$d = 10$ mm

$L = 10$ meter and increased to 60 meters
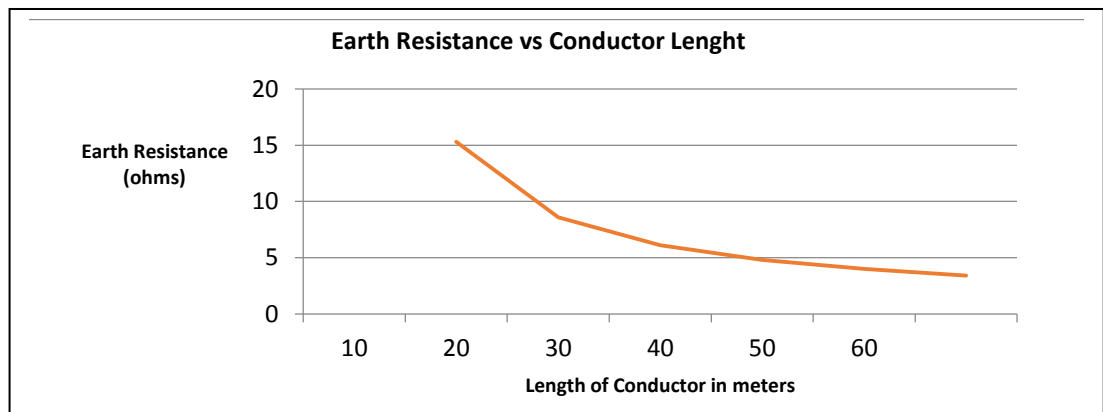
Figure 3.11 Relationship between earth resistance and length of conductor

Figure 3.11 indicated that as the conductor length increases that there is a significant reduction, of 78%, in the earthing value. A further scenario was considered where the length of the conductor was maintained at 50 meters and the depth to which it is buried varied between 0.5 to 4 meters.
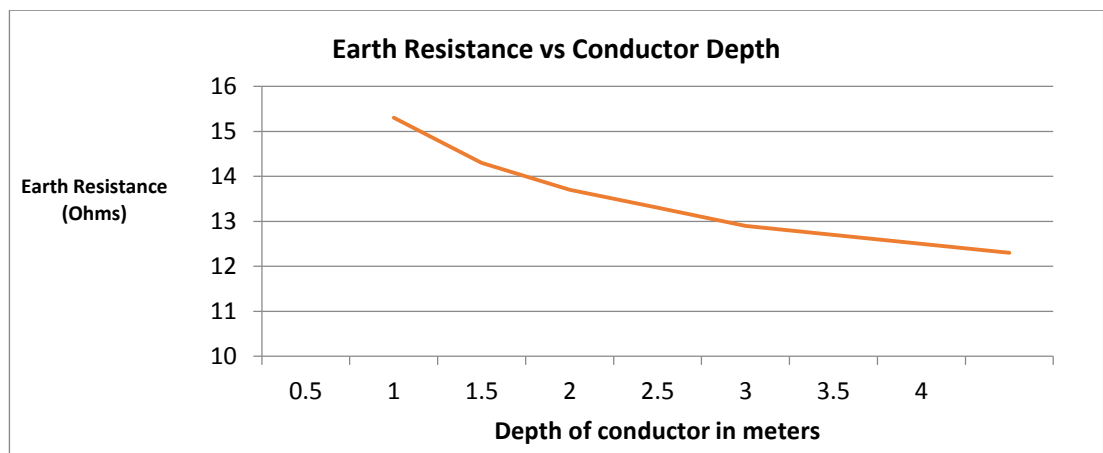
Figure 3.12 Relationship between earth resistance and depth

From figure 3.12, the earth resistance values decreased by 19.6%. In both scenarios, a 'saturation limit' was reached. Hence it is not economically viable to increase the number of electrodes or the depth it is planted at beyond this 'saturation' number.

3.2.4 Radial conductors

For this earthing type, the tower footing resistance was calculated by developing a genetic model in MATLAB based on equation 5 [11, 12].

$$Rg = \rho(ln\left(\frac{4L}{\sqrt{dh}}\right) - 1 + N(n))/n\pi L \tag{5}$$

Where

ρ = Soil resistivity in ohm-meter

L = Buried electrode length (meters)

d = Electrode diameter (meters)

h = buried electrode depth (meters)

n = number of radials

Table 3.4 displays the resistance values obtained for various numbers of radial conductors. The following unit parameter values were used: $\rho = 90$, L = 50, d = 0.01, h = 0.5

Table 3.4: Number of radials and resistance

N*	2	3	4	6	8	12
N(n)	0.7	1.5	2.45	4.42	6.5	11
Rg-ohms	2.1	1.6	1.34	1.09	0.96	0.85

*Number of radial conductors

Graph of Resistance values vs No of Conductor
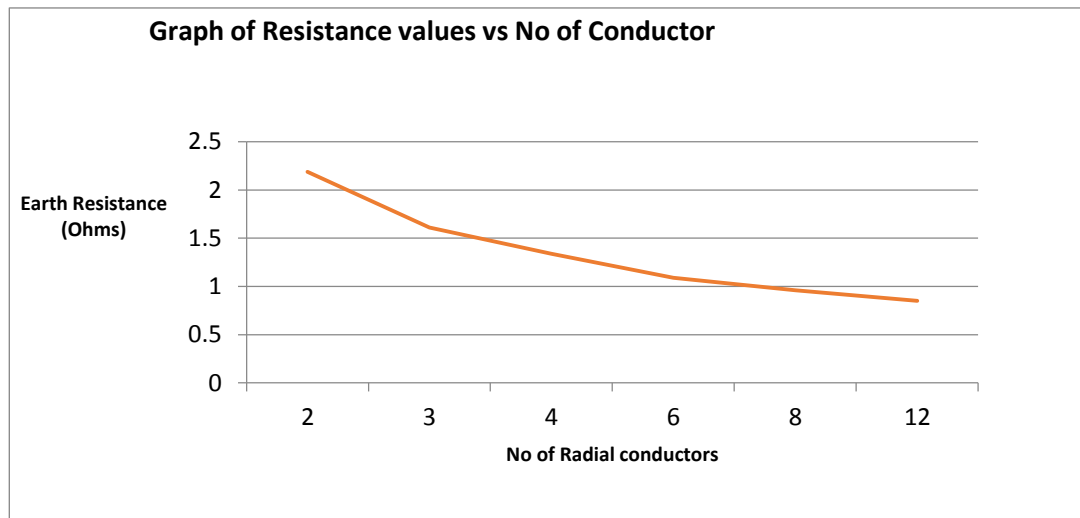
Figure 3.13 Relationship between number of radial conductor and resistance values.

Figure 3.13 displays a 'saturation limit', in terms of the number of electrodes used against further benefit of a reduction of resistance values.

3.2.5 Suggested options to improve high tower footing resistance

By adopting the following techniques, the tower footing resistance can be minimized by:

(i.)   One may utilise short radial conductor lengths bonded at the injection point, instead of a single long conductor length. This results in having a number of conductors in parallel.

(ii.)   In low to medium soil resistivity, one may terminate radial conductors with vertical electrodes.

(iii.)   Sharp bends tend to increase the inductance, hence one may utilise large bending radii when changing the direction of horizontal conductors.

(iv.)   There are earths enhancing compounds available to better the soil resistivity in the proximity of the conductor. This will reduce the tower footing resistance.

3.2.6 Tower Footing Resistance Factors

Tower footing resistance (TFR) can be affected by a number of factors, which must be considered when designing grounding system for transmission line tower. Some of these are;

- Electrode configuration.
- Configuration available for improving TFR: Vertical electrode (Driven rod).
- Grounding System design.

a) Electrode Configuration

An earth electrode can be a conductor, plate or a metal pipe. This is electrically connected to earth and can be made of aluminium, copper, galvanised steel or mild steel. The factors affecting the earthing are:

- Electrode depth.
- Soil moisture content.
- Soil temperature.
- Electrode resistance.
- Soil composition at the site.

b) Configuration available for improving TFR: Vertical electrode (Driven rod)

During earthing system design, should the acceptable value for soil resistance be exceeded, then the soil resistance may be enhanced using different methods. These methods include vertical rods, salting and chemical treatment. The earth of the towers can be improved by the using vertical electrode method. Furthermore for the vertical rod configuration, addition electrodes can be can be driven into the ground in parallel to meet tower footing resistance value. The following formula may be used for the parallel rods configuration.

$$R = \rho \frac{\left| \ln\left(\left(\frac{L}{a} \right) + \left((r-1)*D \right) \right) \right|}{2*r*L*3.14} \tag{6}$$

c). Grounding System design

The grounding system design requirements for large substations and for enhancing the existing tower footing resistance will require the accurate value of soil resistivity on the site. The IEEE suggests that two layers shall be used throughout the computation of earth grid. This resistivity was obtained by the following formulae used for two layers

$$P_a = \frac{p_1}{\left[1 + \left| \frac{p_1}{p_2} - 1 \right| \times \left| 1 - e^{\frac{1}{-k(d+2h)}} \right| \right]} \tag{7}$$

It makes design sense that a deep electrode to be used to reach the lower resistivity layers, i.e should be driven through the upper level, this enhancing the performance of the earth grid. Parallel vertical electrodes configuration is recommended if the resistance is more than the required value.

1. Location 1: DUT wet soil condition

For location 1 under wet conditions the resistance decreased as the number of rods increased. Upon increasing the length of the rod from 5 to 10 meters, the resistances decreased further. Both curves showed the same slope.

2. Location 1: DUT dry soil condition

The apparent resistivity for the dry soil is higher compared to wet soil. Due to the dryness the soil, the number of rods required is more than of the wet soil. Table 3.4 shows that for the resistance to be below 10 Ω, about 4 or more rods should be used.

3. Location 2: KCHS wet soil condition

The same pattern of resistance at DUT was encountered at Kwa-Makhutha. Here highly resistive layer overlaid low resistivity layer due to the different soil types. Vertical electrode configuration can be employed for resistance correction. As shown in table 3.5, 5 and 10 meters rod are simulated to see the change in resistance. Rods with a length of 5 meters require a total of 16 rods or the resistance to be approximately 10 Ω. Should the rod lengths be increased to 10 meters, the number of required rods would be at least 10.

Table 3.5 Relationship between earth resistance and number of rods under wet and dry conditions

Fig 3.5a Relationship between earth resistance and number of rods for DUT under wet soil condition	Fig 3.5b Relationship between earth resistance and number of rods for DUT under dry soil condition.
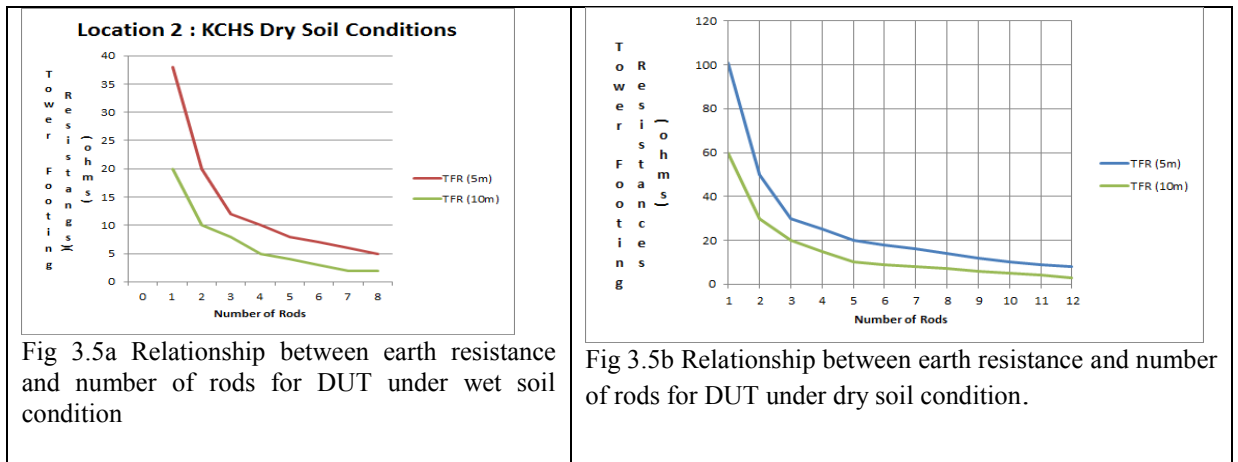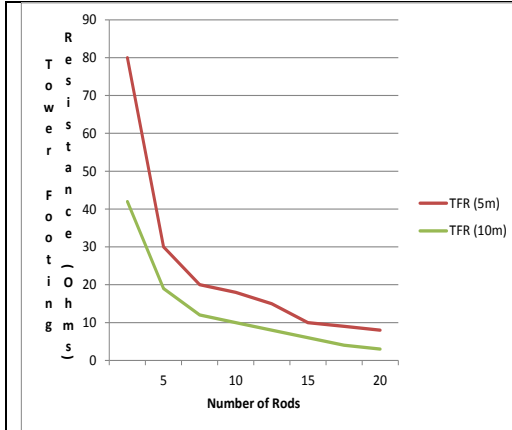
Fig 3.5c Relationship between earth resistance and number of rods for KCHS under wet soil condition	Fig 3.5d Relationship between earth resistance and number of rods for KCHS under dry soil conditions
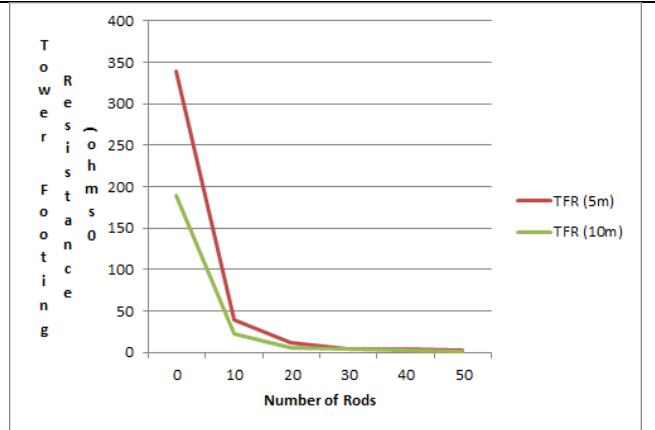
At Kwa-Makhutha, about 35 rods were required to correct the resistance when using a 5 meters long rod (see fig 3.5d).

The investigation shows the by increasing the number of rod, the tower footing resistance would decrease. This is for both set of readings. The results obtained from the dry conditions shown higher readings than the wet cases. The depth at which the readings was taken remain consistent. This confirms the theroical study that by increasing the numer of rods the tower footing resistance would decrease. This would have the net effect of improving network performance.

CHAPTER FOUR   METHOLOGY FOR EVALUATING HVAC AND EHVDC LINE PERFORMANCE

4.0. High Voltage Alternating Current (HVAC) and EHVDC systems

In this sub chapter the methodology is to determine the over-voltages resulting from pre -determined lightning stroke magnitudes. Also the required number of surge arrestors to drain the power surge to ground is calculated. The process that is followed for both systems is that shown in Figure 4.1. The soil resistivity and tower footing resistance are discussed in detail in Chapter 3 and is not repeated here. However the outputs of these studies are briefly discussed for continuity purposes.
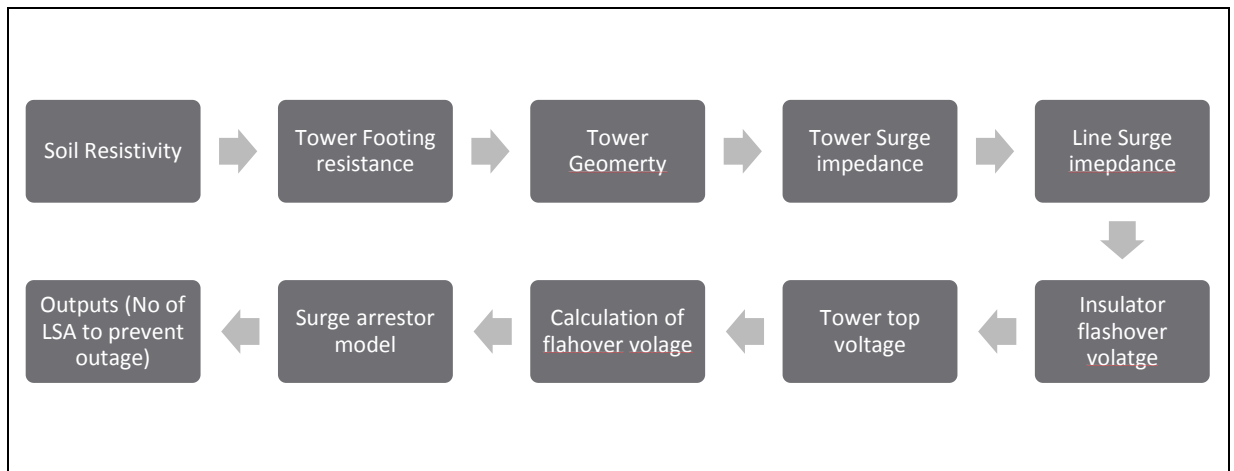
Figure 4.1 Flow chart to determine number of line surge arrestors to prevent breaker operations

4.1. Tower Footing Resistance

MATLAB sub routines were created to determine Tower Footing Resistance for both HVAC and EHVDC systems and are displayed in Appendix A. The program, including sub routines, were created with the inputs been the variables and the output been the tower footing resistance. The soil resistivity is assumed to be uniform, as in Chapter 3.1 and is also an input to the model.

Driven Rod:

$$R \; = \; \rho \frac{\left|\ln\left(\left(\frac{L}{a}\right) + ((r-1)*D)\right)\right|}{2*r*L*3.14} \tag{4.1}$$

Horizontal electrode (crows foot)

$$Rg = \rho(\ln\left(\frac{4L}{\sqrt{dh}}\right) - 1)/\pi L \tag{4.2}$$

Radial conductors

$$Rg = \rho(\ln\left(\frac{4L}{\sqrt{dh}}\right) - 1 + N(n))/n\pi L \qquad (4.3)$$

Where:

R = Tower footing resistance
ρ = Soil resistivity in ohm-meter
L = Conductor length (meters)
a = Conductor radius (meters)
D = Distance between rods (meters)
L = Buried electrode length (meters)
r = Number of electrodes
d = Electrode diameter (meters)
h = buried depth of the electrode (meters)
n = number of radials

Once again the sub-routines created in MATLAB showed the variables as the inputs to the program and the outputs been the tower footing resistance values. The sub-routine then compares the expected tower footing resistance of the three cases as discussed in Chapter 3. Thereafter the method that provides the lowest tower footing resistance is identified and that value is used further in the program. This flow process is shown in Figure 4.2
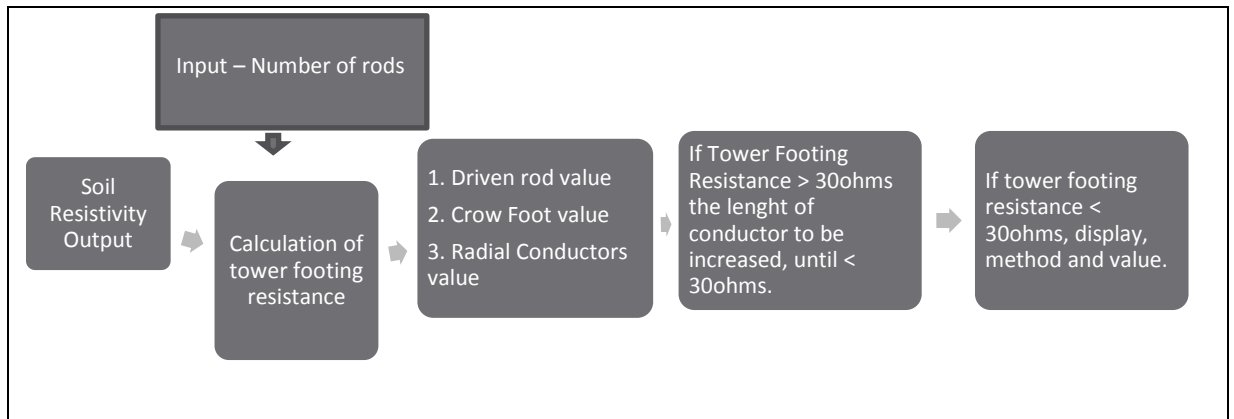
Figure 4.2 Flow diagram - Calculation of Tower Footing Resistance

4.2 Procedure and method to determine the surge impedance of the tower and line

The process that is followed is that shown in figure 4.1.

4.2.1 Tower Model

A MATLAB subroutine was created, using the process in figure 4.3, to calculate the tower surge impedance. This is based on the lumped inductance model and the modeling is based on the following equation.

$$Z_T = 60\ln\left(\cot\left[0.5\tan^{-1}\left(\frac{r_{avg}}{H_t}\right)\right]\right) \qquad (4.4)$$

Where $r_{avg} = \dfrac{r_1 h_1 + r_{2(h_1 + h_2)} + r_3 h_1}{h_1 + h_2}$ \qquad (4.5)

Z_T = average tower surge impedance

r_1 = tower top radius

r_2 = tower mid-section radius

r_3 = tower base radius

h_1 = height from base of tower to mid-span

h_2 = height of mid span to top

Figure 4.3 shows the process to calculate the tower surge impedance.
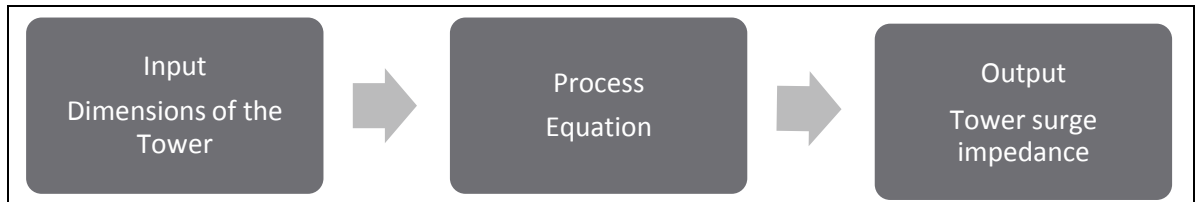
Figure 4.3 Flow diagram - Calculation of Tower Surge Impedance

4.1.2 Line Model

As discussed in Chapter 2 section 2.8, the following equation may be used to calculate the line impedance.

$$Z_g = 60\ln\left(\frac{2h}{r_g}\right) \qquad (4.6)$$

Utilisation equation 4.4, 4.5 and 4.6, a sub-routine was developed to calculate the surge impedances. For the HVAC system, the tower surge impedance was 117 and 416 ohms for the conductor. For the EHVDC system, the tower surge impedance was 121 and 417 ohms for the conductor.

4.3 Procedure and method to determine the tower top voltage for the HVAC and EHVDC systems.

The process that is followed is that shown in the flowchart in Figure 4.4
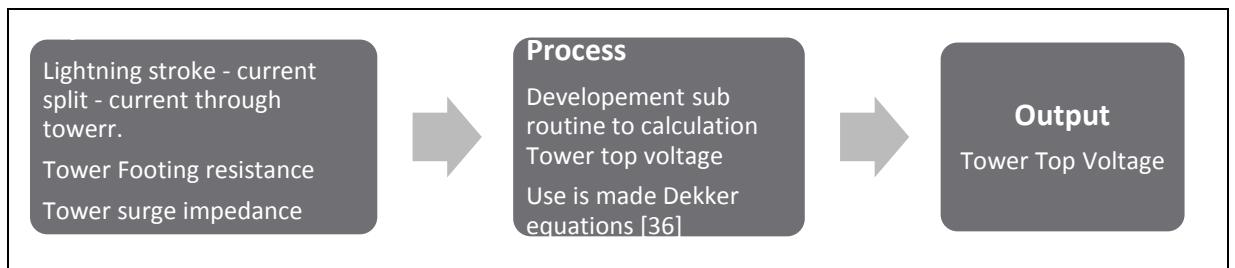
Figure 4.4 Flow chart to determine the Tower Top Voltage

A subroutine was development in MATLAB to calculate the tower top voltages for both the HVAC and EHVDC systems. This subroutine is based on the theory and example as per Dekker [36]. The process following is shown in Figure 4.4. The following parameters are used as inputs to the program

Ic -Current through the tower, which is determined by the lightning stroke.

Zt -Tower surge impedance.

Zs - Line surge impedance.

R - Tower footing resistance.

The damping factor is a function of the line and tower surge impedance and the tower footing resistance. Ic is a function of the wave travel time within the tower. These parameters are calculated as part of other routines and those outputs are used as input into determining the tower top voltage. The subroutine in MATLAB provides one with the tower top voltage for various lightning strokes. The subroutines contain a small database that contains the magnitude of the lightning that could be chosen. Figure 4.5 shows the lightning stroke magnitude and current that could be expected through the tower. This highlights the effect of the lightning stroke split.

| Tower Top Voltage for HVAC lines | Tower Top Voltage for EHVDC lines |
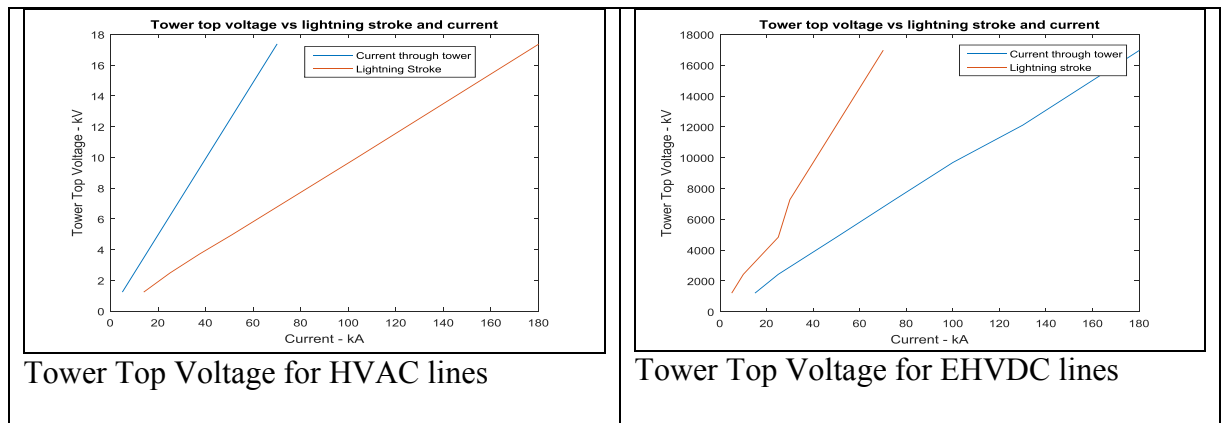
Figure 4.5 Tower Top voltage vs lightning current through tower

With the magnitude of the lightning stroke been the only variable, the graph would indicate a linear relationship. Of importance is the magnitude of the tower top voltage corresponding to that lightning current that flows through the tower. Due to the current splitting (refer to Chapter 2.2.9), 15kA of a 37.5kA stroke would flow through the tower. This would give a peak overvoltage 3720kV. This is based on 8/20 micro second lightning waveform.

Graph of Lightning overvoltages vs time	Graph of Lightning overvoltages vs time
Overvoltage caused by a 37.5kA Lightning Stroke to a HVAC line	Overvoltage caused by a 51kA Lightning Stroke to a EHVDC line
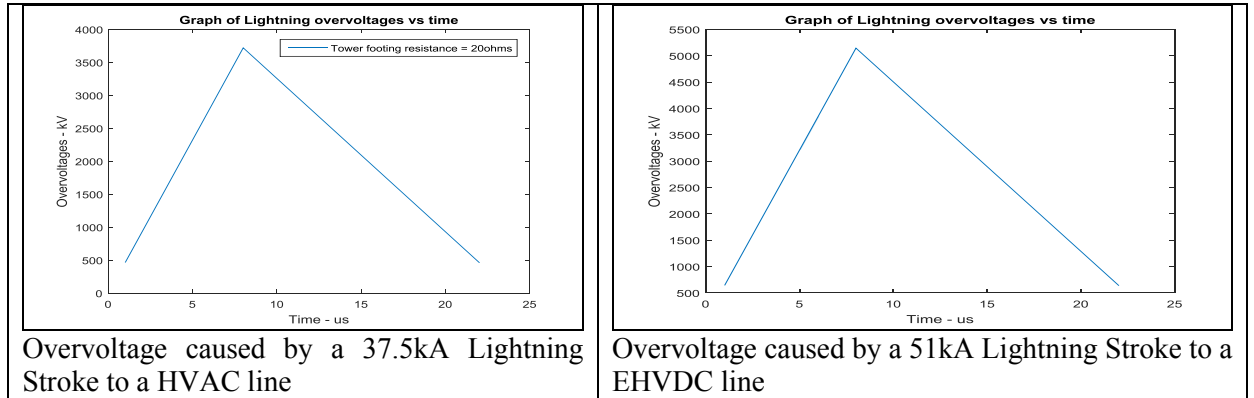
Figure 4.6. Over voltages caused by lightning stroke to overhead lines

4.4 Procedure and method to calculate the Insulator flashover voltage.

The process that is to be followed is shown below in Figure 4.1
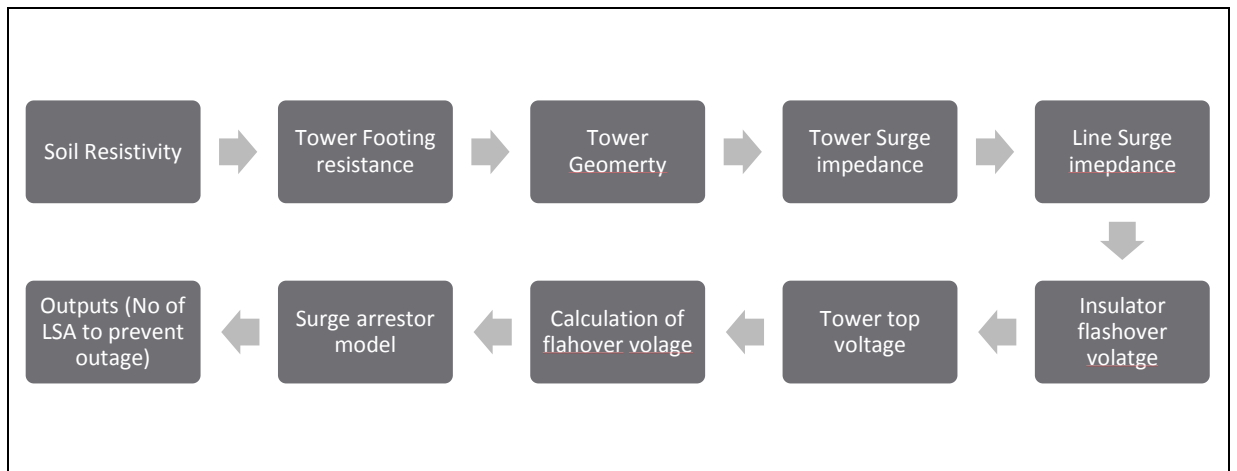
Figure 4.7 Flow chart to determine number of line surge arrestors to prevent breaker operations

As discussed in chapter 2 section 4.5, the insulator may be modelled as a stray capacitance, which can be connected between the a phase and the tower. Furthermore, the proposed voltage time characteristics by CIGRE is used for the simulations. Furthermore the time withstand capability of the insulator is calculated utilizing the following :

$$V_{flashover} = K_1 \ + \ \frac{K_2}{t^{0.75}} \tag{4.7}$$

where

K_1 = 400L

K_2 = 710L

L = insulator length (meters)

t = elapsed time after lightning stoke (us)

The flow chart in figure 4.8 shows the steps used in the sub routine to determine the insulator over voltages.
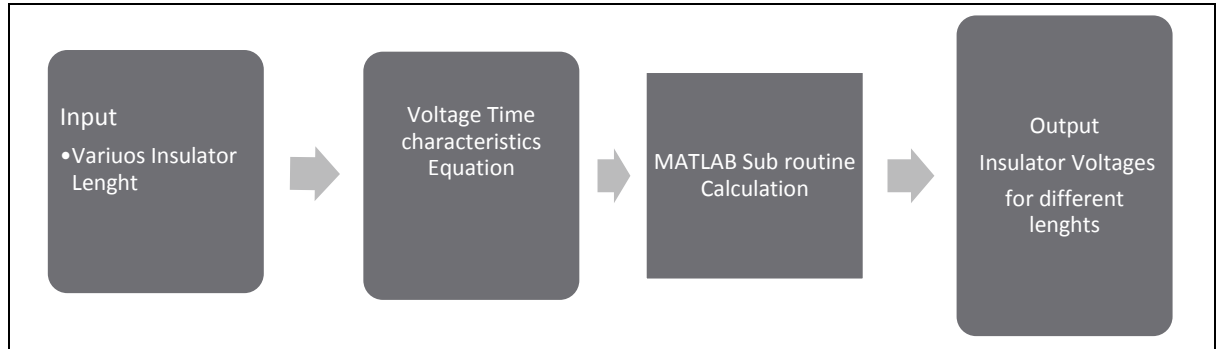
Figure 4.8 Flow Chart to determine Insulator Overvoltages

The sub-routine is created in MATLAB for both the HVAC and EHVDC systems. The variable is the length of the insulator. Some of the voltage time curve for different lengths of HVAC and EHVDC insulators is shown in figure 4.9. These lengths of the insulator would be for different high voltage categories.
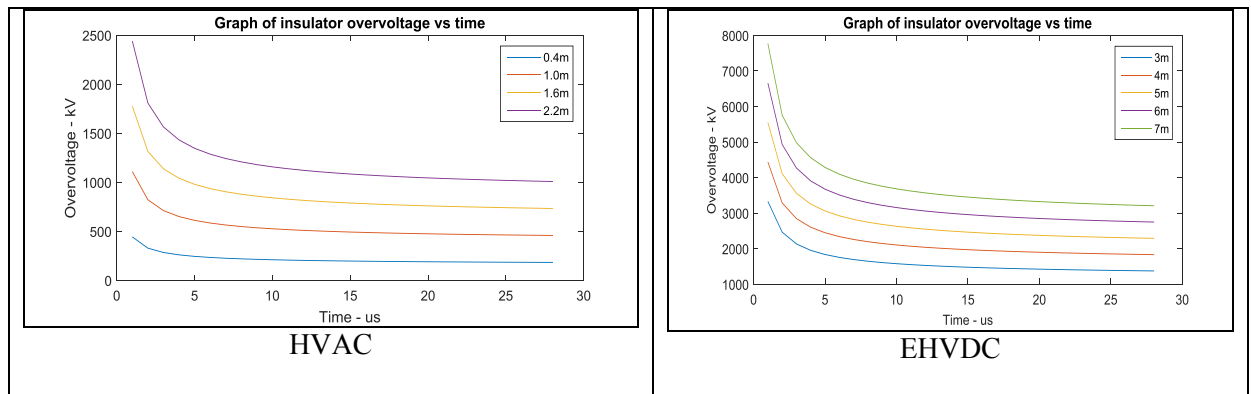
Figure 4.9 Graph of insulator overvoltage vs time

As expected, the increased insulator length leads to an increase on the insulator flashover voltage. This over-voltage curve would tend to 'flatten' out as time proceeds

4.5 Modeling of surge arrestors

The process that is followed is that shown below in Figure 4.10
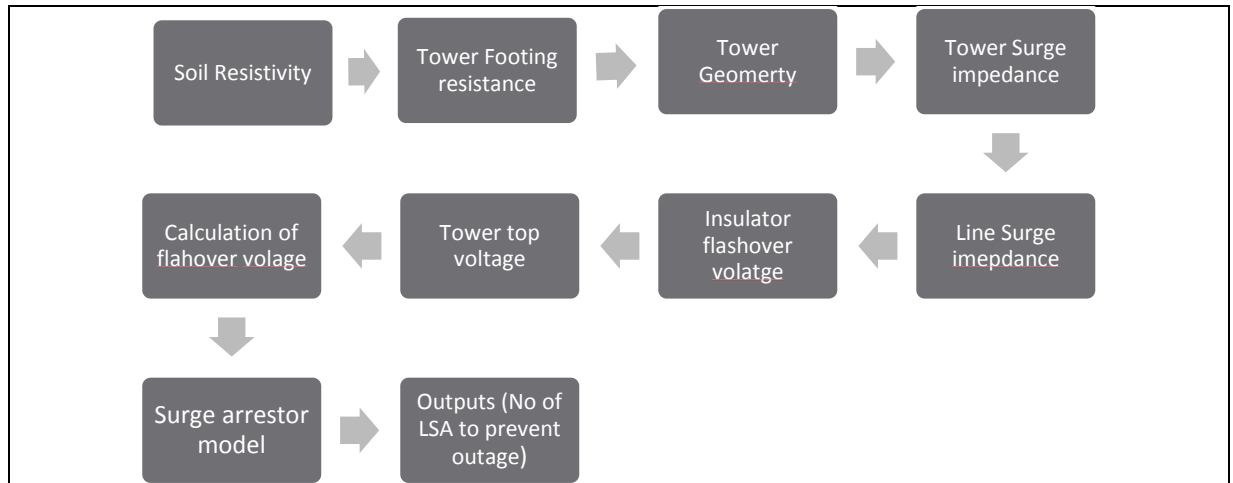
Figure 4.10 Flow chart to determine required number of LSA to prevent breaker operations

4.6 Operating voltage of the surge arrestor.

The model of the surge arrestor used is as per Chapter 2.1.11. A MATLAB sub routine has written that would interrogate a database and obtain the voltage at which the surge arrestor would begin to operate. This is based on the following formula.

For A_0, the

$$V_d = B_o \frac{V_{10}}{1.6}$$ (4.8)

Likewise, for A_1,

$$V_d = B_1 \frac{V_{10}}{1.6}$$ (4.9)

where B_o = Relative IR in pu for A_0

B_1 = Relative IR in pu for A_1

V_d = Discharge voltage

4.7 Selection and size of the surge arrestors for the HVAC system

The selection of the surge arrestor is based on the following simplified flow diagram courtesy of ABB buyer's guide [29]. This process is shown in figure 4.11.
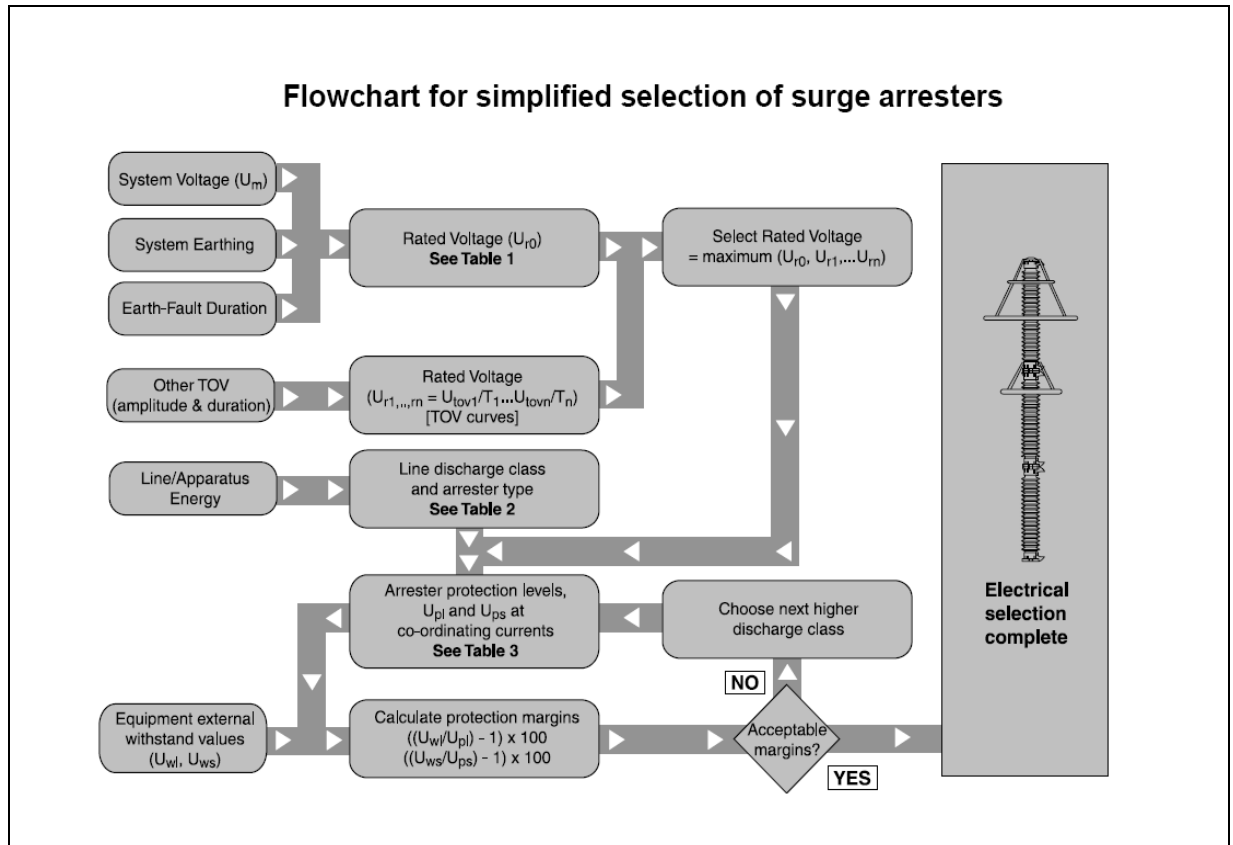
Figure 4.11 Flow chart for the selection of line surge arrestors.
Reproduced from reference [62]

The maximum system voltage (Um) for the line is 92kV. The system earthing is effective and fault clearance time < 1 second. The rated voltage (Ur) was 0.8xUm= 74kV. A higher standard Ur was chosen, i.e. 96kV. The decision to increase the rated voltage is influenced by the number of surge arrestors that would be installed and the need to minimize the effect of leakage current, which could result in nuisance tripping of the breaker.

A common surge arrestor for the system voltage Um of 92 kV would be a Pexlim R. This is a class 2 surge arrestor, with an Upl/Ur of 2.59. This gives an Upl (Lightning impulse protective level) of 249kV at 10kA. The insulation on the line normally has a lightning impulse withstand level (Uwl) of at least 450kV, the protective margin is ((Uwl/Upl) – 1) x 100 = 80.7%. The pexlim R has an energy capability of 5.1.

Should one decide to use a surge arrestor with a higher energy capability, then the Pexlim Q can be chosen. This has a higher energy capability of 7.8. This has an Upl/Ur of 2.35, which provided a protection margin of 100%, i.e the surge arrestor would withstand any instances of 100% over voltages. Hence a lightning impulse protective level Upl of 249 at 10kA is obtained.

4.8 Selection of surge arrestors for the EHVDC system

The selection of the EHVDC surge arrestor may follow the same process as that for the HVAC surge arrestor. Alternatively, data sheets, obtainable from manufactures may be used for obtain the V_{10} value.

Note: The selection of the surge arrestor is also based on standard surge arrestor sizes and ratings as provided by ABB.

4.9 Calculation of the discharge voltage of the surge arrestor)
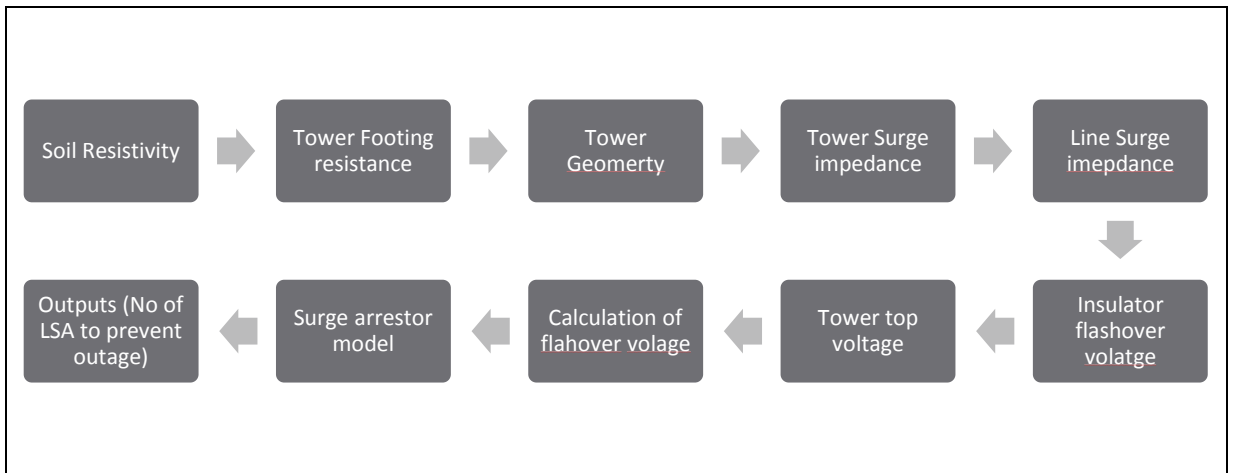
Figure 4.12 Flow chart to determine number of line surge arrestors to prevent breaker operations

Utilising the current rating and the MCOV of the surge arrestor, the discharge voltage can be calculated, using equations 4.8 or 4.9 and with reference to the data as shown in figure 4.11.
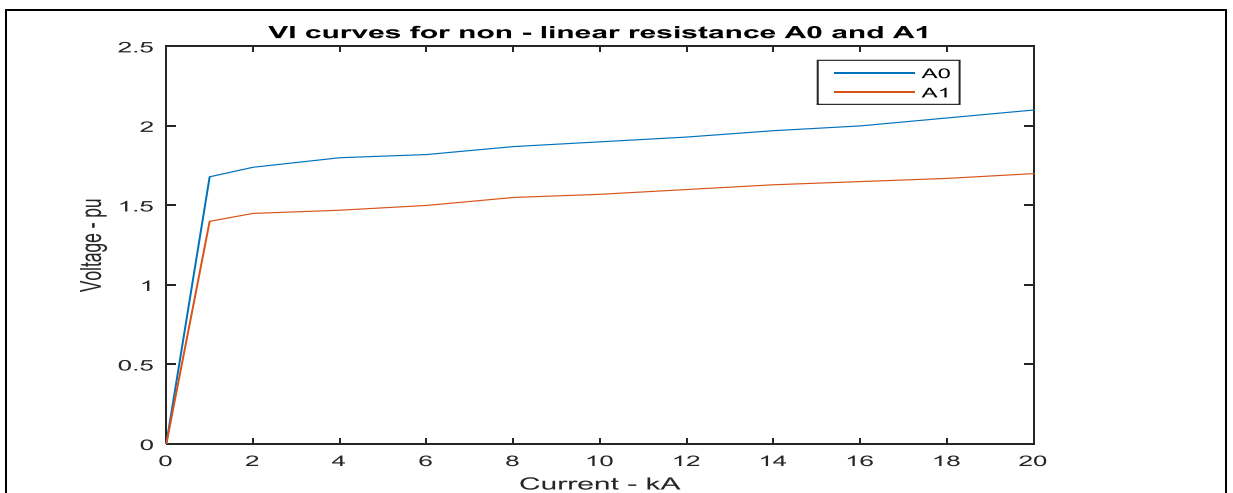
Figure 4.13 V-I non-linear characteristic for A0 and A1

The associated V-I voltage for the nonlinear resistor, A0 is determined by reading the "Relative IR" for a 10kA current from Fig 4.13. Figure 4.13 show that the "Relative IR" for a 10 kA current is 1.9pu.

Therefore the discharge kV for associated with l0kA is:

$$V_d = \frac{1.9 * 249}{1.6} kV = 296 kV$$

4.10 Selection and calculation of the discharge current for a EHVDC surge arrestor

The associated V-I voltage for the nonlinear resistor, A0 is determined by reading the "Relative IR" for a 20kA current from Fig 4.13. From this figure the "Relative IR" for a 20 kA current is 2.1pu. Therefore, the discharge kV for associated with 20kA for a 533dc system is:

$$V_d = \frac{2.1 * 1014}{1.6} kV = 1331 kV$$

Once the discharge voltage, or a voltage greater then this appears across the surge arrestor, it will start conducting and to dissipate the surge. This surge travels at the speed of light and hence the voltage will remain at the surge arrestor terminals for a very short time. It is during this time that the surge arrestor will conduct and reduce the power surge by draining the discharge voltage.

4.11 Method to calculate the required number of surge arrestors. -

The power surge caused by the lightning stroke would either be completely drained to ground via the tower or a back flash over would occur. The number of surge arrestors required is thus a simple process of deduction the overvoltage on the phase conductor (remember that this splits into two) by the V_{10} calculated value, until the power surge is completely eliminated. This would indicate the required number of surge arrestors. Figure 4.14 shows this calculation process.
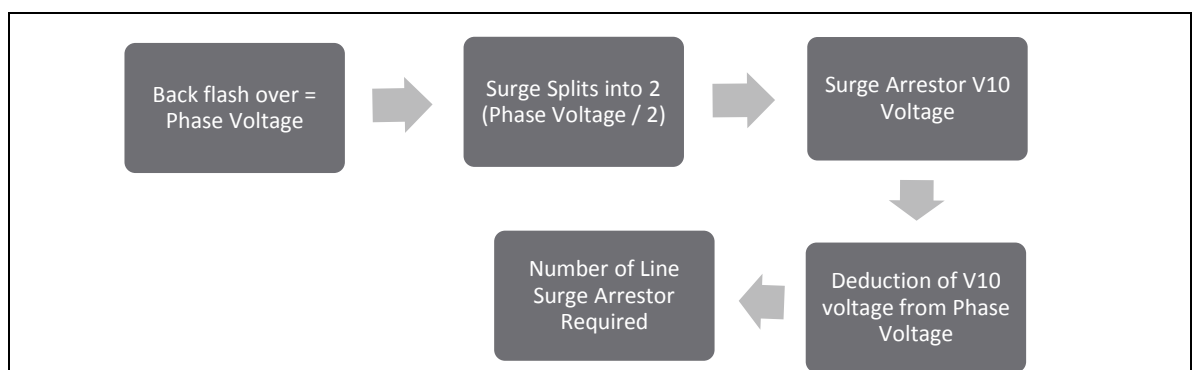
Figure 4.14 Flow diagram for the calculation of number of line surge arrestors

Once this voltage or a voltage greater then this appears across the surge arrestor, it will start conducting and to dissipate the surge. This surge travels at the speed of light and hence the voltage will remain at the surge arrestor terminals for a very short time. It is during this time that the surge arrestor will conduct and reduce the power surge by draining the discharge voltage.

CHAPTER FIVE   RESULTS AND DISCUSSION

5.1 Analyses and discussion of the HVAC results

5.1.1 Soil Resistivity

The parameters as shown in table 5.1 were entered in the sub-routines that were developed based on the flow chart/formulas as illustrated in Chapter 4. The sub-routines are found in Appendix A1.

Table 5.1 The variables required for the calculations of soil resistivity

Variable	Value
Upper layer thickness	7 meter
Soil resistivity (upper layer)	500 Ohm meter
Soil resistivity (Lower layer)	1000 Ohm meter

The outputs of the soil resistivity subroutine, in Appendix A1, are shown in figures 5.1 and 5.2.
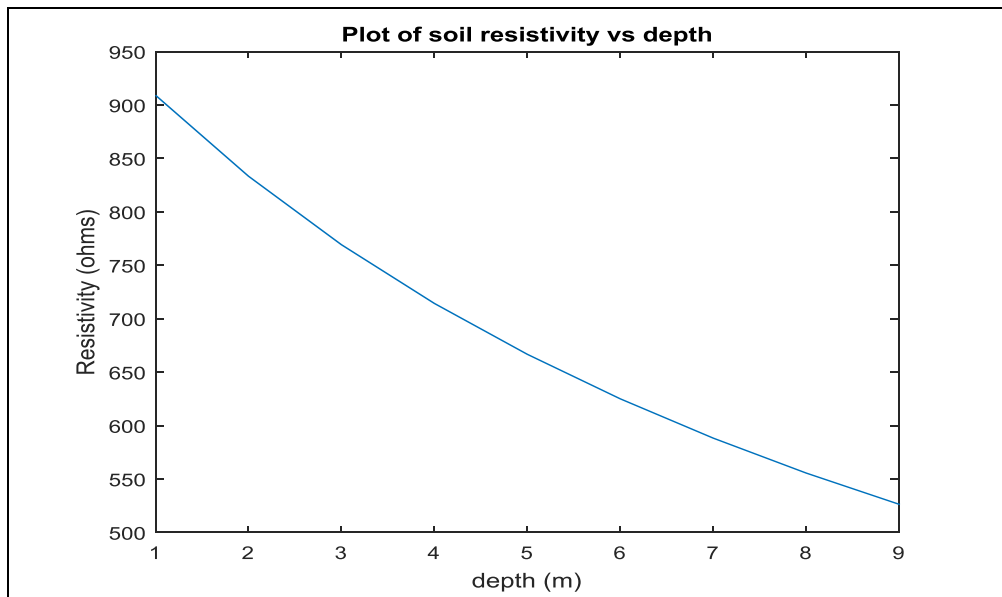
Figure 5.1 illustrates the relationship between soil resistivity and depth

Should the upper and lower layer values of soil resistivity be interchanged the following graph is obtained.
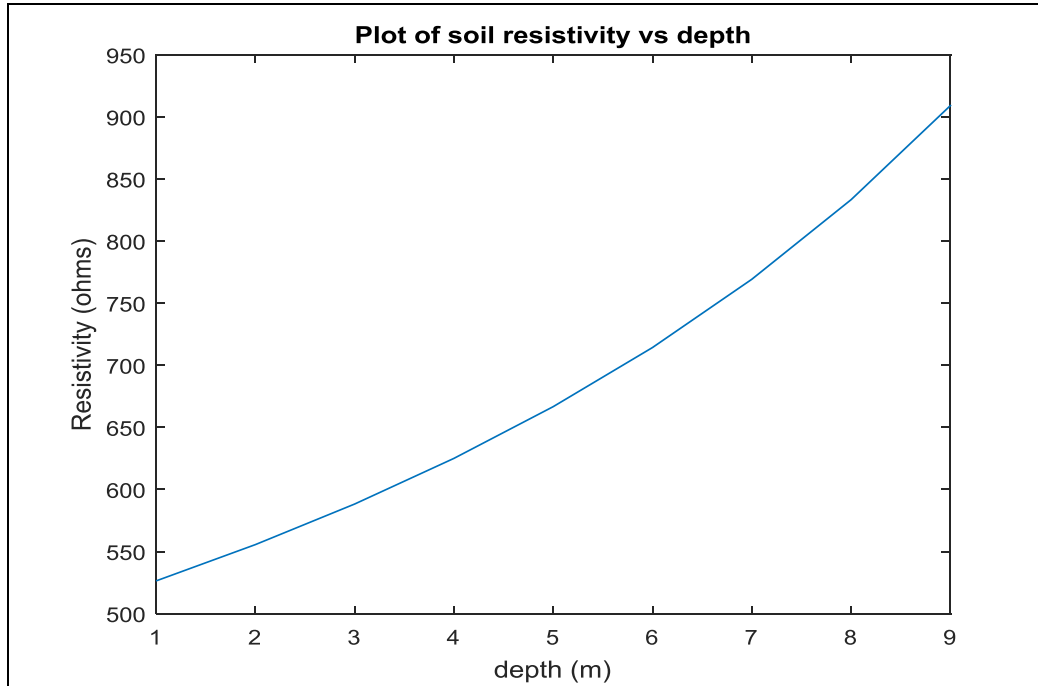
Figure 5.2 Increasing depth leads to higher soil resistivity

As expected the soil resistivity of the upper level dominates. However we can reduce the resistivity by having the electrodes penetrate the lower level as much as possible. However, it is not always possible, both from a financial and practical perspective.

5.1.2. Tower Footing Resistance

Using the programs (sub routines), displayed in Appendix A2, which is created for Tower footing resistance, one can change the soil resistivity values and hence the Tower Footing Resistance values as shown in table 5.2 is obtained for four case studies.

Table 5.2 Tower Footing Resistance for different soil conditions

	Case Study 1	Case Study 2	Case Study 3	Case Study 4
Upper Level (ohm m)	1862	1000	600	200
Lower Level (ohm m)	500	500	200	50
Depth of upper level (m)	7	7	7	7
Overall Soil Resistivity(ohm m)*	1025	763	375	105
Tower footing resistance (ohm)*	143	107	52.5	14.7

*Calculated values

For HVAC lines the overall tower footing resistances should be less than 30ohms. Soil resistivity values around 200 ohm meters would correspond to wet soil conditions while soil resistivity values greater than 1500 ohm meter would be dry for soil conditions. This phenomenon is discussion in

Chapter 3. The results show that for decreasing soil resistivity, the tower footing resistances would decrease. Study 1, 2 and 3 displays values in excess of 30 ohms. To reduce the values to that below 30 ohms, one could increase either the number of rods or conductor lengths. The calculated values are shown in tables 5.3, 5.4 and 5.5. These conditions are simulated for case study 1, 2 and 3. Case study 4 is below 30ohms.

Table 5.3 Radial Conductors required in obtaining a TFR below 30 ohms

Radial Conductor						
	Case Study 1		Case Study 2		Case Study 3	
No of conductors	Length (m)	Resistance (ohms)	Length (m)	Resistance (ohms)	Length (m)	Resistance (ohms)
2	50	24.94	30	29.12	20	20.09
3	30	28.87	30	21.67	10	27.33
6	30	24.15	20	25.96	10	23.24
8	20	28.41	20	21.33	10	19.41
12	20	25.54	20	19.18	10	17.66
13	20	23.15	20	17.38	10	16.25

.

Table 5.3 shows the various configurations, in terms of length and number of conductors, which could be employed to obtain a desired Tower footing resistance of less than 30ohms for each case study.

Arising from case study 1, the best combination is 13 conductors with a length of 20 meters each will provide a TFR of 23.2 ohms. The total conductor length would be 260 meters. For case study 2, the same combination will result in the lowest tower footing resistance, which is 25% less than the value obtained in case study 1. Case study 3 will require 13 conductors with a length of 10 meters each to obtain a tower footing resistance value of 16.25. These results are expected as the soil resistivity decreases from case study 1 to 3. From case study 3, to obtaining a tower footing resistance of 23.2, it would require 6 conductors of 10 meters each. This material length is 60 meters is much less than that of case study 1. Again this can be attributed to the better soil conditions. It must be note that any of these combinations would suffice to give a tower footing resistances less than 30 ohms.

Table 5.4 explores the Driven Rod option. The model varies the number of rods and hence the length of the conductor required in obtaining a TFR value of less than 30 ohms for each case study. The number of rods is user specified.

Table 5.4 Relationship between rods, length and tower footing resistance

	Driven Rod											
	Case Study 1				Case Study 2				Case Study 2			
No of Rods	1	2	3	4	1	2	3	4	1	2	3	4
Lenghts (m)	22	17	16	15	17	13	12	11	8	7	6	6
Resistance (ohms)	30	30	28	29	29	29	28	29	30	26	28	26

The length, of the rods required to reduce the tower footing resistance values to less than 30 ohms, decreases as the soil resistivity values decreases.

Table 5.5 Crows Foot

	Crows Foot	
	Rg(Ohms)	Length(m)
Case 1	27.3	90
Case 2	29.1	60
Case 3	25.6	30

Table 5.5 illustrates the length of conductor needed to reduce the tower footing resistance values to that less than 30ohms. The sub routine created in MATLAB would then compare the results from all three methods and would display the technical solution that would provide the lowest tower footing resistance as shown in table 5.6.

Table 5.6 Method with lowest tower resistance values

	Method	Tower footing resistance value
Case 1	Radial	23.4
Case 2	Radial	17.3
Case 3	Radial	16.25
Case 4	All values less than 30 ohms	

5.1.2 Tower and Line models

Utilising the sub-routines and process as indicated in Chapter 4.1.2, the tower and line surge impedance is obtained. Figure 5.3 show a typical 88kV HVAC tower.

Figure 5.3 Typical tower for HVAC transmission lines.

Based on the dimensions of a typical HV tower, the following standard dimensions were be entered into the sub-routine

r_1 = 4.2m

r_2 = 4.2m

r_3 = 3.8m

h_1 = 9.74m

h_2 = 18.48m

These parameters are variables into the programs and a tower surge impedance of 117 is obtained. Similarly a line surge impedance of 416 was obtained for the conductor.

5.1.3 Insulator Over-voltage vs Time

The insulator modelled is for a HVAC transmission line. The length of the insulator used in the simulations is 1.6 meters. This is typical insulator length used on 88 or 132kV systems. Figure 5.4 indicates insulator over-voltages for different insulator lengths.
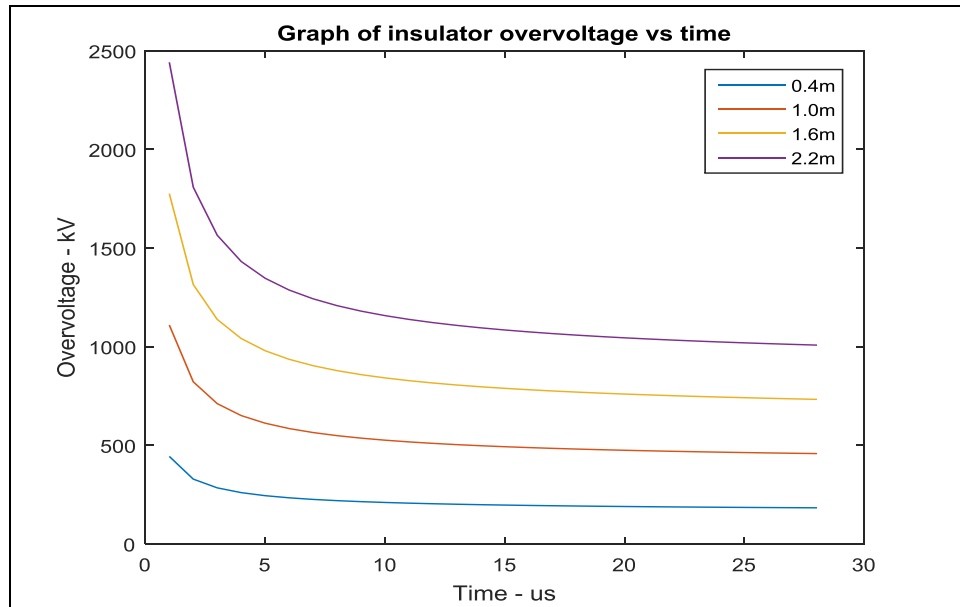
Figure 5.4 Over-voltages for different insulator length

5.1.4 Tower top voltage

Utilising the model created in MATLAB, it is crucial to calculate the tower top voltage. This subroutine is based on the theory and example as illustrated by Dekker [36]. The following parameters are used as inputs to the program

Ic - Current through the tower, which is determined by the lightning stroke.

R - Tower footing resistance.

Zs – Line surge impedance.

Zt – Tower surge impedance.

These parameters are calculated as part of other routines and those outputs are used as input into determining the tower top voltage. The subroutine in MATLAB is developed as per the flow chart in Chapter 4. Figure 5.5 shows with the tower top voltage for various lightning strokes.
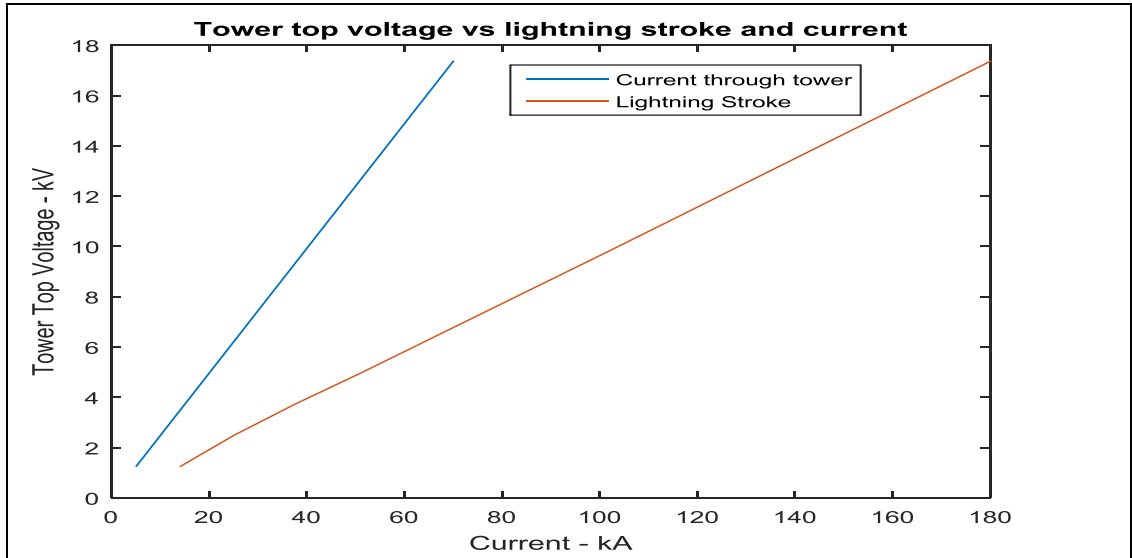
Figure 5.5 Tower Top voltage vs lightnning current through tower

With the magnitude of the lightning stroke been the only variable, the graph would indicate a linear relationship. Of importance is the magnitude of the tower top voltage corresponding to that lightning current that flows through the tower. Due to the current splitting (refer to Chapter 2.2.9), 15kA of a 37.5kA stroke would flow through the tower. This would give a peak overvoltage 3720kV. This is based on 8/20 micro second lightning waveform.
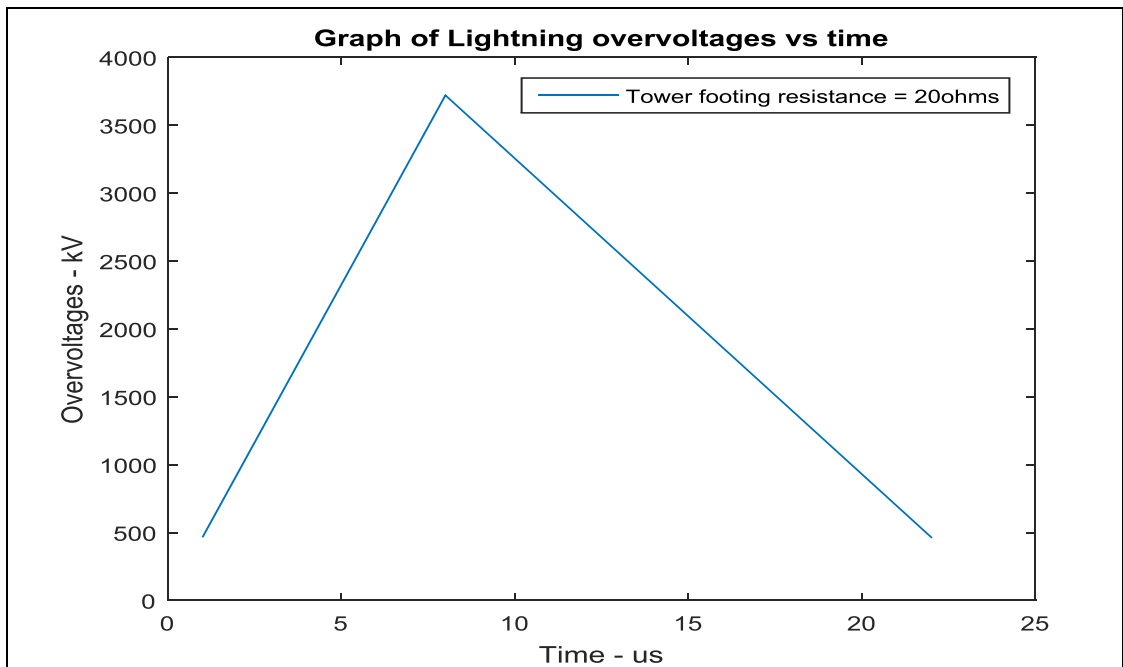
Figure 5.6 Over voltages caused by a 37.5kA lightning stroke

Figure 5.7 provides the over voltage curves for different tower footing resistance and lightning strokes.
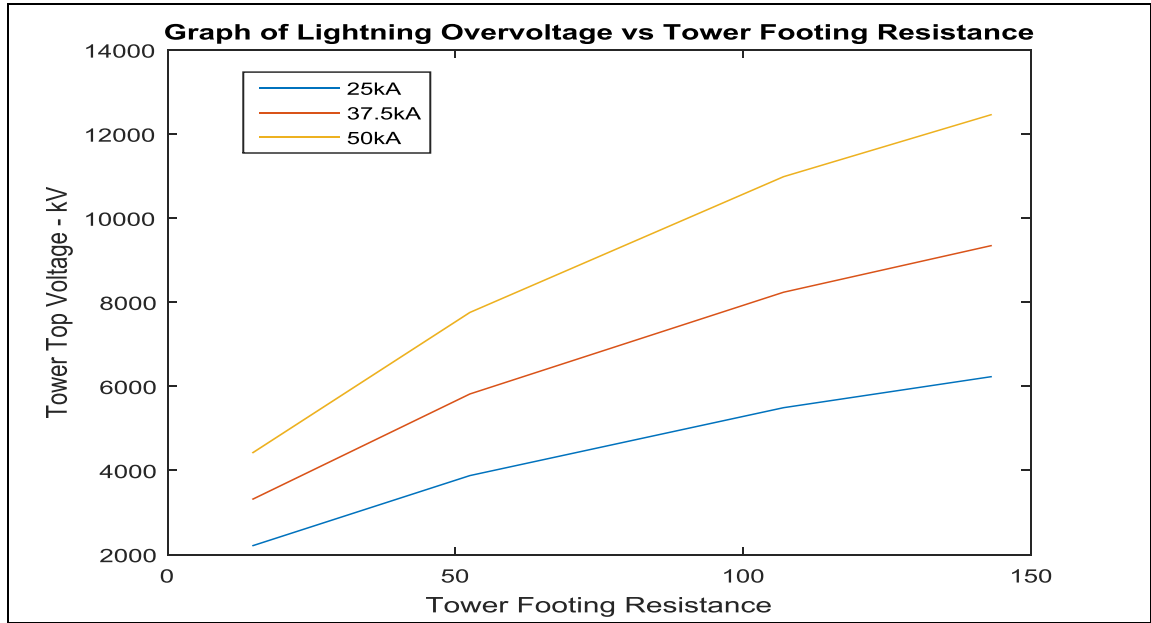
Figure 5.7 Tower Top Voltage variation vs Tower Footing Resistance

With a constant lightning stroke magnitude, the tower voltage top would increase with an increasing tower footing resistance. No earthing enhancement techniques were considered for the earthing values used as per figure 5.7. Utilising earthing enhancement techniques as discussed in Chapter 3, which reduces the tower footing resistance value below 30ohms, the graph shown in figure 5.8 is obtained.
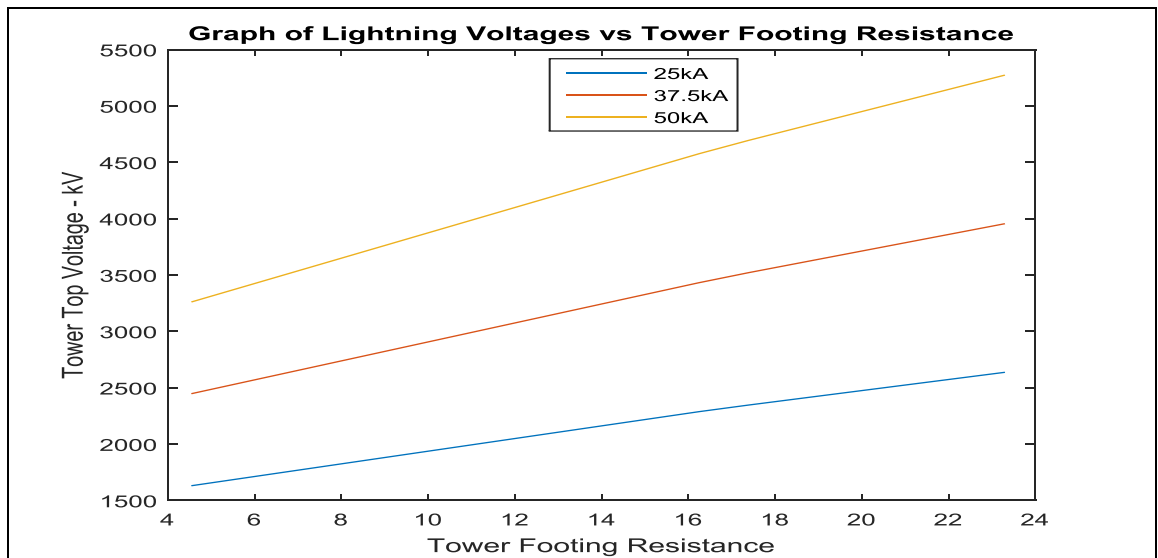
Figure 5.8 Enhance earthing (less than 30ohms) vs over voltages

Figures 5.7 and 5.8 shows that the tower top voltage is almost halved. This is a substantial reduction. This highlights the need to have acceptable tower footing resistance. It may be costly to reduce the footing resistance to single digit figures.

5.1.5. Insulator Flashover Voltage

The insulator length is directly proportional to the voltage, which must be exceeded for a back flashover to occur. The following graph indicates the expected insulator flashover voltage versus line length. The length of an 88 or 132kV insulator used in the simulations is 1.6 metres.
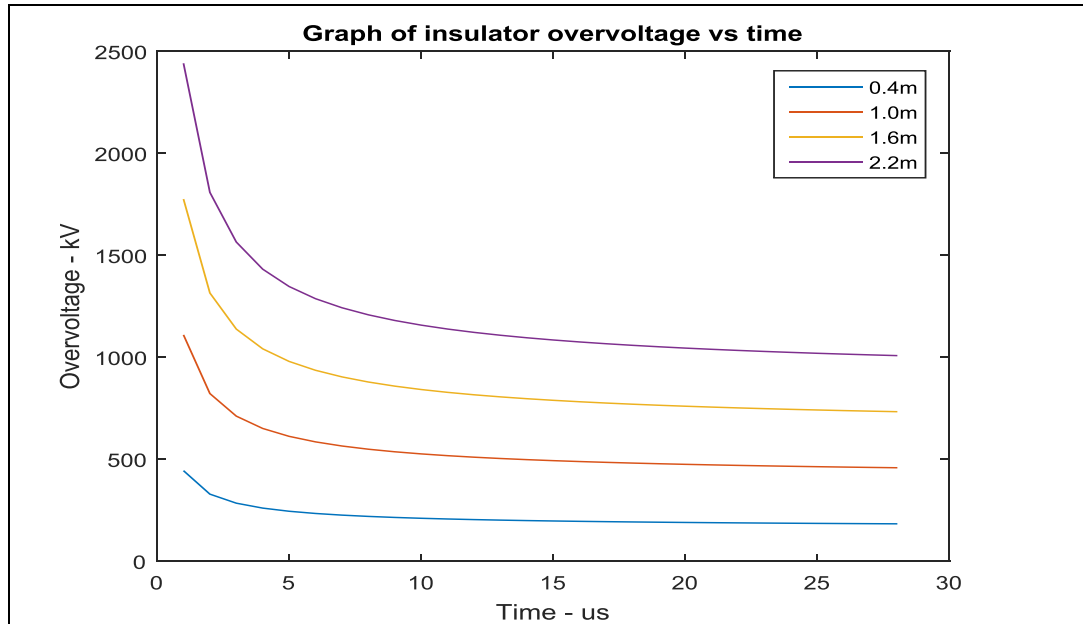
Figure 5.9 Graph of insulator over-voltage vs time

Neither the lightning stroke magnitude nor the tower footing resistance may a substantial part on determining the insulator over voltage. It must be noted that a back flash over would occur for all the parameters as shown in figure 5.9 as the insulator flashover voltage will be exceeded. Over designing or increasing the length of the insulator to 2.2 meters would still result in the tower top voltage been exceed, resulting in a flashover. To improve the network performance, this power surge needs to be drain to ground. Line Surge Arrestor may be used to facilitate this process.

5.1.6 Surge Arrestor discharge voltage

For the nonlinear resistor A_0, the associated V-I voltage for a l0kA current is determined by reading the "Relative IR" for a 10kA current from Fig 5.10.
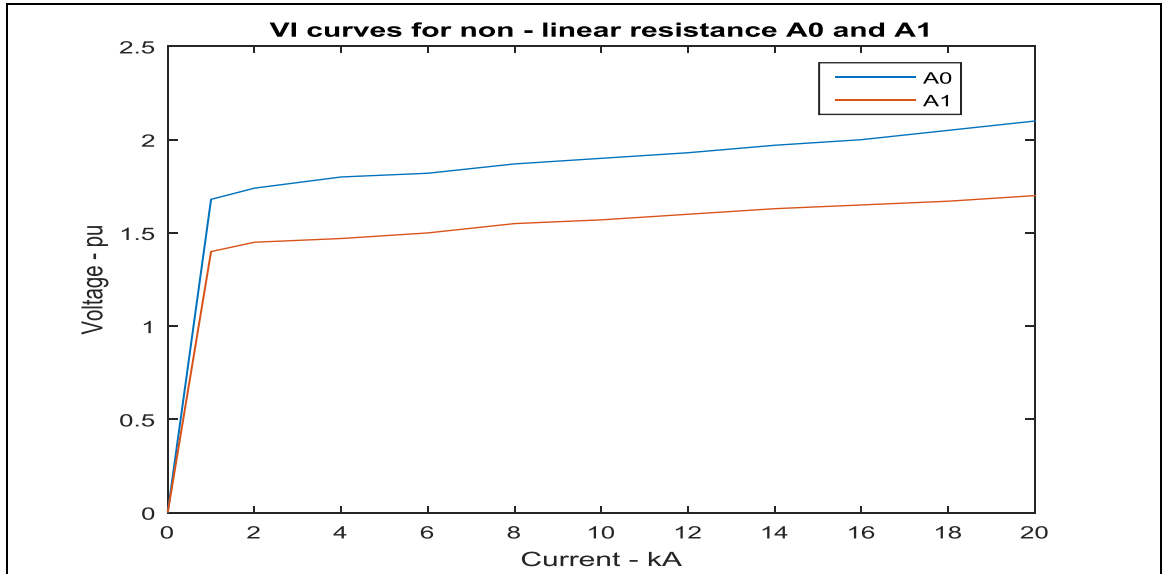
Figure 5.10 VI Curves for non-linear resistance

Figure 5.10 show that the "Relative IR" for a 10 kA current is 1.9pu. The operating voltage for this surge arrestor specification is 249kV - Refer to Chapter 4.2.10. Hence the discharge kV for associated with l0kA is:

$$V_d = \frac{1.9 * 249}{1.6} kV = 296kV$$

Once this voltage or a voltage greater then this appears across the surge arrestor, it will start conducting and begin to dissipate the surge. This surge travels at the speed of light and hence the voltage will remain at the surge arrestor terminals for a very short time. It is during this short time that the surge arrestor will conduct and reduce the power surge by draining the discharge voltage.

5.1.7. Required number of surge arrestors to dissipate the lightning surge on phase conductor.

At this stage the power surge caused by the lightning stroke would either be completely drained to ground via the tower or a back flash over would occur. The required number of surge arrestors, thus is a simple process of deducting the overvoltage on the phase conductor (remember that this splits into two) by the V_{10} calculated value, until the power surge is completely eliminated. This would indicate the required number of surge arrestors.

A lightning stroke current of 25kA would require four 88kV surge arrestors connected in parallel to dissipate the lightning stroke. This would prevent the line breaker from operating and causing small duration outages. The surge arrestor connectivity is shown in figure 5.11.
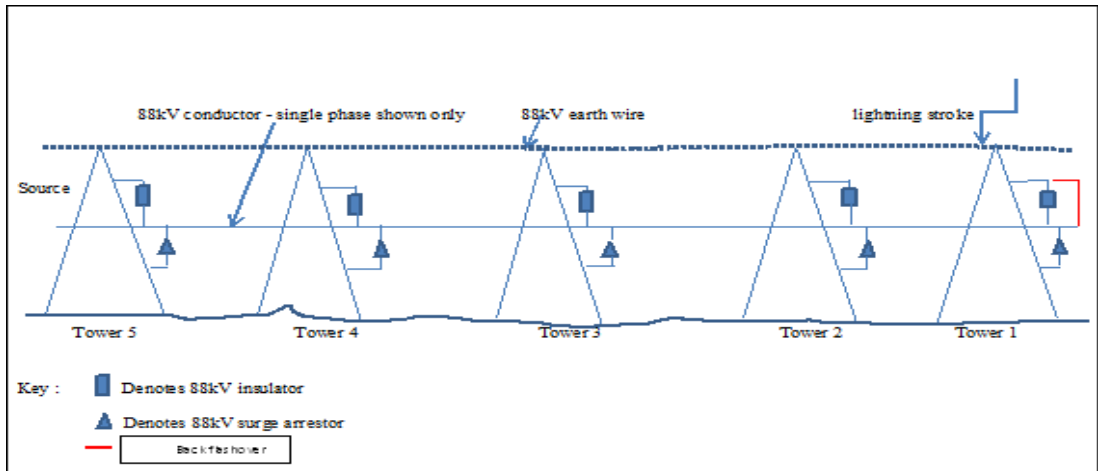
Figure 5.11. Parallel connection of surge arrestors on a number of towers

Figure 5.12 illustrates the reduction of the over-voltages, which is caused by a 25kA lightning stroke. Surge arrestors of the same rating were used and the tower footing resistance is 17.38ohms.
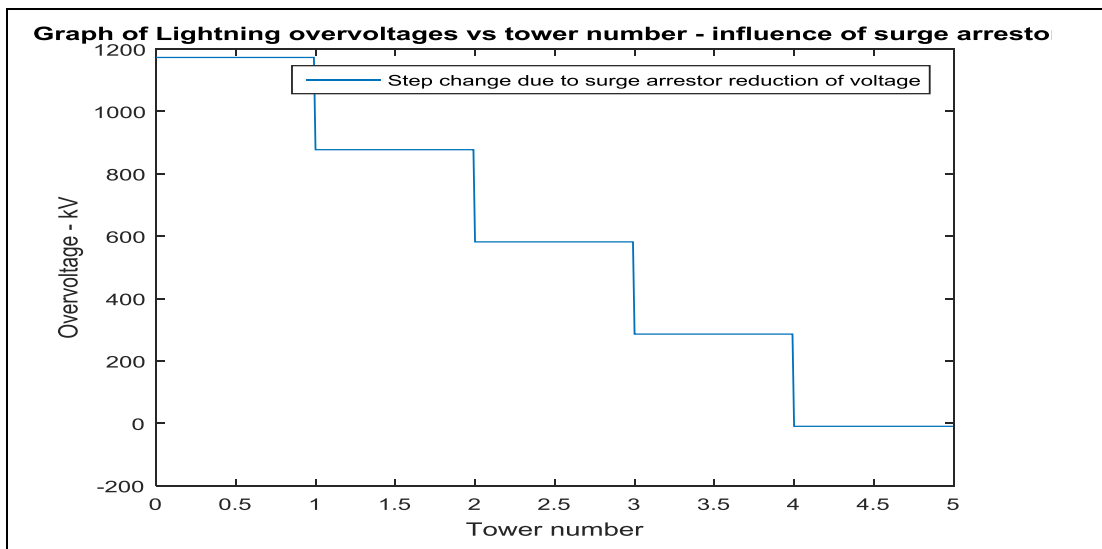
Figure 5.12 Lightning over voltages vs tower number – influence of surge line arrestors

Table 5.7 – 5.10 shows the required number of surge arrestors to drain the over-voltages caused by lightning strokes of different magnitude and for different soil parameters to ground. The soil parameters are taken from case studies 1 to 4.

Table 5.7 Tower Footing resistance of 23.1 and different lightning strokes

Lightning current kA	Insulator voltage kV	Tower footing resistance	Tower top voltage -kV	Back flash over	Phase voltage	Required SA, to prevent outage
12	849	23.2	1318	yes	659	2
25	849	23.2	2636	yes	1318	5
37.5	849	23.2	3955	yes	1978	7
50	849	23.2	5273	yes	2637	9

Table 5.8 Tower Footing resistance of 17.4 and different lightning strokes

Lightning current kA	Insulator voltage kV	Tower footing resistance	Tower top voltage -kV	Back flash over	Phase voltage	Required SA, to prevent outage
12	849	17.38	1173	yes	587	2
25	849	17.38	2346	yes	1113	4
37.5	849	17.38	3510	yes	1760	6
50	849	17.38	4693	yes	2346	8

Table 5.9 Tower Footing resistance of 16.3 and different lightning strokes

Lightning current kA	Insulator voltage kV	Tower footing resistance	Tower top voltage -kV	Back flash over	Phase voltage	Required SA, to prevent outage
12	849	16.3	1144	yes	571	2
25	849	16.3	2288	yes	1144	4
37.5	849	16.3	3431	yes	1716	6
50	849	16.3	4578	yes	2288	8

Table 5.10 Tower Footing resistance of 4.56 and different lightning strokes

Lightning current kA	Insulator voltage kV	Tower footing resistance	Tower top voltage -kV	Back flash over	Phase voltage	Required SA, to prevent outage
12	849	4.56	816	No	0	0
25	849	4.56	1632	yes	816	3
37.5	849	4.56	2449	yes	1225	5
50	849	4.56	3265	yes	1633	6

Even with low tower footing resistance and lightning strokes greater than 25kA will still cause a back flash over. These cases would require line surge arrestors to drain the power surge to earth. The two figures 5.13 and 5.14 illustrate the lightning stroke pattern in terms of value and magnitude for an 88kV, 49km overhead transmission line.
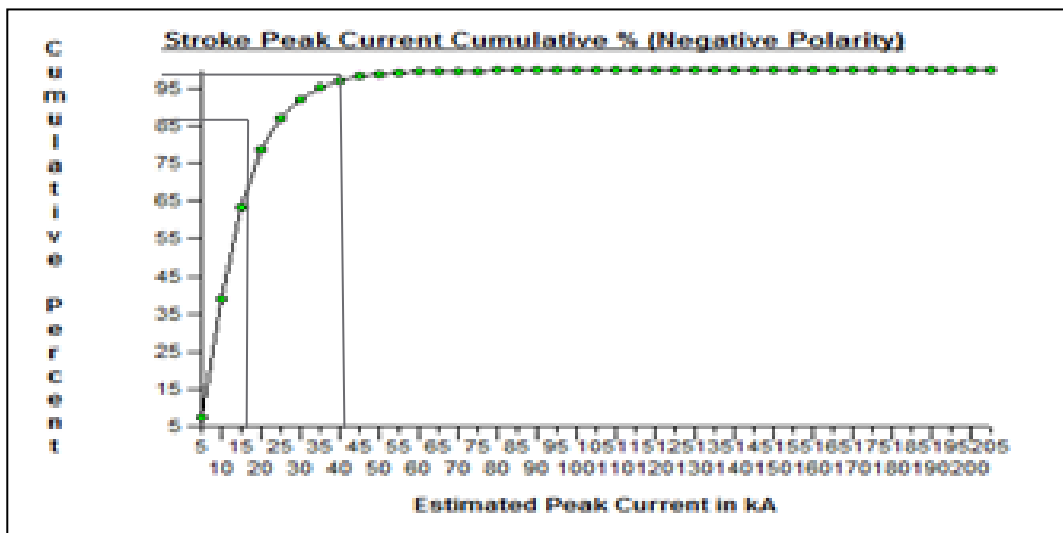
Figure 5.13 Cumulative percentage of peak lightning current
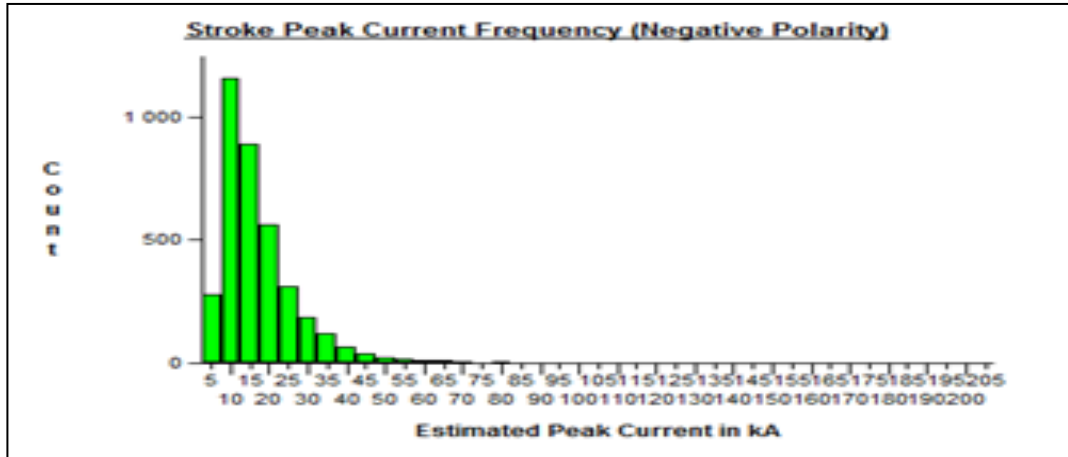
Figure 5.14 Stroke magnitude frequency of peak current.

Almost 85% of the recorded strokes are less than 25kA and over 95% of the strokes are below 50kA. This implies, with correct tower footing resistance and utilizing 9 sets of surge arrestors, the outages should be substantial reduced.

Figure 5.15 illustrates the number of breaker interruptions over a 4 year period. All these interruptions resulted from lightning strokes within a diameter of 1km of the line. The corresponding stroke magnitude for the breaker interruptions time was obtained from the FALLS system.
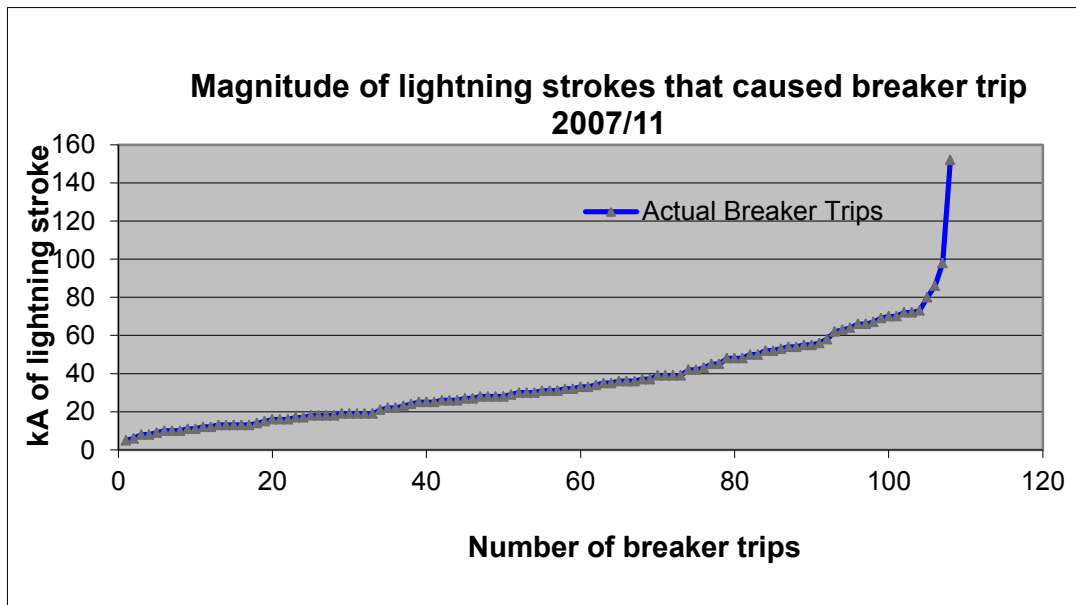
Figure 5.15 Incident of breaker interruptions vs Stroke magnitude

Analysis of the data revealed that there were 106 lightning induced trips over a four storm cycles. 84 of these interruptions resulted due to lightning strokes less than 50kA. This is about 79% of the interruptions. Hence by installing 9 sets of surge arrestors, we can prevent a

further 73 interruptions. This would be an average of 18 per year. To overcome more lightning related breaker interruptions additional surge arrestors maybe required.

5.1.8 Effect of increased insulator length on flashover voltage

Table 5.11 shows the effect of changing the insulator length from 1.6 to 2.2 meters. The soil resistivity for case study 1 was used.

Table 5.11 Tower Footing resistance of 17.4 ohms, longer insulator and different lightning strokes

Lightning current kA	Insulator voltage kV	Tower footing resistance	Tower top voltage -kV	Back flash over	Phase voltage	Required SA, to prevent outage
12	1208	17.38	1173	No	0	0
25	1208	17.38	2346	yes	1113	4
37.5	1208	17.38	3510	Yes	1760	6
50	1208	17.38	4693	Yes	2346	8

Increasing the insulator length from 1.6 meters to 2.2 meters, increases the withstand capability of the insulator and will eliminate the low magnitude lightning strokes. However, it must be noted that the cost implications of re-insulation an 88kV line is costly and in cases unpractical.

5.1.9 Financial Evaluation for HVAC Sytems

The financial evaluation is done based on the following

- Annual expected number of voltage dips and momentary outages due to lightning

  Performance monitoring of a sub transmission overhead line revealed that for a period between 2007 and 2011, there was 106 lightning induced momentary interruptions. This is an average of 26 lightning related interruptions per year.

- Estimate the cost associated with voltage dips and momentary outages.

  A study undertaken by Nzimande [3] revealed that lightning related dips lead to losses of between US $5357 and US $35714 per annum for 10 storm related dips, and average of between US$535.7 and US $3571 per dip. These figures are escalated to 2018 and are US$1143 and US$7425.

- Cost of 27 surge arrestors to effectively militate against lightning back flashover.

Table 5.12 - High level cost to install 27 sub transmission LSA

Item	Year 2018
Cost of a surge arrestor and counter	$ 35 76
Cost of 27 surge arrestor and counters	$ 96 564
Labour and transport	$ 31 060
Total	$127 623

5.1.10 Capital Recovery Period

Based on an 10% annual escalation rate both in terms of capital and savings cost the following figure 5.16 can be generated. It must be noted that the maintenance cost of the surge arrestor are negligible. Visual inspections can be built into the cost of the routine line inspections. Furthermore the additional sales that the power utility would receive, is also not included in the financial evaluation.
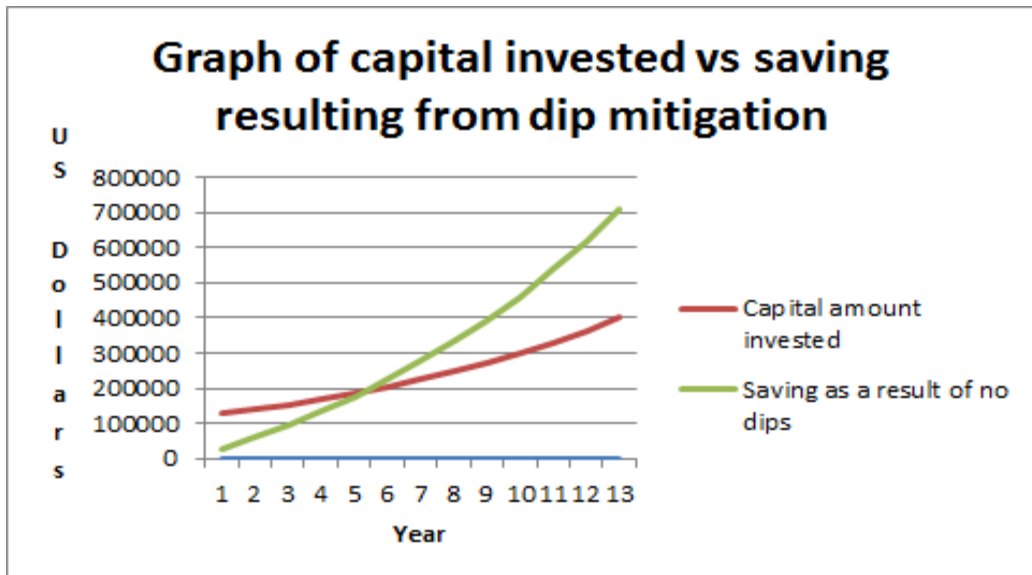
Figure 5.16 Capital invested vs cost saving resulting from dips

The breakeven point should occur in year 6. Savings after this year should be viewed as a savings, not only to the power utility, customer, but to the general economy as well.

5.2 Analysis and discussion of the EHVDC modelling results

The following figure illustrates the amount of lighting strokes that can occur within a corridor of an overhead EHVDC line. The strokes would be of different magnitude.
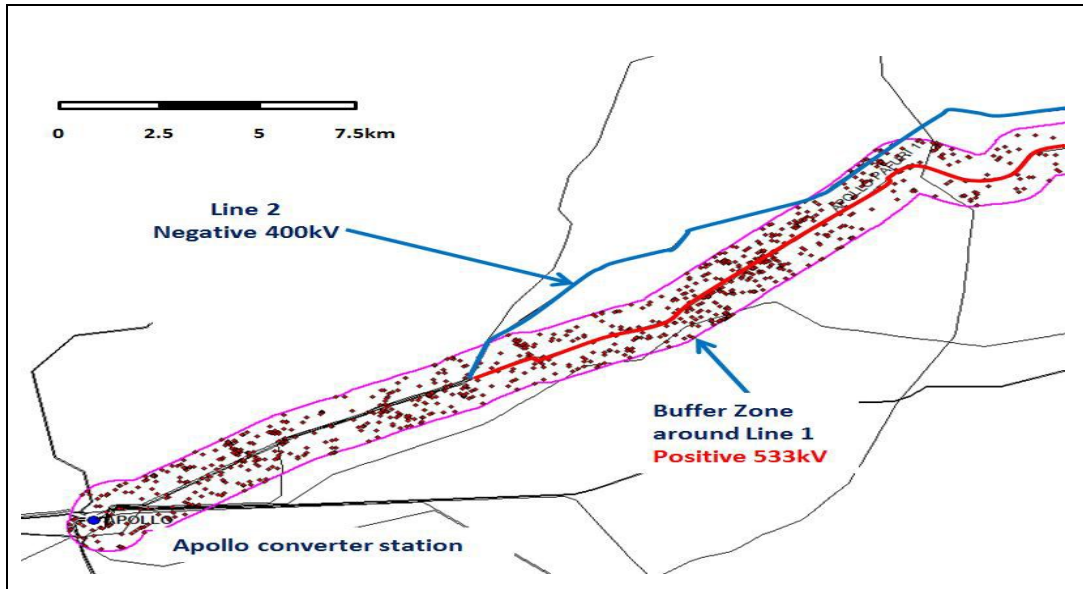
Figure 5.17 Lightning activity within the 1km buffer of the EHVDC line

In figures 5.17, 5.18 and 5.19 the lightning strokes experiences by a 533kV DC line is shown [15]. The first graph shows the peak current frequency for the positive pole of the line and the second show same, but for the negative pole.
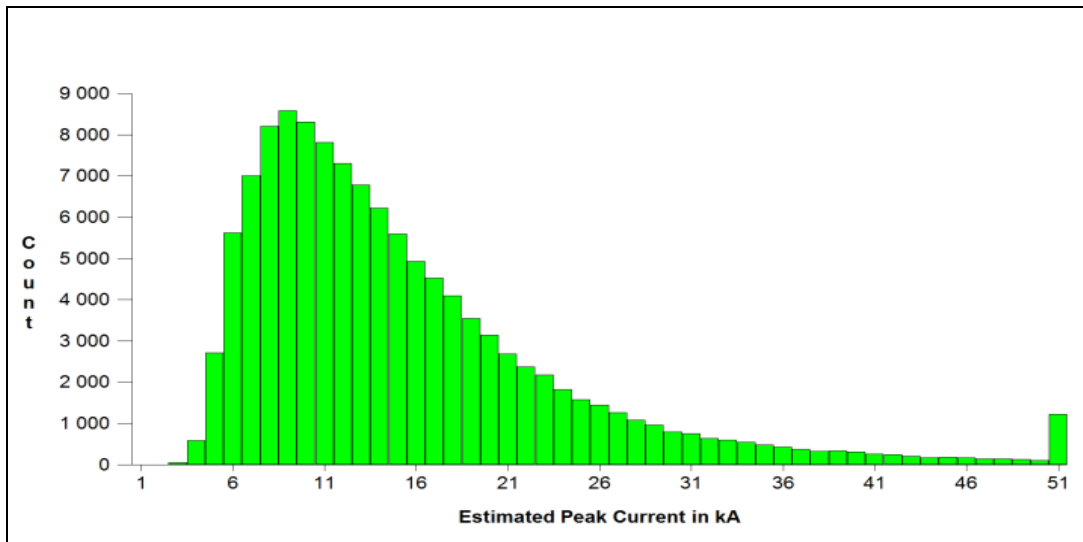
Figure 5.18 Positive pole (Line 1) stroke peak current frequency for strokes of negative polarity
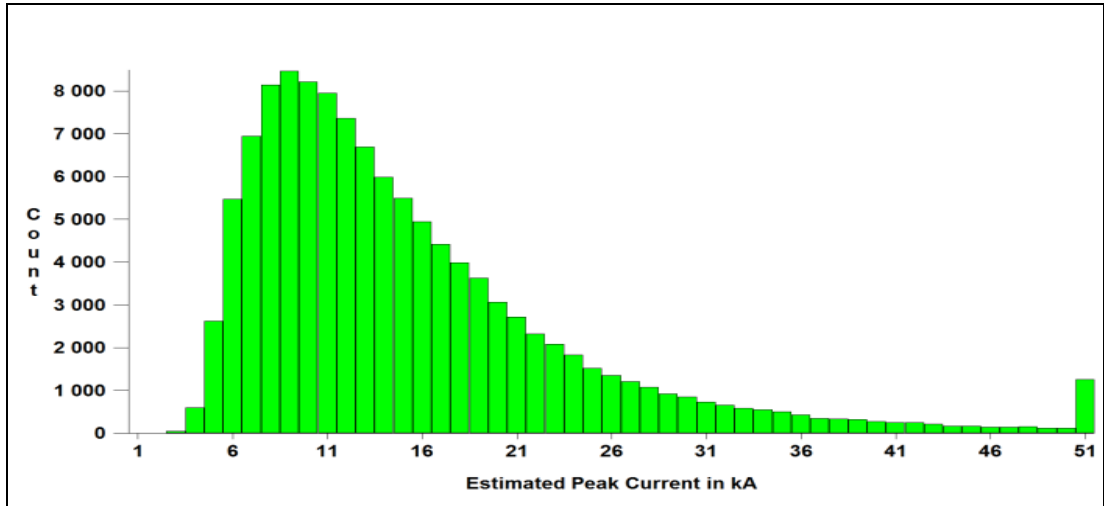
Figure 5.19 Negative pole (Line 1) stroke peak current frequency for strokes of negative polarity

From figure 5.18 and 5.19, majority of the lightning strokes are less than 26kA. It is expected that for the standard line BIL and tower footing resistance, no back flash over would occur. The two layer model is used to determine the soil resistivity. The top layer was a variable into the MATLAB program. Hence we would be able to ascertain, which of the three earthing methods would be the most appropriate for this application. It this particular case the radial conductor is the most suit earthing type and provides earthing values of less than 30ohms. The calculations are as in Chapter 5.1.1 and 5.1.2.

5.2.1. Insulator Flashover Voltage

The standard insulator length for 533kV line is 6 meters. Utilising the sub-routine created in Chapter 4, different insulator length would provide different flashover voltages as displayed in figure 5.20.
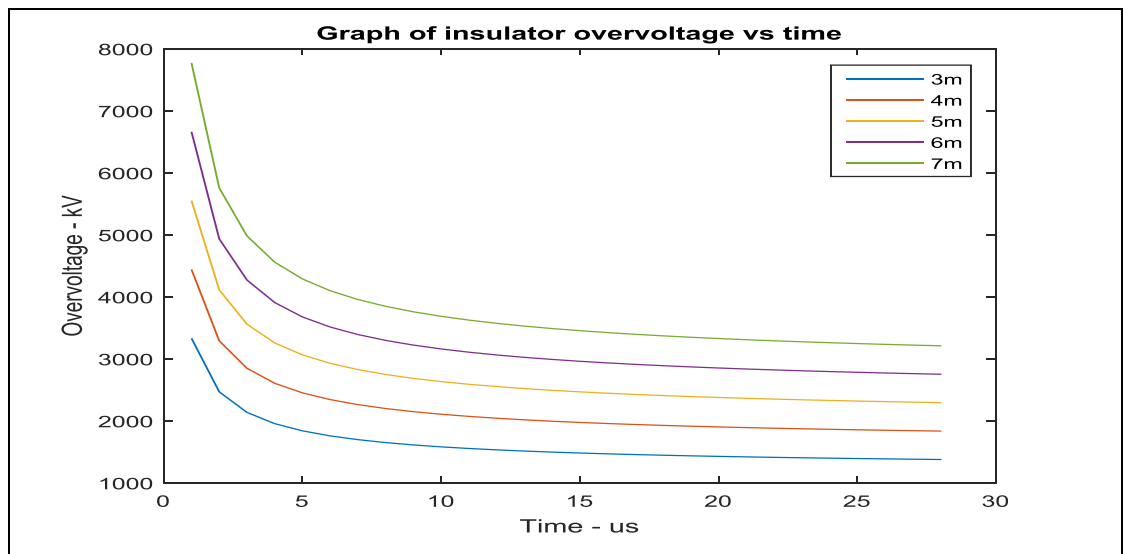
Figure 5.20 Insulator flashover voltage vs Time

From the graph one can deduce that the flash over voltage of the insulator would increase as the length of the insulator increased. These voltages would tend to converge towards a voltage level. The flashover over voltage for a 6 meter insulator would be 3196kV for an 8/10us waveform

5.2.2 Tower and Line surge impedance

For an EHVDC transmission tower the following dimension can be used.

r_1 = 7.75m

r_1 = 7.75m

r_3 = 3.9m

h_1 = 11.9m

h_1 = 34.0m

These parameters are variables into the programs and a tower surge impedance of 111 is obtained. Similarly a line surge impedance of 417 was obtained for the conductor.

5.2.3 Tower top voltage

The programs used a lightning stroke magnitude of 50kA and a tower footing resistance value of 17.38 ohms. Utilising the standard 533kV tower dimension and the physical size of the conductor, the tower top overvoltage is shown in figure 5.21.
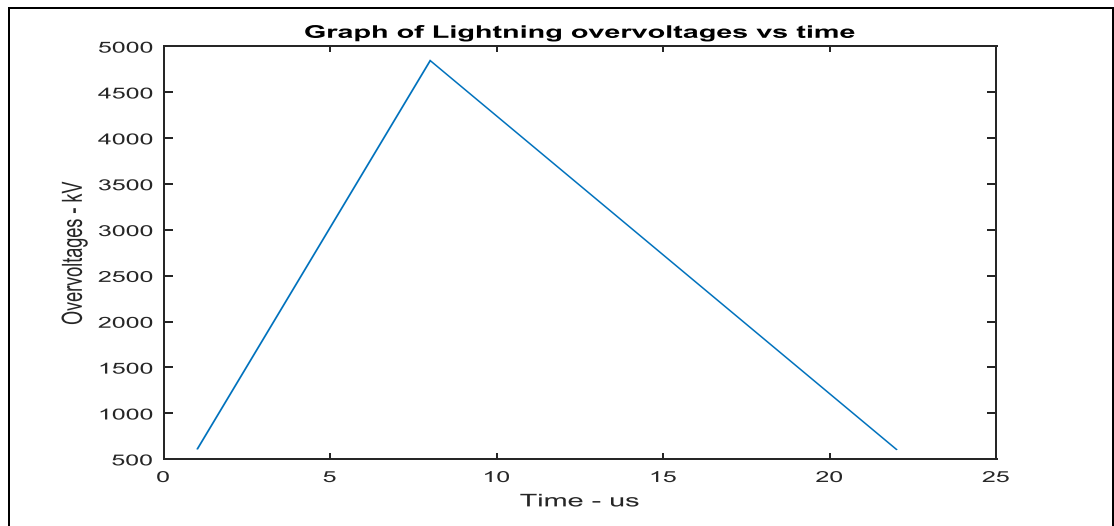
Figure 5.21 Graph of Tower Top Voltage vs Time

An over-voltage greater 4588kV.at 8 micro-seconds is obtained. From figure 5.20 the withstand voltage of the insulator is 3196kV. This would result in a back flash over. Figure 5.22 was generated using various lightning stroke magnitudes.
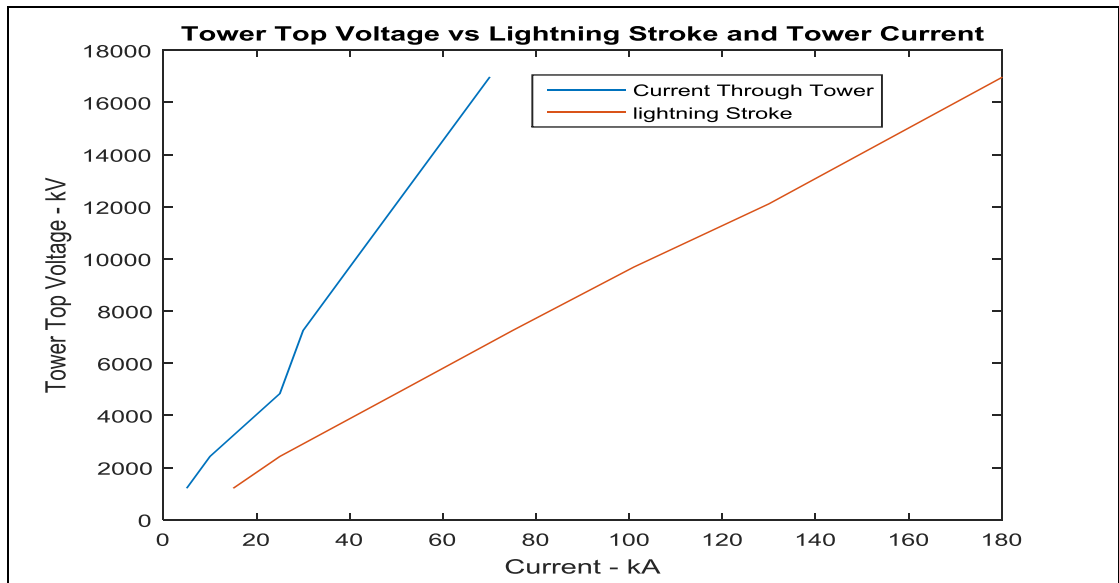
Figure 5.22 Tower top voltage vs lightning current through the tower

With the stroke current been the only variable, a linear relationship with the tower top voltage is obtained. It must be noted that this over voltage is generated using the current flowing through the tower. This is due to the current splitting effect. From the above figure a lightning stroke of 50kA would give rise to a short duration over-voltage of 4475kV. Figure 5.23 illustrates the tower top voltage for various lightning strokes as a function of tower footing resistance.
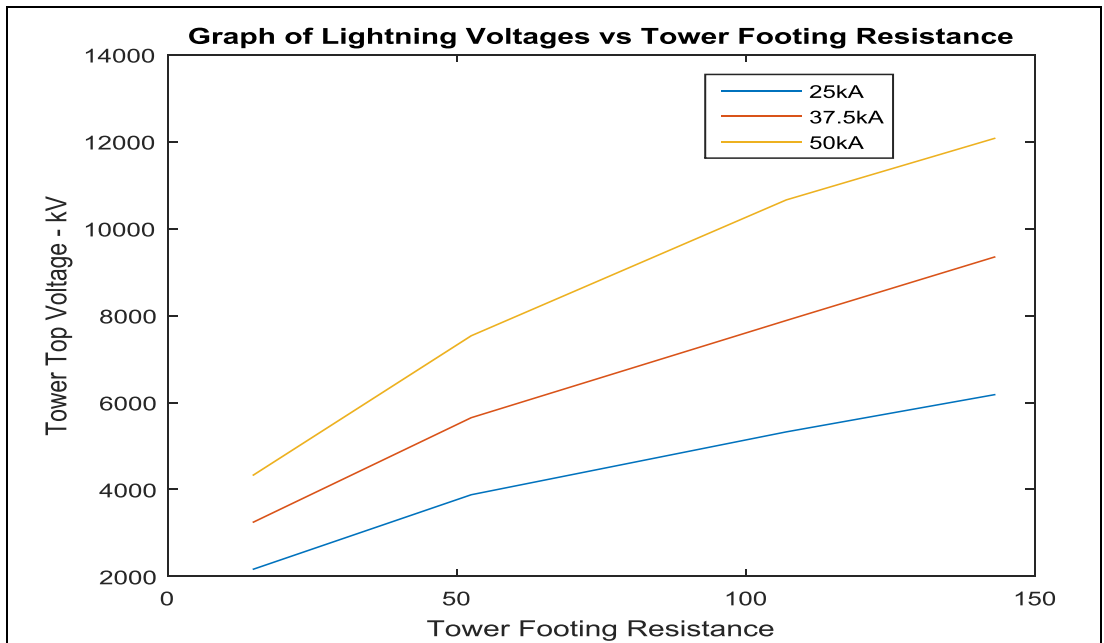
Figure 5.23 Tower Top over Voltage variation vs Tower footing resistance

With a constant lightning stroke magnitude, the tower voltage top would increase with an increasing tower footing resistance. No earthing enhancement is considered for the earthing values used as per figure 5.23. Utilising earthing enhancement techniques as discussed in Chapters 3, 5.1.1 and 5.1.2, which reduces the tower footing resistance value to less than 30 ohms, the graph shown in figure 5.24, is obtained.
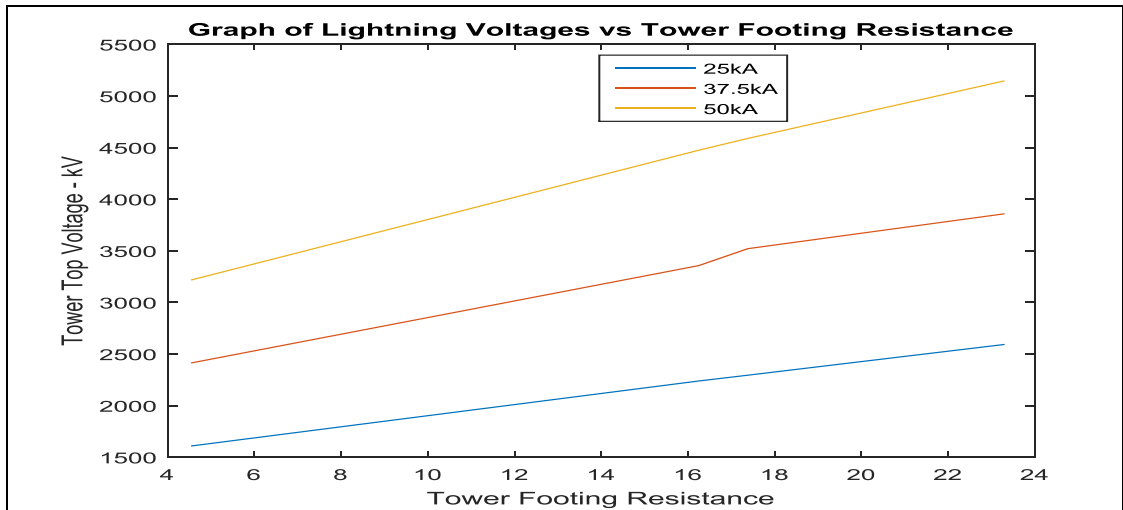
Figure 5.24 Modified Tower Footing Resistance vs Tower Top Voltage

Figures 5.23 and 5.24 indicate a substantial reduction in the tower top voltages. This highlights the need to have acceptable tower footing resistance. It may be costly to reduce the footing resistance to single digit figures.

5.2.4 Surge Arrestor discharge voltage

The nonlinear resistor, A_0, associated V-I voltage determined by reading the "Relative IR" for a 20kA current from Fig 5.25.
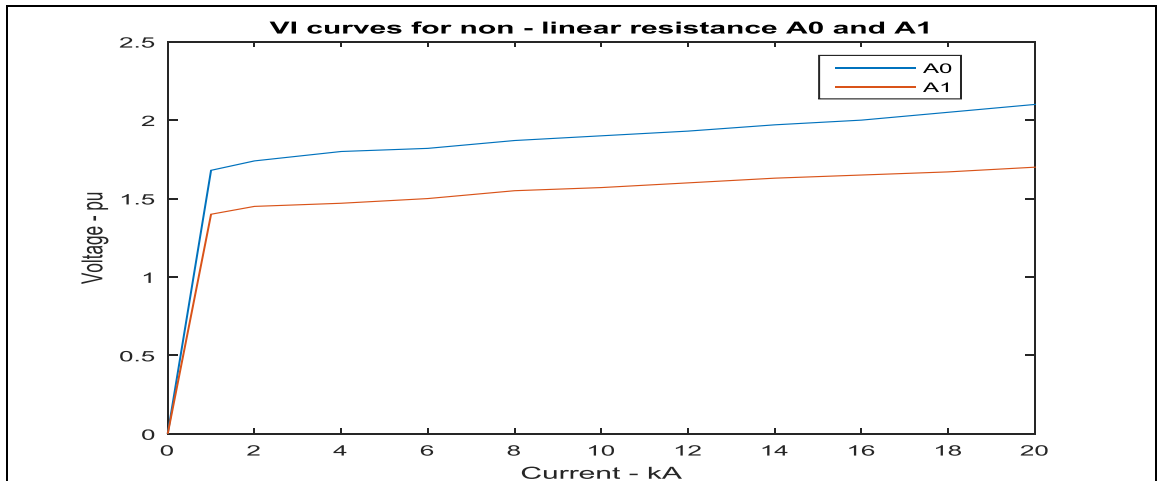
Figure 5.25 VI Curves for non-linear resistance

Figure 5.25 shows that the "Relative IR" for a 20 kA current is 1.9pu. The operating voltage for this surge arrestor specification is 976kV – Refer to surge arrestor data sheets in Appendix B. Therefore, the associated discharge kV for a 20kA surge arrestor is:

$$V_d = \frac{2.1 * 1014}{1.6} kV = 1331 kV$$

Once this voltage or a voltage greater then this appears across the surge arrestor, it will start conducting and begin to dissipate the surge. This surge travels at the speed of light and hence the voltage will remain at the surge arrestor terminals for a very short time. It is during this short time that the surge arrestor will conduct and reduce the power surge by draining the discharge voltage.

5.2.5 Required surge arrestors

When the back flash over has occurred, the voltage on phase conductor would be almost equal to the back flash over voltage. On the conductor the power surge will further separatet into two. One half of the power surge would travel towards the source bus bar and the other towards the end of the line.

Placing the surge arrestor be placed at this node would result in a three way power surge split, which would be a function of the line impedance and the amount of energy the surge arrestor may conduct in that short time interval. This time interval is normally less than 1us. A number of line surge arrestors would have to be connected in parallel to dissipate the power surge and prevent a breaker operation.

A lightning stroke current of 50kA would require three 550kV 20kA surge arrestors connected on parallel to dissipate the lightning stroke. This should prevent the line breaker from operating and causing small duration outages.

Figure 5.26 shows the reduction of the over-voltage caused cause by a 50kA lightning stroke. The same rating surge arrestors were used.
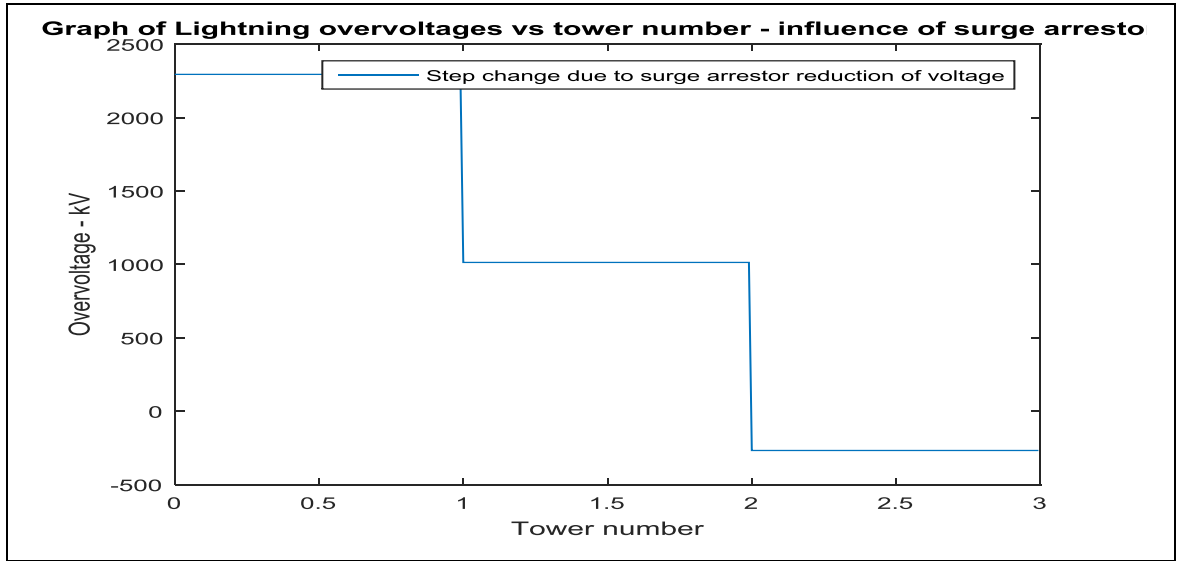
Figure 5.26 Reduction of lightning over voltages due to the introduction of line surge arrestors

Table 5.13 – 5.16 shows the required number of surge arrestors to drain the over voltages caused by lightning strokes of different magnitudes and different soil parameters. The soil parameters are taken from case studies 1 – 4.

Table 5.13 Tower Footing resistance of 23.1 and different lightning strokes

Lightning current - kA	Insulator Voltage kV	Tower Footing Resistance	Tower top Voltage kV	Back Flash over	Phase Voltage	Required SA - Prevent outage
12	3296	4.56	804	No	402	0
25	3296	4.56	1609	No	805	0
37.5	3296	4.56	1415	No	1107	0
50	3296	4.56	3119	No	1609	0
98	3296	4.56	6194	Yes	3147	3

Table 5.14 Tower Footing resistance of 16.25 and different lightning strokes

Lightning current - kA	Insulator Voltage kV	Tower Footing Resistance	Tower top Voltage kV	Back Flash over	Phase Voltage	Required SA - Prevent outage
12	3296	16.25	1118	No	559	0
25	3296	16.25	1134	No	1119	0
37.5	3296	16.25	3356	Yes	1678	2
50	3296	16.25	4475	Yes	1137	2
98	3296	16.25	8950	Yes	4475	4

Table 5.15 Tower Footing resistance of 17.3 and different lightning strokes

Lightning current - kA	Insulator Voltage kV	Tower Footing Resistance	Tower top Voltage kV	Back Flash over	Phase Voltage	Required SA - Prevent outage
12	3296	17.33	1143	No	573	0
25	3296	17.33	2349	No	1174	0
37.5	3296	17.33	3440	Yes	1720	2
50	3296	17.33	4588	Yes	2294	2
98	3296	17.33	9175	Yes	4587	4

Table 5.16 Tower Footing resistance of 23.15 and different lightning strokes

Lightning current - kA	Insulator Voltage kV	Tower Footing Resistance	Tower top Voltage kV	Back Flash over	Phase Voltage	Required SA - Prevent outage
12	3296	23.15	1186	No	643	0
25	3296	23.15	2573	No	1286	0
37.5	3296	23.15	3859	Yes	1929	2
50	3296	23.15	5145	Yes	2573	2
98	3296	23.15	10290	Yes	5145	4

Figure 5.27 shows the correlated breaker interruptions due to lightning for an 533kV EHVDC line for the 2009 calendar year. All these interruptions resulted from lightning strokes within a diameter of 1km of the line. The corresponding stroke magnitude for the breaker trip time was obtained from the FALLS system.
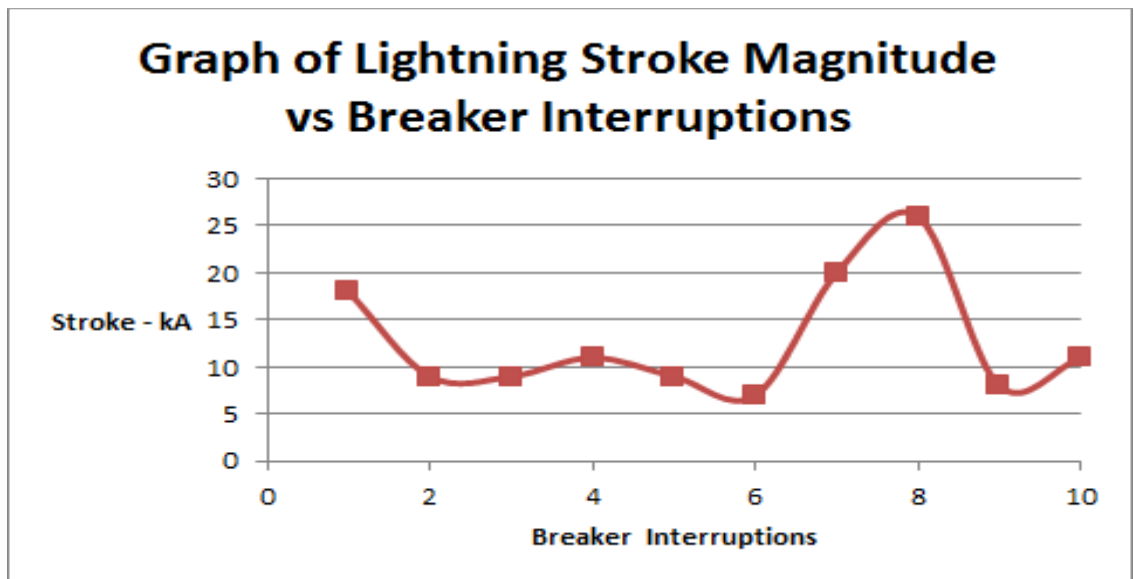
Figure 5.27 Stroke magnitude vs breaker interruptions

Analysis of the data revealed that that the peak lightning stroke that resulted in a breaker interruption was 26kA. Table 5.16 shows that the insulation level would comfortable withstand this lightning

stroke. From figures 5.18 and 5.19 the lightning stroke magnitude can reach 50kA and above, albeit by a small percentage. Hence by utilising three sets of surge arrestors, this percentage can be reduced to almost zero.

5.2.6. Financial Evaluation for EHVDC systems

(a) Annual expected number of voltage dips and momentary outages due to lightning

Performance monitoring of a 533kV overhead line revealed that in the year 2009 there was 124 momentary interruptions. Of these 10 was due to lightning. [15]

(b) Estimate the cost associated with voltage dips and momentary outages.

A study undertaken by Nzimande [16] revealed that lightning (storm) related dips lead to losses of between US$5357 and US$35714 per annum for 10 storm related dips, an average of between US$357 and US$3571 per dip. These figures are escalated to 2018 and are US$1143 and US$7425.

(c) Cost of 4 x 550kV DC line surge arrestors to effectively mitigate against lightning back flashover.

The following table 5.17 illustrates the high level costing required to install 4x550kV surge arrestors, i.e 2 surge arrestor per phase, required to mitigate against a 50kA lightning stroke

Table 5.17 Illustrating the costs to install 4 surge arrestors

Item	Year 2018
Cost of a surge arrestor and counter	USD 38 835
Cost of 4 surge arrestor and counters	USD 158 700
Labour and transport	USD 4 601
Total	USD 163 302

The following figure 5.28 shows that it would take 6 years to recover the capital invested in the surge arrestors to mitigate against dips, providing the inflation is 5%. Should the inflation be 10%, the capital will be recovered after 8 years.
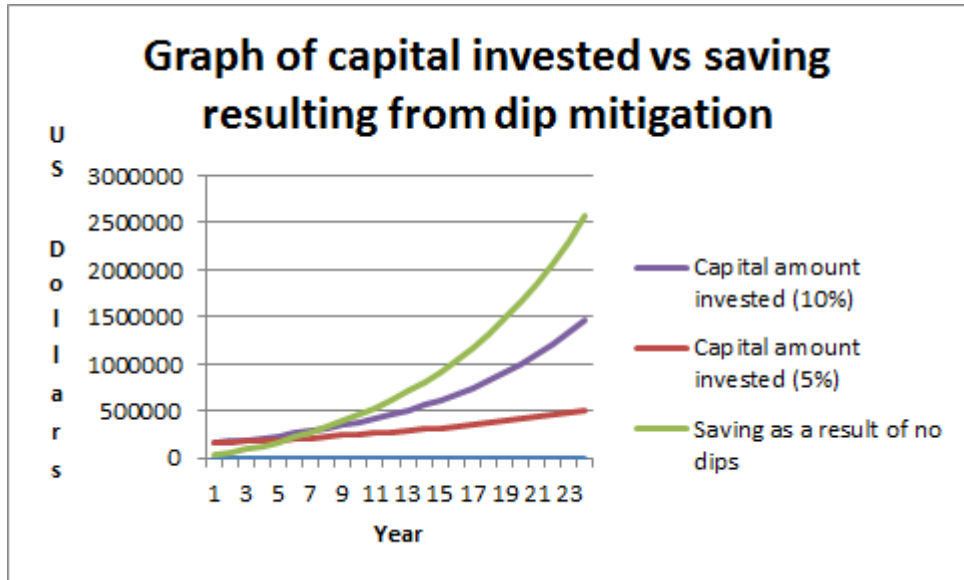
Figure 5.28 Break-even point occurs in year 6 (5% inflation rate)

CHAPTER SIX   CONCLUSION

Power utilities utilise overhead transmission lines, which are aging, to transmit electrical power to consumers. Most of these consumers have electrical equipment that is sensitive to short duration interruptions such as dips One of the main causes of dips are breaker operations, which can originate from lightning strokes.

In this thesis, MATLAB programs have been created to determine earthing configuration for HVAC and EHVDC overhead lines. Based on lightning strokes of different magnitudes and tower footing resistance values, the voltage at the tower top can be determined. Should the tower top voltage exceed the insulator flash over voltage, a back flash over would occur. MATLAB programs have been developed to calculate the tower top voltages and the phase voltage on the conductor. Thereafter the required number of surge arrestors to drain the lightning surge current to ground is calculated.

Soil conditions, in particular, resistivity varies for different soil conditions. Clay and sand mix soil been in the regions of 100 ohm meter and sand been in the range of 200 ohm meter. As the soil depth increases, it may tend to become moister and hence the soil resistivity would decrease. Practical testing done to determine soil resistivity revealed that under dry conditions the value is ~1800 and drops down to ~200 ohms meter under wet conditions. This is for a depth of 0.5 meters.

The profile of the tower footing resistance curve would follow that of soil resistivity results, provided the type of soil is uniform. Dry conditions would lead to high tower footing resistance and vice versa. Different models were created in MATLAB to establish the earthing resistance for the driven rod, crow foot and radial conductor's configurations.

Using earthing enhancement techniques, such as additional conductors, which would reduce the tower footing resistance substantially and bring it a pre determinate value. This can be less than 30ohms. This has been undertaken for different earthing configurations. It must be noted that during the storm cycle, the soil conditions would initially be dry and then be wet.

The program can determine the earthing systems that can be designed to obtain very low values of tower footing resistances. However, one must also consider the financial aspect of installing additional conductor and rods to achieve this.

The importance of having a tower footing resistance below 30 ohms is that the tower top voltage is substantially reduced, when compared with scenarios of having no earthing enhancements. The values

calculated by the developed MATLAB programs showed a reduction of almost 50%. Hence it is important that the tower footing resistance be kept to values less than 30 ohms.

The lower the tower footing resistance, the lower the tower top voltage, which reduces the possibility of a short circuit across the insulator. It high lightning areas, consideration should be given to design systems with the tower footing resistance value below 15 ohms. This will reduce the tower top voltages.

Based on tower and line impedance, about 40% of the lightning stroke would flow down the tower and contribute to the tower top voltages. Variables, such as the lighting stroke, line and tower surge impedance and tower footing resistance values, contribute towards tower top voltage. Should the insulator breakdown voltage be exceeded, back flash overs would occur. The same tower top voltage level will be present on the live side of the conductor (surge arrestor), which is due to the 'short circuit' caused by the high current. It must be noted that approximately 20% of the initial lightning stroke would travel along the conductor towards the source or end of line.

Lightning surges travel at the speed of light. Depending on the impedance of the conductor, the waveform may not be eliminated, which would result in the protective devices operating to eliminate the power surge. This creates dips and short duration outages, which leads to consumer interruptions on the network. This leads to a loss of production and negatively impacts the economy. Line Surge Arrestors are devices that can drain the power surge to ground, if placed adequately and in sufficient numbers

Depending on the magnitude and waveform speed, a single LSA may be insufficient arrestor to drain the power surge to ground. Additional surges arrestors would be required. These additional surge arrestors are calculated based on the power surge that would be present on the conductor and is determined by programs developed in MATLAB.

Surge arrestor should be placed parallel to each other and after the operating device. This would prevent the protective device (network breaker) from operating. Dips and short duration outages would be prevented.

It is important to select and size the surge arrestor accordingly. Some surge arrestor manufacturers are able to manufacture special lightning surge arrestors for the maximum system voltage e.g. 88kV and 533kV. It is advisable to choose surge arrestor with a higher energy capability, pending financial availability. To prevent nuisance breaker operation and minimise the effect of leakage current, one

needs to increase the rated voltage. This is influenced by the number of surge arrestors that would be installed on the line. The pexlim R surge arrestor, which has an energy capability of 5.1, would be suitable sized to drain the surge current from the 88kV line.

The maximum magnitude of the lightning strokes with the corridor of a HVAC line could be as high as 150kA. However the bulk of the stroke magnitude, approximately 97%, is less than 51kA. There are strokes above 51kA, but these are less than 3%. Hence it is advisable to install an adequate number of surge arrestor that would drain strokes of the value of 51kA to ground. Mitigation against a lightning stoke of 51kA will require 9 surge arrestors per phase, which would depend on the tower footing resistance. For this amount of surge arrestors the break-even point will be six years. It must be noted that certain factors such as potential loss of sales to the power utility, additional maintenance is excluded from the financial evaluation

For EHVDC overhead line, the majority of strokes magnitude is between 3 and 51kA. Strokes are evident beyond its magnitude, but the percentage of these are small. Simulations revealed that a tower footing resistance of 23.15ohms two surge arrestor per phase would be sufficient to drain stroke magnitudes of 37.5 and 51kA.

The main effect of preventing breaker operation would be to prevent dips and therefore production loss. Studies have been concluded to ascertain the cost of a dip. Depending on the number of surge arrestors used, the breakeven point would vary as well. The breakeven point is the capital cost of the number of surge arrestors offset against saving. Furthermore damage to overhead line components will be minimized as the power surge will be removed from the line. Routine maintenance of the protective device will be minimized as the operations will be reduced.

By using tower footing resistance enhancement techniques, the tower over voltage is reduced by 50%. Should this not be enhanced the tower top voltage will be twice as much and the simulation results indicate that 8 surge arrestors would be required to drain a lightning stroke of 51kA to ground.

New contributions of this thesis
The major contributions to knowledge of this thesis include:
- Soil resistivity measurements and earthing calculations. Physical measurements were carried out on site under wet and dry conditions. Various tower footing resistance methodologies are examined, modelled and simulated to reduce tower footing resistance values.

- The development of various MATLAB programs to calculate the tower top voltages for given lightning strokes and Tower Footing Resistances, insulator flashover voltage, etc. These programs would ultimately determine the required number of surge arrestors to prevent BFO for a specific lightning stroke.

- The correlation of the existing lightning activities of a HVAC line to that of its actual performance, i.e outage caused by the lightning strokes. This was done using breaker trip time information, which was then matched to the actual lightning strokes within the corridor of the line. Only these breaker trips were utilised in this thesis. The magnitude of the lightning is thus known.

- The correlation of the existing lightning activities with EHVDC line to that of actual performance of a 533kV line. The breaker trip time information was used, which was subsequently matched to lightning strokes within the corridor of the line. This also provided us with the priority and magnitude of the stroke. Only these breaker trips were utilised in this thesis.

- The economic analysis for the HVAC system. This involves quantified production losses associated with dips arising from lightning strokes. These dips would arise from the lightning induced operations for an 88kV overhead line trips. The breakeven point thus determined utilising amongst other capital and installation costs of the system against savings arising from production losses.

- The economic analysis for the EHVDC system. The breakeven point thus determined utilising amongst other capital and installation costs of the system. This cost is offset against quantified production losses associated with dips arising from correlated lightning strokes for a particular 533kV Overhead DC line.

- The development of the overall MATLAB program, which satisfies the primary aim of thesis, which is to determine the required number of surge arrestors to prevent line (power consumer) outages for a given lightning stroke, earthing , line and tower configurations.

CHAPTER SEVEN   RECOMMENDATIONS

The following are recommendations for future studies:

- A financial analysis should be undertaken to determine the breakeven point between the costs of installing earthing systems to lower the tower footing resistance value against the financial benefits of improved system performance.

- A detailed analysis should be done to calculate the lightning stroke percentage that terminated on the phase conductor, shielding failures. Information from the FALLS system is to be used.

- A computer program should be developed to convert the developed MATLAB programs into a user friendly input/output unit

- The financial evaluation should be enhanced by including certain factors such as potential loss of sales to the power utility, reduced maintenance on the operating device and the deferred replacement of line components.

- The EHVDC lines are normally in excess of 400km. Line surge arrestors need to be placed at both the source and receiving end.

- The database for the lightning parameters used in the program may be expanded.

References

[1] G. A. Inc, "Vaisala-GAI fault Analysis and Lightning Location Systems (FALLS) Version 3.2.4," Tucson, Arizona, USA, 2002.

[2] J, Williams., "Lightning Protection and Surge Arrestor Application on NB Power Transmission Lines," in *IEEE PES Transmission and Distribution Conference and Exposition*, Chicago, 2008.

[3] W. K. Glossop, "Performance comparison of existing AC and DC transmission lines within southern Africa with predictions for lines above 765kV," Master of Engineering Dissertation, University of Witwatersrand, Johannesburg, South Africa, 2008.

[4] M. Ahmeda, "Earthing performance of transmission line towers," Doctor of Philosophy in Engineering, Cardiff University, Cardiff, Wales, 2012.

[5] M. Bhavan, "Performance of High Voltage Direct Current (HVDC) systems with line commutated convertors," *IEC/TR 60919-2,* 2008.

[6] J He, Y Tu, R Zeng, J B Lee, S H Chang, Z Guan, "Numeral analysis model for shielding failure of transmission line under lightning stroke," *IEEE Transactions on Power Delivery,* pp. 815-822, 2005.

[7] E. Singh, "Fault Mitigation and Performance Improvement of an 88kV line using Line Surge Arrestors and Counters," University of Kwa Zulu Natal, Postgraduate Research Day, Durban, South Africa, November 2016.

[8] *NRS 048-2, Electricity Supply − Quality of Supply Standards − Part 2: Minimum Standards,* Johannesburg, 2004.

[9] T. Nzimande, "Voltage Dip Performance Analysis," Master of Science in Engineering, University of KwaZulu-Natal, Durban, South Africa, 2009.

[10] HF, Vosloo, "The Need for and Contents of a Life Cycle Management Plan for Eskom Transmission Line Servitudes," Rand Afrikaans University, Johannesburg, 2005.

[11] MJH, Bollen, "Understanding Power Quality Problems: Voltage Dips and Interruptions," in *IEEE Press*, New York, 2000.

[12] H. Hamzehbahmani, H. Griffiths, A Haddad and D Guo, "Earthing Requirements for HVDC Systems," *In 2015 50th International Universities Power Engineering Conference (UPEC) IEEE,* pp. 1-7, 2015.

[13] K. Meah, S. Ula, "Comparative evaluation of HVDC and HVAC Transmission Systems," in *2007*

IEEE Power Engineering Society General Meeting, 24 June 2007, pp. 1-5.

[14] L. A. Bateman, R.W Haywood, "Nelson River DC Transmission Project," *IEEE Transactions on Power Apparatus and Systems,* Vols. Vol. PAS-88, no. 5, pp. 688-693, 1969.

[15] J. Arrillaga, "High Voltage Direct Current Transmission," *2nd Edition, IEE power and energy series 29,* 1998.

[16] P.S. Maruvada , R.D. Dallaire, O.C. Norris-Elye, C.V. Thio, and J.S.Goodman, "Environmental Effects of the Nelson River HVDC Transmission Lines – RI, AN, Electric Field, Induced Voltage, and Ion Current Distribution Tests," *IEEE Transactions on Power Apparatus and Systems,* Vols. PAS-101, no. 4, pp. 951-959, April 1992.

[17] Globe Circuit, "Different-types-hvdc-links.," [Online]. Available: https://circuitglobe.com/ different-types-hvdc-links.html. [Accessed 2019].

[18] U.S. Energy Information Administration, "Assessing HVDC Transmission for Impacts of Non-Dispatchable Generation.," [Online]. Available: https://www.eia.gov/analysis/studies /electricity/hvdctransmission/. [Accessed 2019].

[19] Kumar, Prashant, "MTDC System," Northern India Engineering College, New Delhi, India, 2015. [Online]. Available: https://www.slideshare.net/bunttyy/mtdc-47321069. [Accessed 2020].

[20] O.E. Gouda, G.M.Amer and T.M El-Saied, "Factors Affecting the Apparent Soil Resistivity of Mult-Layer Soil," in *Proceedings of the XIVth International Symposium on High Voltage Engineering*, Tsinghua University, Beijing, China, 25-29 August 2005.

[21] G.A. Adegboyega, K.O. Odeyemi, "Assessment of Soil Resistivity on Grounding of Electrical Systems: A case study of North-East Zone, Nigeria," *Journal of Academic and Applied Studies,* vol. 1(3), pp. 28-38, September 2011.

[22] D. Mukhedka, F. Dawalibi, *IEEE Guide for Measuring Earth Resistivity, Ground Impedance, and Earth Surface Potentials of a Ground System,* IEEE Standards Board.

[23] E&S Grounding Solutions, "www.esgroundingsolutions.com," [Online]. Available: https://www.esgroundingsolutions.com/what-is-step-and-touch-potential. [Accessed 2019].

[24] S. C. Malanda, E. Buraimob, I. Davidson and E. Singh, "Analysis of Soil Resistivity and it's Impact on Grounding System Design," in *Proceedings of the IEEE Power Africa Conference*, Cape Town, Soutrh Africa, 26 - 29 June 2018.

[25] H. B. Dwight, "Calculation of Resistance to Ground," *American Institute of Electrical Engineers,* vol. 55, no. 12, pp. 1319-1328, 1936.

[26] Sunde, Erling D, *Earth conduction effects in transmission systems,* New York: D. Van Nostrand

Company, Inc, 1949.

[27] G. F. Tagg, "Earth resistance," [Online]. Available: http://www.lightningman.com.au/ Earthing.pdf. [Accessed 2017].

[28] R. J. Holt, J. Dabkowski, R.L. Hauth, "HVDC Power Transmission Electrode Siting and Design," Oak Ridge National laboratory, USA, 1997.

[29] Et Al, "General guidelines for HVDC Electrode Design," Cigre, January 2017.

[30] Circuit Globe , "Direct Current Ohms law," [Online]. Available: https://circuitglobe.com/different-types-hvdc-links.html. [Accessed 2019].

[31] C. F. Dalziel, "Deleterious Effects of Electric Shock," International Labour Office, California, 1961.

[32] "IEEE Guide for Safety in AC Substation Grounding," IEEE Std. 80-2000.

[33] Suresh K, Paranthaman S K, "Transferred Potential—A Hidden Killer of Many Linemen," *IEEE Transactions on Industry Applications,* vol. 51, no. 3, pp. 2691 - 2699, May - June 2015.

[34] Working Group on Estimating the Lightning Performance of Transmission Lines, "Working group report estimating lightning performance of transmission lines II-updates to," *IEEE Transaction on Power Delivery,* vol. 8, no. 3, p. 1254 – 1267, 1993.

[35] W. A. Chisholm, Y. L. Chow and K. D. Srivastava, "Travel time of transmission Towers," *IEEE Transaction on Power Apparatus and Systems,* Vols. PAS-104, no. 10, pp. 2922-2928, 1985.

[36] IEEE Guide for the Application of Insulation Coordination, IEEE Std 1313.2-, June 1999.

[37] IEEE Guide for Improving the Lightning Performance of Transmission Lines, IEEE Std 1243, 1997.

[38] Goertz. M, Wenig. S, Gorges. S, Kahl. M, Beckler. S, Christrian. J, Suriyah. M, Leibfried. T, "Lightning Overvoltages in a HVDC Transmission," in *International Conference on Power Systems Transients*, Seoul, South Korea, June 2017.

[39] Tomohiro Hayashi, Tomohiro Hayashi, Yukio Mizuno and Katsuhiko Naito, "Study on Transmission line arresters for tower with high footing resistance," *IEEE Transaction on Power Delivery,* vol. 23, no. 4, pp. 2456-2460, 2008.

[40] Makoto Takeuchi, Yoh Yasuda and Hidenobu Fukuzono, "Impulse characharcteristics of a 500kV transmission tower footing base with various groungrounding electrodes," in *International Conference on Lightning Protection (ICLICLPP)*, UK, 1998.

[41] T. Hayashi, Y. Mizuno and K. Naito, "Study on Transmission – Line Arresters for Tower with High Footing Resistance," *IEEE Transaction on Power Delivery,* vol. 23, no. 4, pp. 2456-2460, October 2008.

[42] C. Li-Hsiung, C. Jiann-Fuh, L.Tsorng-Juu and W. Wen-I, "Calculation of ground resistance and step voltage for buried ground rod with insulation lead," *Electric Power Systems Research 78,* p. 995– 1007, 2008.

[43] E. Singh, I.E. Davidson, G.K. Venayagamoorthy, "Methodology for measuring and enhancing Tower Footing Resistance for Lightning Protection for an 88kV line," in *Proceedings of the 25th South African Universities Power Engineering Conference*, Stellenbosch, South Africa, 30 January - 1 February 2017.

[44] I. E. Davidson, "A Mathematical Algorithm for Investigating Soil Resistivity," in *Proceedings of the 6th Southern African Universities Power Engineering Conference. University of the Witwatersrand*, Johannesburg, South Africa, January 1996.

[45] Y. LIU, "Transient Response of Grounding Systems Caused by Lightning: Modelling and Experiments," ACTA UNIVERSITATIS UPSALIENSIS, UPPSALA, 2004.

[46] C. A. Nucci, F. Rachidi, "Lightning Induced Voltages," in *IEEE '99 T&D Conference Panel Session. Distribution Lightning Protection*, New Orleans, April 1999.

[47] G.A. Adegboyega, K.O. Odeyemi, "Assessment of Soil Resistivity on Grounding of Electrical Systems: A case study of North-East Zone, Nigeria," *Journal of Academic and Applied Studies,* vol. 1, no. 3, pp. 28-38, September 2011.

[48] N.H.N. Hassan, A.H.A. Bakar, H. Mokhlis and H. A. Illis, "Analysis of Arrestor Energy for 132kV Overhead Transmission Line due to Back Flashover and Shielding failure," *Proceedings Of the 16th IEEE International Conference on Power and Energy,* pp. 683-688, December 2012.

[49] E. Singh, I.E. Davidson, "Improving Overhead HV AC Line Performance using Line Surge Arrestors under Lightning Conditions with economic anaylsis," *International Journal of Applied Engineering Research,* vol. 14, no. 22, pp. 4126-4135, 2019.

[50] Dekker. M, "Lightning Surge Analysis," [Online]. Available: http://197.14.51.10:81/pmb/ informatique/computer%20aid%20analys/0824706994/PDFs/DK1913_CH13.pdf. [Accessed 2017].

[51] C.F. Wagner, H.R. Hileman, "Lightning Performance of Transmission lines 3," *AIEE Power Apparatus and Systems,* p. 903, November 1960.

[52] G. Radhika, M. Suryakalavathi and G. Soujanya, "Effective Placement of Surge Arrestor during Lightning," *International Journal of Computer Communication and Information System,* vol. 2, no. 1, pp. 167-172, 2010.

[53] Mohd Z.A Ab Kadir, Zawati Mohd Nawi and Junainah Sardi, "Numerical Modeling and Simulation

in Electro Magnetic Transient Program for Estimating Line Back Flashover Performance," November 2010. [Online]. Available: https://www.researchgate.net/profile/Zainal_Kadir/ publication/303494666_Numerical_Modeling_and_Simulation_in_Electromagnetic_Transient_ Program_for_Estimating_Line_Backflashover_Performance/links/0fcfd51012a01f1d52000000/ Numerical-Modeling-and-Simulation-i. [Accessed 2017].

[54] IEEE Working group 3.4.11, "Modeling of metal oxide surge arrestors," *IEEE transaction on Power Delivery,* vol. 7, no. 1, pp. 302-309, January 1999.

[55] P. Pinceti, M Giannettoni, "A simplified model for the zine oxide surge arrestor," *IEEE Transaction on Power Delivery,* vol. 14, no. 2, pp. 393-398, April 1999.

[56] "Soil Measurements," [Online]. Available: https://learn.weatherstem.com/modules/learn/ lessons/77/09.html. [Accessed 2019].

[57] Sajad Samadinasab*, Farhad Namdari and Mohammad Bakhshipour, "The Influence of Moisture and Temperature on the Behavior of Soil Resistivity in Earthing Design Using Finite Element Method," *Indonesian Journal of Electrical Engineering and Computer Science,* vol. 2, no. 1, p. 11 12, April 2016.

[58] Johnson. A. Ivan, "Methods of measuring soil moisture in the field," US Government Printing Office, Washington., 1962.

[59] Black C.A., "Methods of Soil Analysis: Part I Physical and mineralogical," American Society of Agronomy, Madison, Wisconsin, USA, 1965.

[60] "Earthing Fundalmental," [Online]. Available: http://www.lightningman.com.au/Earthing.pdf. [Accessed 2017].

[61] Stierman, "Field Techniques," August 2005. [Online]. Available: http://www.eeescience.utoledo.edu/faculty/stierman/EEG/notes/FT.htm. [Accessed 2018].

[62] ABB, "High Voltage Surge Arrestors," *www.abb.com,* p. 6, 2002.

Appendix A - Subroutines for HVAC Systems

Appendix A1 – Calculation of Soil Resistivity

```
clear all
% Initialising of variables
J=0;
p=3.14;

% Obtaining the variables
I=10;
P1=input ('Enter Upper layer soil resistivity   ');
P2=input ('Enter Lower layer soil resistivity   ');
H=input ('Enter upper layer thickness in meters ');
h=0;
for J=1:H
Pa(J) = I*(P1*P2)/(P2*(J-h) + P1*(I+h-J));
Ex(J) = J;
Soil_Resist(J)=Pa(J);
end
plot (Ex, Soil_Resist);
title('Plot of soil resistivity vs depth');
ylabel('Resistivity (ohms)');
xlabel('depth (m)');

Soil_Resistance = Soil_Resist(H);
```

Appendix A2 – Calculation of Tower Footing Resistance

```
%This subroutine calculates the earthing resistances of the three earthing
%types, which must be less than 30ohms. This compares the results and
display the method that produces the
%best earthing results. The program uses the soil resistivity from the
%SoilR subroutine.

clear all
run SoilR
rods=[];

% Driven rods
rods = input ('Enter number of rods  ');
Rnew=[];
%single rod
L=3;
a=7.9/(100);
p=Soil_Resistance;
S=5;
T=0.3;

R11 = p*[log(L/a)]/(2*pi*L);
Fr1 =log((L/a)*(1+sqrt(1+((a/L)*(a/L))))) + a/L - (sqrt(1 +
((a/L)*(a/L))))+
log(((2*(L+T))*(1+sqrt(1+((a*(L+T)/2)*(a*(L+T)/2)))))/((L+(2*T))*(1+(sqrt(1
+((a/(L+(2*a)))*(a/(L+(2*a))))))))));
Fr2 =
(T/L)*log((2*(L+T)*((1+sqrt(1+((a*(L+T)/2)*(a*(L+T)/2)))))*(2*T)*((1+sqrt(1
+(a/(2*T*2*T)))))))/((L+(2*T))*((1+(sqrt(1+((a/(L+2*a))*(a/(L+2*a)))))))*(1+(
sqrt(1+((a/(L+2*a))*(a/(L+2*a))))))))));
Fr3= (1+(T/L))*(sqrt(1+((a/(2*(L+T)))*(a/(2*(L+T)))))));
Fr4= (1+(2*T/L))*(sqrt(1+(a/(L+(2*T)))*(a/(L+(2*T))))) -
(T/L)*(sqrt(1+((a/2*T)*(a/2*T))));
Fr = Fr1+Fr2-Fr3+Fr4;
Rnew = p*Fr/(2*pi*L);


%two rods
D=3;
a=7.9/100;
p=Soil_Resistance;
L=3;
R21 = p*[log((L/a)+ D)]/(4*pi*L);
Fr1 =log((L/a)*(1+sqrt(1+((a/L)*(a/L))))) + a/L-(sqrt(1 + ((a/L)*(a/L))))+
log(((2*(L+T))*(1+sqrt(1+((a*(L+T)/2)*(a*(L+T)/2)))))/((L+(2*T))*(1+(sqrt(1
+((a/(L+(2*a)))*(a/(L+(2*a))))))))));
Fr2 =
(T/L)*log((2*(L+T)*((1+sqrt(1+((a*(L+T)/2)*(a*(L+T)/2)))))*(2*T)*((1+sqrt(1
+(a/(2*T*2*T)))))))/((L+(2*T))*((1+(sqrt(1+((a/(L+2*a))*(a/(L+2*a)))))))*(1+(
sqrt(1+((a/(L+2*a))*(a/(L+2*a))))))))));
Fr3= (1+(T/L))*(sqrt(1+((a/(2*(L+T)))*(a/(2*(L+T)))))));
Fr4= (1+(2*T/L))*(sqrt(1+(a/(L+(2*T)))*(a/(L+(2*T))))) -
(T/L)*(sqrt(1+((a/2*T)*(a/2*T))));
Fr = Fr1+Fr2-Fr3+Fr4;
a=D/3;
```

```matlab
Fr1D =log((L/a)*(1+sqrt(1+((a/L)*(a/L))))) + a/L - (sqrt(1 +
((a/L)*(a/L))))+
log(((2*(L+T))*(1+sqrt(1+((a*(L+T)/2)*(a*(L+T)/2)))))/((L+(2*T))*(1+(sqrt(1
+((a/(L+(2*a)))*(a/(L+(2*a)))))))));
Fr2D =
(T/L)*log((2*(L+T)*((1+sqrt(1+((a*(L+T)/2)*(a*(L+T)/2)))))*(2*T)*((1+sqrt(1
+(a/(2*T*2*T)))))))/((L+(2*T))*((1+(sqrt(1+((a/(L+2*a))*(a/(L+2*a))))))*(1+(
sqrt(1+((a/(L+2*a))*(a/(L+2*a)))))))));
Fr3D= (1+(T/L))*(sqrt(1+((a/(2*(L+T)))*(a/(2*(L+T))))));
Fr4D= (1+(2*T/L))*(sqrt(1+(a/(L+(2*T)))*(a/(L+(2*T))))) -
(T/L)*(sqrt(1+((a/2*T)*(a/2*T))));
FrD = Fr1D+Fr2D-Fr3D+Fr4D;
R2new = p*(Fr+FrD)/(4*pi*L);

%three rods
D=3;
a=7.9/100;
p=Soil_Resistance;
L=3;
R31 = p*[log((L/a)+ (2*D))]/(6*pi*L);
R3new = p*(Fr+(2*FrD))/(6*pi*L);

%four rods
D=3;
a=7.9/100;
p=Soil_Resistance;
L=3;
R41 = p*[log((L/a)+ (3*D))]/(8*pi*L);
R4new = p*(Fr+(3*FrD))/(8*pi*L);

%five rods
D=3;
a=7.9/100;
p=Soil_Resistance;
L=3;
R51 = p*[log((L/a)+ (4*D))]/(10*pi*L);
R5new = p*(Fr+(4*FrD))/(10*pi*L);

TFR=33;
nn=0;
for I=1:rods
    TFR=33;
    L=3;
    a=7.9/100;
    nn(I)=I;
while TFR > 30
  test = (I)-1;
 R115(I)= p*[log((L/a)+ ((test*D)))]/((2*(I))*pi*L);
 R15new(I) = p*(Fr+(test*FrD))/((2*(I))*pi*L);
 Lenght(I) = L;
 Radius(I) = a;
L=L+1;
a=a+0.01;
if a>0.10
    a=0.1;
    end
TFR = R15new(I);
end
end
```

```matlab
disp (' ');
disp (' ');
disp( '          Driven Rod');
if rods==5
fprintf('%s %2.2g\t %2.2g\t %2.2g\t %2.2g\t %2.2g\r', 'No_of_Rods', nn,
'Lenghts(m)', Lenght, 'Resistance', R15new');
else if rods==6
        fprintf('%s %2.2g\t %2.2g\t %2.2g\t %2.2g\t %2.2g\r',
'No_of_Rods', nn, 'Lenghts(m)', Lenght, 'Resistance', R15new');
    else if rods==4
            fprintf('%s %2.2g\t %2.2g\t %2.2g\t %2.2g\r', 'No_of_Rods', nn,
'Lenghts(m)', Lenght, 'Resistance', R15new');
        end
    end
end


x=combine(TFR, L)';
disp('' );
disp('' );
disp('' );
% Horizontal Electrodes buried under the surface
d=10/1000;
L=10;
p=Soil_Resistance;
h=0.5;
Rg = 33;
while Rg > 30
Rg = (p/(pi*L))*(log((4*L)/(sqrt(d*h))) - 1);
if Rg > 30
    L=L+10;
end
end

disp (' ');
disp (' ');
disp( '          Crows Foot');
disp( '    Rg(Ohms)      Lenght(m)');
y=combine(Rg, L)';
disp (y);


disp('' );
disp('' );
disp('' );

% radial conductors
Rrad = 100;
L=0;
II=0;
n=2;
while n < 13
if n==2
    N(n) = 0.7;
else if n==3
        ResRad2=ResRad;
        Resistance = min(ResRad2);
        No = n-1;
        ResRad=[];
```

```matlab
        Lo=L;
        first = combine (No, Lo, Resistance);
        first = first';
            N(n) = 1.53;
    else if n==4
            ResRad3=ResRad;
            Resistance = min(ResRad3);
            No=n-1;
            Lo=L;
            second = combine (No, Lo, Resistance);
            second = second';
            ResRad=[];
            N(n) = 2.45;
    else if n==6
            ResRad4=ResRad(II);
            Resistance = min(ResRad4);
            No=n;
            Lo=L;
            third = combine (No, Lo, Resistance);
            third = third';
            ResRad=[];
        N(n) = 4.42;
    else if n==8
            ResRad6=ResRad(II);
            Resistance = min(ResRad6);
            No=n;
            Lo=L;
            fourth = combine (No, Lo, Resistance);
            fourth = fourth';
            ResRad=[];
            N(n) = 6.5;
        else if n==12
                ResRad8=ResRad(II);
                Resistance = min(ResRad8);
            No=n;
            Lo=L;
            fifth = combine (No, Lo, Resistance);
            fifth = fifth';
            ResRad=[];
                N(n) = 11;
            end
        end
            end
        end
    end
end

L=0;
II=0;

while Rrad > 30
L=L+10;
II=II+1;
Rrad = (p/(n*pi*L))*(log((4*L)/(sqrt(d*h))) - 1 + N(n));
ResRad(II) =Rrad;
end
Rrad = 100;
if Rrad > 30
        n=n+1;
        if n==5
```

```matlab
                n=6;
            end
        if n==7
                    n=8;
                end
if n==9
        n=12;
            end


            else if Rrad < 30
            break
        end
end
end
ResRad12=ResRad(II);
Resistance = min(ResRad12);
    No=n;
    Lo=L;
    sixth = combine (No, Lo, Resistance);
    sixth = sixth';

disp (' ');
disp (' ');
disp  (     ' Radial Conductors    ');
disp  (     'No_of_conductors   Lenght(m)   Resistance(ohms)   ');
fprintf('%10.4g\t %10.4g\t %10.4g\n', first, second, third, fourth, fifth,
sixth);

%display the minimum value
 Rcr = combine(ResRad2, ResRad3, ResRad4, ResRad6, ResRad8, ResRad12);
 Rcr1 = min (Rcr);
 Rcr2 = max (Rcr1);

  Rdr = min(R15new);
 TFRBest=min(combine(Rdr, Rg, Rcr2));

 if TFRBest==Rdr
     Name = 'Driven Rod';
 else if TFRBest==Rg
     Name = 'Crows Foot';
     else if TFRBest==Rcr2
     Name = 'Radical Conductors';
         end
     end
 end

 disp (' ');
 disp (' ');

 disp (' Best suited earthing method');
 disp( Name);
 disp (TFRBest)
```

Appendix A3 – Calculation of Induced Lightning Voltage

```matlab
clear all

h= 23;
Zo=20;
Imax = 10;
d=50;

Imax = [10, 20, 30, 40, 50, 60, 70, 80, 90, 100];

for I = 1:10
    Umax (I) = Zo*Imax(I)*h/d
    I = I +1;
end

plot (Imax, Umax)
pause
dis = [30, 50, 70, 90, 110, 130, 150, 170, 190, 210];

Imax =10
while Imax < 101

    for J = 1:10
    Umax (J)= Zo*Imax*h/dis(J)
    J = J + 1;
    plot (dis, Umax)
    end

J = 1
 if Imax==10
 Umax10 = Umax
 else if Imax==20
        Umax20 = Umax
 else if Imax==30
        Umax30 = Umax
 else if Imax==40
        Umax40 = Umax
 else if Imax==50
        Umax50 = Umax
 else if Imax==60
        Umax60 = Umax
        else if Imax==70
        Umax70 = Umax
 else if Imax==80
        Umax80 = Umax
 else if Imax==90
        Umax90 = Umax
 else if Imax==100
        Umax100 = Umax
    end
    end
    end
            end
    end
    end
```

```
        end
        end
        end
 end
 Imax = Imax + 10;
end
plot (dis, Umax10, dis, Umax20, dis, Umax30, dis, Umax40, dis, Umax50, dis,
Umax60, dis, Umax70,dis, Umax80, dis, Umax90, dis, Umax100)
title ('Overvoltage vs distance from line')
xlabel ('Meters')
ylabel ('Over voltage - kV')
legend ('10kA','20kA', '30kA','40kA','50kA', '60kA', '70kA','80kA', '90kA',
'100kA')
```

Appendix A4 – Calculation of Tower Top Voltage

```matlab
R = [TFRBest, 20, TFRBest];
for O = 1:3
Tt = 0.3*10^(-6);
T0 = 2*10^(-6);
T01 = T0/4;
T01 = T01;
T02 = T01+T01;
T03 = T02+T01;
T04 = T03+T01;
TCO = combine (T01, T02, T03, T04);
TCO =TCO';


Tr=8*10^-6;
Tf=20*10^-6;
Tf1 = Tf/10;
Tr1 = Tr/8;
dum = Tr1;
dumm = Tf1;
Trt = Tr1
for I = 2:8
    Trt(I) = dum + Trt(I-1);
end


for I = 9:15
    Trt(I) = dumm + Trt(I-1);
end
%data base for lightning stroke magnitude in kA
I = [5, 10, 15, 20, 30, 40, 50, 70, 80, 90, 100, 150];
LC=I;
sd=find (LC==PLS);

%calculation of tower top voltage
for J = sd:sd
Zi = Zg*Zt/(Zg+2*Zt);
Zw = (Zt*(Zg*Zg))/(Zg+(2*Zt*Zt))*((Zt-R(O))/(Zt+R(O)));



Dc = ((2*Zt - Zg)/(2*Zt + Zg))*((Zt - R(O))/(Zt+R(O)));
Ic(J) = (2*Tt/T0)*I(J);


II=10;
for E = 1:4
IcNew(E) = (2*TCO(E)/Tt)*II;
VtNew(E) = Zi*II - Zw*((II/(1-Dc)) - IcNew(E)/((1-Dc)*(1-Dc)));
end

Vt(J) = Zi*I(J) - Zw*((I(J)/(1-Dc)) - Ic(J)/((1-Dc)*(1-Dc)));
Vt(J) = Zi*I(J) - Zw*((I(J)/(1-Dc)) - Ic(J)/((1-Dc)*(1-Dc)));
%Tower Top Voltage
Vt(J) = -Vt(J);


end


if O==1
Zo1 = Vt;
else if O==2
```

```
    Zo2 = Vt;
      else if O==3
Zo3 = Vt;

    end
     end
end

end

Diff1 = abs(Zo2-Zo1)
Zo1 = Zo2-Diff1
Zo2 = Zo2
Diff3 = abs(Zo2-Zo3)
Zo3 = Zo2+Diff3



if TFRBest > 20
    Zo2 = Zo3
else if TFRBest < 20
        Zo2 = Zo1
        else if TFRBest == 20
        Zo2 = Zo2
    end
    end
end
```

Appendix A5 – Calculation of Insulator withstand Voltage

```
L = 0.4;
H = 28;

while L < 2.3

K1 = 400*L;
K2 = 710*L;
t=8;
f=20;
G=round(t);
tt=t/G;
dr= 0;
for I=1:28
    dr(I) = 0;
    Vfo(I) = 0;
end


dr = 1
for I=2:28
    dr(I) = dr(I-1) + tt;
end

for I = 1:28
Vfo(I) = K1 + K2/(dr(I)^0.75);
end

for I=1:28
    dr(I) = dr(I);
    Vfo(I) = Vfo(I);

end

drr = 0;
for I = 2:21
    drr(I) = drr(I-1) + 1;
end
%for I = 1:28

 %   Vfon(I-7) = Vfo(I);
%end

if L==1.0
    VfoA = Vfo;
%    VfonA = Vfon;
end

if L==0.4
    VfoB = Vfo;
%    VfonB = Vfon;
end

    if L==1.6
    VfoD = Vfo;
%    VfonD = Vfon;
```

```matlab
    end

        if L==2.2
    VfoE = Vfo;
%    VfonE = Vfon;
            end
L = L + 0.6;

end



plot (dr, VfoB, dr, VfoA, dr, VfoD, dr, VfoE)
xlabel ('Time - us');
ylabel ('Overvoltage - kV');
title ('Graph of insulator overvoltage vs time');
legend('0.4m', '1.0m' ,'1.6m' ,'2.2m')
```

Appendix A6 – Calculation of Surge Arrestor impulse withstand voltage (V10)

```matlab
%Obtain variables from previous sub routines
run TFRNew
%Pre-determined lightning stroke
PLS1 = input('Enter peak lightning stroke in kA      ');
PLS2 = PLS1/2;
% Using a 10 or 20kA surge arrestor
SAR = input('Enter surge arrestor rating in kA      ');
BIL = 450;
for I=1:1
To(I) = 30;
end
T1 = TFRBest;
T2 = TFRBest;
T3 = TFRBest;
R1 = 400;
R2 = 400;
R3 = 400;
R4 = 400;
Lsec1 = 400;
Lsec2 = 400;

Load = 1;


%Zt=60*log(cotd(0.5*(atand(8/28))))

%Surge impedance of ground wire
%Radius of fox conductor = (3.74mm*7);
%height of tower (earthwire) is 27m
 Zg = 60*log(27/0.026);
 h = 28.22;
h1 = 9.74;
h2 = 18.48;

r1 = 4.2
r2 = 4.2;
r3 = 3.8;
Ravg1 = r1*h1 + r2*h + r3*h2;
Ravg = Ravg1/h;
Zt = 60*log(cot(0.5*atan(Ravg/h)));


 %Surge impedance of tower
 %Radius of tower is 4 meters
 %Zt=60*log(cotd(0.5*(atand(8/28))))
R1=Zg;
R2=Zg;
R3=Zg;
R4=Zg;
%Z4 = (R4*T3)/(T3+R4);t1
%Z3 = ((R3+Z4)*T2)/(T2+R3+Z4);
%Z2 = ((R2+Z3)*T1)/(Z3+R2+T1);
%Z1 = R1+Z2;
%Current through tower
Itower = PLS2*Zg/(Zt+Zg);
```

```matlab
%Current through earthwire
Iearthwire = PLS2*Zt/(Zt+Zg);

PLS = round(Itower)


for I=1:1
    Zeq=(R1*R2*T3)/((R1*R2)+(R1*T3)+(R2*T3));
Veq = Zeq*PLS;
I1=Veq/R1;
I2=Veq/R2;
I3=Veq/T3;
end


i = [0,1,2,4,6,8,10,12,14,16,18,20];
Vpu = [0,1.68,1.74,1.8,1.82,1.87,1.9,1.93,1.97,2.0,2.05, 2.1];
Va1 = [0, 1.4, 1.45, 1.47, 1.5, 1.55, 1.57, 1.6, 1.63, 1.65, 1.67, 1.7];

FF=find (i==SAR);

for K=FF:FF
    V10=Vpu(FF);
end

DV = V10*248/1.6;
```

Appendix A7 – Calculation of Required No of Surge Arrestors

```matlab
clear all
run Tower
run TTVoltage
run Insulator_foTEST


% Arrestor energy discharged by the line arrestor stroke to ground wire
% Ea = Arrestor discharge voltage
Ri = TFRBest;
Ts = 220/(3*10^8);
sd=find (LC==PLS);



for k=sd:sd
T = Zg*Ts/Ri;
Ia = PLS*1000;
OV = Zo2(k);
BIL = OV;
Ea(k) = Zo2(k)*10^3;
Wa(k) = Ia*Ea(k)*T;

% Amount of energy required for the surge arrestor
Esav(k) = Wa(k)/1000;;
Esa = Esav(k)/132000;
end
Esa
% Arrestor energy discharged by the line arrestor stroke to phase conductor

Ts = 220/(3*10^8);
K1 = 1;
T = Zg*Ts/Ri;
Alpha = -80*10^-6/T;
for YY=1:12
for kk=sd:sd
Ia(YY) = LC(YY)*1000;
Ea(kk) = Zo2(kk)*10^3;
Wap(YY,kk) = K1*Ia(YY)*Ea(kk)*T/(1+(1/Alpha));

%Amount of energy required for the surge arrestor
Esavp(YY,kk) = Wap(YY,kk)/1000;
Esap(YY,kk) = Esavp(YY,kk)/88000;
end
end
Wap;
Esap;

OV = OV/8;
OV1 = OV;
OVT = OV1
for J = 2:8
    OVT(1) = OV1
    OVT(J) = OV1 + OVT(J-1)
end
OVTT = OVT
for J = 9:15
```

```matlab
    if J==16, break, end
    OVT(J) = OVT(17-(J+1))
end


plot (Trt*10^6, (OVT))

xlabel ('Time - us');
ylabel ('Overvoltages - kV');
title ('Graph of Lightning overvoltages vs time');

pause
BFO = OVT(8) - VfoE(8)
if BFO > 0
    disp (' flash over will occur')
    outage = 1
else if BFO < 0
        disp (' flash over will not occur')
        outage = 0
    end
end

i = [0,1,2,4,6,8,10,12,14,16,18,20];
Vpu = [0,1.68,1.74,1.8,1.82,1.87,1.9,1.93,1.97,2.0,2.05, 2.1];
Va1 = [0, 1.4, 1.45, 1.47, 1.5, 1.55, 1.57, 1.6, 1.63, 1.65, 1.67, 1.7];

FF=find (i==SAR);

for K=FF:FF
    V10=Vpu(FF);
end

DV = V10*249/1.6;

for I=1:15
    if OVT(I) > DV
        Overvoltage2(I) = OVT(I) - DV;
    else Overvoltage2(I) = OVT(I);
    end
end

%Number of surge arrestors required
OVTT = OVT(8)/2;
J=0
I =1
for I = 3:20
    W=I-2;
    I = I + J;
    ID(1) = OVT(8)/2;
    ID(2) = OVT(8)/2;
    IDD(1) = 0;
    IDD(2) = 0 + 0.99;
    ID
    NSA = OVTT - DV;
    ID(I) = NSA;
    ID(I+1) = NSA
    IDD(I) = W;
    IDD (I+1) = W + 0.99;
```

```
    J=J+1;
OVTT = NSA;

if OVTT < 1
      break, end
end
if BFO < 0
    NLSA = 0;
    W=0;
    IDD=0;
else
NLSA = I
end




disp ('       VfoE    Max Overvoltage (kV)  Required Surge Arrestor  Tower
Foot Resis outage')
fprintf('%10.4g\t %10.4g\t %10.4g\t %10.4g\t %10.4g\n', VfoE(8),
(OVT(8)/2), W, TFRBest, outage);




plot (IDD,ID)




xlabel ('Tower number');
ylabel ('Overvoltage - kV');
title ('Graph of Lightning overvoltages vs tower number - influence of
surge arrestors');
legend ('Step change due to surge arrestor reduction of voltage');
```

Appendix B - Subroutines for EHVDC Systems

Appendix B1 – Calculation of Insulator Flashover Voltage

```
L = 3;
H = 46;

while L < 7.2

K1 = 400*L;
K2 = 710*L;
%t = (H)/(3*10^8);
%t = t*10^6;
t=8;
f=20;
G=round(t);
tt=t/G;
dr= 0;
for I=1:28
    dr(I) = 0;
    Vfo(I) = 0;
end


dr = 1
for I=2:28
    dr(I) = dr(I-1) + tt;
end

for I = 1:28
Vfo(I) = K1 + K2/(dr(I)^0.75);
end

for I=1:28
    dr(I) = dr(I);
    Vfo(I) = Vfo(I);

end

drr = 0;
for I = 2:21
    drr(I) = drr(I-1) + 1;
end
%for I = 1:28

 %   Vfon(I-7) = Vfo(I);
%end

if L==3
    VfoA = Vfo;
%    VfonA = Vfon;
end

if L==4
    VfoB = Vfo;
%    VfonB = Vfon;
```

```matlab
end


    if L==5
    VfoD = Vfo;
%    VfonD = Vfon;
    end


      if L==6
    VfoE = Vfo;
%    VfonE = Vfon;
      end


      if L==7
      VfoF = Vfo;
%    VfonF = Vfon;
            end
L = L + 1;

end



plot (dr, VfoA, dr, VfoB, dr, VfoD, dr, VfoE, dr, VfoF)
xlabel ('Time - us');
ylabel ('Overvoltage - kV');
title ('Graph of insulator overvoltage vs time');
legend('3m', '4m' ,'5m' ,'6m','7m')
```

Appendix B2 – Calculation of Induced Voltage Caused by Lightning Stroke

```
h= 47;
Zo=20;
Imax = 10;
d=50;

Imax = [10, 20, 30, 40, 50, 60, 70, 80, 90, 100];

for I = 1:10
    Umax (I) = Zo*Imax(I)*h/d
    I = I +1;
end

plot (Imax, Umax)
pause
dis = [30, 50, 70, 90, 110, 130, 150, 170, 190, 210];

Imax =10
while Imax < 101

    for J = 1:10
    Umax (J)= Zo*Imax*h/dis(J)
    J = J + 1;
    plot (dis, Umax)
    end

J = 1
 if Imax==10
 Umax10 = Umax
 else if Imax==20
        Umax20 = Umax
 else if Imax==30
        Umax30 = Umax
 else if Imax==40
        Umax40 = Umax
 else if Imax==50
        Umax50 = Umax
 else if Imax==60
        Umax60 = Umax
        else if Imax==70
        Umax70 = Umax
 else if Imax==80
        Umax80 = Umax
 else if Imax==90
        Umax90 = Umax
 else if Imax==100
        Umax100 = Umax
    end
    end
    end
            end
    end
    end
    end
    end
```

```
        end
   end
   Imax = Imax + 10;
end
plot (dis, Umax10, dis, Umax20, dis, Umax30, dis, Umax40, dis, Umax50, dis,
Umax60, dis, Umax70,dis, Umax80, dis, Umax90, dis, Umax100)
title ('Overvoltage vs distance from line')
xlabel ('Meters')
ylabel ('Over voltage - kV')
legend ('10kA','20kA', '30kA','40kA','50kA', '60kA', '70kA','80kA', '90kA',
'100kA')
```

Appendix B3 – Calculation of Tower Top Voltage

```
I = [5, 10, 15, 20, 30, 40, 50, 70, 80, 90, 100, 150];
LC=I;
sd=find (LC==PLS);
for J = sd:sd
Zi = Zg*Zt/(Zg+2*Zt);
Zw = (Zt*(Zg*Zg))/(Zg+(2*Zt*Zt))*((Zt-R(O))/(Zt+R(O)));


Dc = ((2*Zt - Zg)/(2*Zt + Zg))*((Zt - R(O))/(Zt+R(O)));
Ic(J) = (2*Tt/T0)*I(J);

II=10;
for E = 1:4
IcNew(E) = (2*TCO(E)/Tt)*II;
VtNew(E) = Zi*II - Zw*((II/(1-Dc)) - IcNew(E)/((1-Dc)*(1-Dc)));
end

Vt(J) = Zi*I(J) - Zw*((I(J)/(1-Dc)) - Ic(J)/((1-Dc)*(1-Dc)));
Vt(J) = Zi*I(J) - Zw*((I(J)/(1-Dc)) - Ic(J)/((1-Dc)*(1-Dc)));
Vt(J) = -Vt(J);



Main = -Zi*I(J);
Decay2 = -Ic(J)/((1-Dc)*(1-Dc));
Decay1 = -Zw*((I(J)/(1-Dc)));
end

if O==1
Zo1 = Vt;
else if O==2
   Zo2 = Vt;
    else if O==3
Zo3 = Vt;
   end
    end
end

end
Diff1 = abs(Zo2-Zo1)
Zo1 = Zo2-Diff1
Zo2 = Zo2
Diff3 = abs(Zo2-Zo3)
Zo3 = Zo2+Diff3

if TFRBest > 20
    Zo2 = Zo3
else if TFRBest < 20
        Zo2 = Zo1
        else if TFRBest == 20
        Zo2 = Zo2
    end
    end
end
```

Appendix B4 – Calculation of Surge Arrestor Lightning Impulse Withstand Voltage (V10)

```matlab
run TFRNew
PLS1 = input('Enter peak lightning stroke in kA     ');
PLS2 = PLS1/2;


SAR = input('Enter surge arrestor rating in kA      ');
BIL = 450;
for I=1:1
To(I) = 30;
end
T1 = TFRBest;
T2 = TFRBest;
T3 = TFRBest;
R1 = 400;
R2 = 400;
R3 = 400;
R4 = 400;
Lsec1 = 400;
Lsec2 = 400;


Load = 1;


Voltage = 132000;
Current = Load/Voltage;
T1=T2;
%Zt=60*log(cotd(0.5*(atand(8/28))))

%Surge impedance of ground wire
%Radius of fox conductor = (3.74mm*12)check;
%height of tower (earthwire) is 46.9m
 Zg = 60*log(46.9/0.045);
 h = 46.9;
h1 = 12.9;
h2 = 34.0;

r1 = 7.75
r2 = 7.75;
r3 = 3.9;
Ravg1 = r1*h1 + r2*h + r3*h2;
Ravg = Ravg1/h;
Zt = 60*log(cot(0.5*atan(Ravg/h)));


 %Surge impedance of tower
 %Radius of tower is 4 meters
 %Zt=60*log(cotd(0.5*(atand(8/28))))
R1=Zg;
R2=Zg;
R3=Zg;
```

```matlab
R4=Zg;
%Z4 = (R4*T3)/(T3+R4);t1
%Z3 = ((R3+Z4)*T2)/(T2+R3+Z4);
%Z2 = ((R2+Z3)*T1)/(Z3+R2+T1);
%Z1 = R1+Z2;
%Current through tower
Itower = PLS2*Zg/(Zt+Zg);

%Current through earthwire
Iearthwire = PLS2*Zt/(Zt+Zg);

PLS = round(Itower)




for I=1:1
    Zeq=(R1*R2*T3)/((R1*R2)+(R1*T3)+(R2*T3));
Veq = Zeq*PLS;
I1=Veq/R1;
I2=Veq/R2;
I3=Veq/T3;
end

XAxis = [0, 0.025, 0.05, 0.1, 0.15, 0.2, 0.25, 0.3, 0.4, 0.5, 0.6, 0.8 0.9
1.0];
Time = [0.0125  0.025   0.0375  0.05    0.0625  0.075   0.0875  0.1 0.1125
0.125   0.1375  0.15    0.1625  0.175   0.1875  0.2 0.2125  0.225   0.2375
0.25    0.2625  0.275   0.2875  0.3 0.3125  0.325   0.3375  0.35    0.3625
0.375   0.3875  0.4 0.4125  0.425   0.4375  0.45    0.4625  0.475   0.4875
0.5 0.5125  0.525   0.5375  0.55    0.5625  0.575   0.5875  0.6 0.6125
0.625   0.6375  0.65    0.6625  0.675   0.6875  0.7 0.7125  0.725   0.7375
0.75    0.7625  0.775   0.7875  0.8 0.8125  0.825   0.8375  0.85    0.8625
0.875   0.8875  0.9 0.9125  0.925   0.9375  0.95    0.9625  0.975   0.9875
1];
Magnitude = [0.05   0.15    0.25    0.3 0.375   0.45    0.5 0.55    0.6
0.65    0.7 0.75    0.8 0.85    0.9 0.95    0.97    0.98    0.99    1
0.99    0.98    0.97    0.95    0.9 0.85    0.8 0.75    0.65    0.6 0.55
0.5 0.45    0.375   0.3 0.25    0.15    0.1 0.05    0   -0.05   -0.15   -
0.25    -0.3    -0.375  -0.45   -0.5    -0.55   -0.6    -0.65   -0.7    -
0.75    -0.8    -0.85   -0.9    -0.95   -0.97   -0.98   -0.99   -1  -0.99
-0.98   -0.97   -0.95   -0.9    -0.85   -0.8    -0.75   -0.65   -0.6    -
0.55    -0.5    -0.45   -0.375  -0.3    -0.25   -0.15   -0.1    -0.05   0];
Time = Time/5;
for T=1:80
    Overvoltage(T) = 0;
    Icurrent(T) = 0;
    Vlnd(T) = 0;

    Current(T) = Magnitude(T)/Load;
plot (Time, Magnitude)
    Magnitude (T) = Magnitude (T)*88;
end

Icurrent= [ 0, 170, 190, 200, 190, 170, 100, 75, 50, 50, 30, 0, 0, 0];

for I = 15:80
```

```matlab
        Icurrent(I) =0;
end
for Q=1:80
    Icurrent(Q) = Icurrent(Q)*I3/200;
    Current_light(Q) = Current(Q) + Icurrent(Q);
end




Max_Current = max (Current_light);

%voltage rise due to resistive component
for T=1:14
Overvoltage(T) = Icurrent(T)*T3;
end


%voltage rise due to inductive component

for T=1:14
Vlnd(T)=(50/1000000)*50/(10/1000000);
end



for T=1:80
    Overvoltage (T) = Overvoltage (T) + Magnitude (T) + Vlnd(T);
end

for T=1:80
    plot(Time, Overvoltage);
end

R=max(Overvoltage);
if R > BIL
    outage = 1;
else outage = 0;

end

i = [0,1,2,4,6,8,10,12,14,16,18,20];
Vpu = [0,1.68,1.74,1.8,1.82,1.87,1.9,1.93,1.97,2.0,2.05, 2.1];
Va1 = [0, 1.4, 1.45, 1.47, 1.5, 1.55, 1.57, 1.6, 1.63, 1.65, 1.67, 1.7];


FF=find (i==SAR);

for K=FF:FF
    V10=Vpu(FF);
end

DV = V10*248/1.6;



for I=1:80
    if Overvoltage(I) > DV
        Overvoltage1(I) = Overvoltage (I) - DV;
    else Overvoltage1(I) = Overvoltage (I);
    end
end
```

```
for T=1:80
    plot (Time, Overvoltage1, Time, Overvoltage)
title('Plot of Time vs voltage');
ylabel('voltage kV');
xlabel('Time S');
legend('Surge Arrestor', 'No Surge Arrestor')


    end
```

Appendix B5 - Calculation of Required Number of Surge Arrestors

```matlab
clear all
run TowerDC
run TTVoltageDC
run InsulatorDC


 % Arrestor energy discharged by the line arrestor stroke to ground wire
 % Ea = Arrestor discharge voltage
 Ri = TFRBest;
 Ts = 220/(3*10^8);
 sd=find (LC==PLS);


 for k=sd:sd
 T = Zg*Ts/Ri;
 Ia = PLS*1000;
 OV = Zo2(k);
 BIL = OV;
 Ea(k) = Zo2(k)*10^3;
 Wa(k) = Ia*Ea(k)*T;

 % Amount of energy required for the surge arrestor
 Esav(k) = Wa(k)/1000;;
 Esa = Esav(k)/132000;
 end
 Esa
% Arrestor energy discharged by the line arrestor stroke to phase conductor

 Ts = 220/(3*10^8);
 K1 = 1;
 T = Zg*Ts/Ri;
 Alpha = -80*10^-6/T;
 for YY=1:12
 for kk=sd:sd
 Ia(YY) = LC(YY)*1000;
 Ea(kk) = Zo2(kk)*10^3;
 Wap(YY,kk) = K1*Ia(YY)*Ea(kk)*T/(1+(1/Alpha));

%Amount of energy required for the surge arrestor
Esavp(YY,kk) = Wap(YY,kk)/1000;
Esap(YY,kk) = Esavp(YY,kk)/88000;
end
end
Wap;
Esap;

OV = OV/8;
OV1 = OV;
OVT = OV1
for J = 2:8
    OVT(1) = OV1
    OVT(J) = OV1 + OVT(J-1)
end
OVTT = OVT
for J = 9:15
```

```matlab
    if J==16, break, end
    OVT(J) = OVT(17-(J+1))
end


plot (Trt*10^6, (OVT))

xlabel ('Time - us');
ylabel ('Overvoltages - kV');
title ('Graph of Lightning overvoltages vs time');

pause
BFO = OVT(8) - VfoE(8)
if BFO > 0
    disp (' flash over will occur')
    outage = 1
else if BFO < 0
        disp (' flash over will not occur')
        outage = 0
    end
end

i = [0,1,2,4,6,8,10,12,14,16,18,20];
Vpu = [0,1.68,1.74,1.8,1.82,1.87,1.9,1.93,1.97,2.0,2.05, 2.1];
Va1 = [0, 1.4, 1.45, 1.47, 1.5, 1.55, 1.57, 1.6, 1.63, 1.65, 1.67, 1.7];

FF=find (i==SAR);

for K=FF:FF
    V10=Vpu(FF);
end

DV = V10*1014/1.6;

for I=1:15
    if OVT(I) > DV
        Overvoltage2(I) = OVT(I) - DV;
    else Overvoltage2(I) = OVT(I);
    end
end

%Number of surge arrestors required
OVTT = OVT(8)/2;
J=0
I =1
for I = 3:20
    W=I-2;
    I = I + J;
    ID(1) = OVT(8)/2;
    ID(2) = OVT(8)/2;
    IDD(1) = 0;
    IDD(2) = 0 + 0.99;
    ID
    NSA = OVTT - DV;
    ID(I) = NSA;
    ID(I+1) = NSA
    IDD(I) = W;
    IDD (I+1) = W + 0.99;
```

```matlab
    J=J+1;
OVTT = NSA;

if OVTT < 1
        break, end
end
if BFO < 0
    NLSA = 0;
    W=0;
    IDD=0;
else
NLSA = I
end




disp ('       VfoE    Max Overvoltage (kV)  Required Surge Arrestor  Tower
Foot Resis outage')
fprintf('%10.4g\t %10.4g\t %10.4g\t %10.4g\t %10.4g\n', VfoE(8),
(OVT(8)/2), W, TFRBest, outage);


plot (IDD,ID)
xlabel ('Tower number');
ylabel ('Overvoltage - kV');
title ('Graph of Lightning overvoltages vs tower number - influence of
surge arrestors');
legend ('Step change due to surge arrestor reduction of voltage');
```

Appendix C – EHVDC Data Sheet

No.	Item	Unit	
1)	Manufacturer		ABB
2)	Arrester functional designation		D
3)	Manufacturer type reference		PEXLIM D609-XD515MEP
4)	Catalogue number		1HSA1281-948
5)	Rated voltage	kV dc/kV(rms)	609 (dc)
6)	CCOV	kV crest	515
7)	PCOV	kV crest	N.A.
8)	ECOV	kV crest	N.A.
9)	Reference current	mA crest	1 (dc)
10)	Reference voltage	kV crest	609
11)	Continuous current at PCOV	mA(crest)	< 1
12)	Maximum discharge voltage for steep front current impulse at following current:		
	1000A crest	kV crest	903
	3000A crest	kV crest	951
	10000A crest	kV crest	1035
	20000A crest	kV crest	1095
13)	Maximum discharge voltage for 8/20μs current wave for following currents:		
	1000A crest	kV crest	857
	3000A crest	kV crest	898
	10000A crest	kV crest	964
	20000A crest	kV crest	1014
14)	Maximum discharge voltage for 30–45/60–90μs current wave for following currents:(Waveshape / μs)		
	300A crest	kV crest	810
	1000A crest	kV crest	844
	3000A crest	kV crest	883
15)	Maximum discharge voltage for 1 ms front time of the current wave for following currents:		
	300A crest	kV crest	810
	1000A crest	kV crest	844
	3000A crest	kV crest	883
16)	Short duration high current withstand(4/10μs)	kA crest	100
17)	Pressure relief capability:		
	High current	kA(rms)	65
	Low current	A crest	600
18)	Arrester housing insulation withstand		
	Lightning impulse	kV crest	1425
	Switching impulse (wet)	kV crest	1175
	AC/DC+(wet)	kV(rms)/kV DC+	N.A.
19)	Arrester housing		
	Average diameter as per IEC 815	mm	148.5
	Minimum creepage distance	mm	26290
	Minimum strike distance	mm	> 5500
20)	Cantilever Strength		
	with the insulator sub base	Nm	N.A. Hanging arrester
	without the insulator sub base	Nm	
21)	Maximum current sharing factor (for multi–column arresters)		1.1
22)	Rated energy absorption capability		
	for single column	kJ/kV rating	5.16
	total for complete arrester	kJ	8700
23)	Maximum temperature rise of block after maximum energy dissipation	K	141
24)	Number of blocks in series		76
25)	Number of parallel column in main current carrying path of arrester		3
26)	Color		Grey